Ammonia Elimination from Protonated Nucleobases

A Thesis presented to the Faculty of the Graduate School

At the University of Missouri-Columbia

In Partial Fulfillment of the Requirements for the Degree

Master of Science

---

by

SHUO YANG

Dr. Rainer Glaser, Thesis Supervisor

AUGUST 2007

The undersigned, appointed by the dean of the Graduate School, have examined the thesis entitled

Ammonia Elimination from Protonated Nucleobases

Presented by Shuo Yang,

A candidate for the degree of Master of Science

And hereby certify that, in their opinion, it is worthy of acceptance

Professor Rainer Glaser

Professor Susan Lever

Professor Peter Tipton

ACKNOWLEDGEMENTS

I would like to express sincere gratitude to my advisor, Professor Rainer Glaser, for his patience, mentorship, guidance and constructive criticism throughout my thesis studies. It's fortunate to work with a person who continuously encouraged me to develop independent thinking and keenness of observation, which I consider are essential for my future study and career.

I also want to thank my parents for their unconditional love, support and inspiration. I am grateful to them for providing me freedom of choice and supporting me in my decisions. Without them, I could not have reached this milestone.

The first two chapters of this dissertation describe results of collaborative efforts in the Glaser research group. Chapter 1 builds on initial studies described in the doctoral thesis of Dr. Sundeep Rayat (University of Missouri-Colubia, 2003) and presents a major and significant extension with regard to the quality and the scope of the theoretical levels (QCI levels, solvation studies), the addition of 4-aminopyrimidine, and the completeness of the potential energy surface exploration (PES scans, isomers of alcohol tautomer). Much has been learned in the meantime, both in the group and elsewhere, that informs the context of the discussion, and the paper has been reconceptualized, restructured, and revised in close collaboration with Dr. Glaser. Chapter 2 builds on synthetic and mass-spectrometric studies by Dr. Ming Qian (PDA, MU 2001-5), Dr. Papiya Majumdar (Ph.D., MU 2007), and Dr. Nathan Leigh (departmental mass spectrometrist), and computational studies by Dr. Hong Wu (Ph.D., MU 2005). My first contribution to this work consisted in the extension of the computations of the proton affinities. My second

and major contribution consists in the exploration of the many plausible paths leading to ammonium ions. The results of this study greatly increased our understanding of the gas phase ion chemistry and has had significant consequences for the interpretation of the experimental results.

I am most grateful to have had these opportunities for collaboration. I have enjoyed all of these activities tremendously and I realize and recognize gratefully that these collaborations have greatly enriched my experience as a graduate student at MU.

TABLE OF CONTENTS

LIST OF TABLES

Table Page

LIST OF SCHEMES

Scheme Page

LIST OF FIGURES

Figure Page

Ammonia Elimination from Protonated Nucleobases

SHUO YANG

Dr. Rainer Glaser, Thesis Supervisor

ABSTRACT

Chapter 1: The dediazoniations of the diazonium ion **1** of 4-aminopyrimidine and of the tautomeric cytosinediazonium ions **2** and **3** are facile and result in the formations of cations **4**, **5**, and **6**. The pyrimidine ring-opening of 4, **5** and **6** form their acyclic isomers **7 – 9**, respectively. The stability of (*E*)- and (*Z*)-isomers is studied.

Chapter 2: The results are discussed of mass-spectrometric studies of the nucleobases adenine **1h** (**1**, R = H), guanine **2h**, and cytosine **3h**. The protonated nucleobases are generated by electrospray ionization of adenosine **1r** (**1**, R = ribose), guanosine **2r**, and deoxycytidine **3d** (**3**, R = deoxyri-bose) and their fragmentations are studied with tandem mass spectrometry. Possible NH_3 elimination fragmentation paths for all the ions are given.

Chapter 3: The conformational and isomer preferences of cyanoamine **1** and carbodiimide **2**, their conjugate acids and the formation of isoguanosine are discussed. Possible NH_3 elimination paths from the protonated cyanoamine **1** and carbodiimide **2** are studied.

CHAPTER 1. 4-Pyrimidyl Cations in 4-Aminopyrimidine Deamination: Controlling Role of Endocyclic Nitrilium Ion Lability

1.1 Introduction

Heteroanalogs of benzynes, the hetarynes, had been discussed even before benzynes,[1] but it was Wittig's discovery of *o*-benzyne[2] in 1940 that led to the systematic exploration of benzynes[3,4] and hetarynes.[5,6,7] The simplest neutral and cationic *N*-hetarynes, the azarynes, result by isoelectronic (=CH– / =N–) and (≡C– / ≡N^+–) replacements (Scheme 1.1). The combination of both types of replacements results in diazaryne cations, and these include 4-pyrimidyl cation. We are interested in 4-pyrimidyl cation **4** and its derivatives **5** and **6** (Scheme 1.2). These cations are readily accessible[8] from the diazonium ions **1** - **3**, respectively, and this chemistry is important in the context of nitrosative cytosine deamination.[9,10] DNA cytosine methyl-transferases[11] methylate and/or deaminate cytosine (C) to form 5-methylcytosine (5meC), thymine (T), and uracil (U), and nitrosation is a second important path for the conversion of cytosine to uracil. C-to-U damage can be repaired via enzymatic base excision and cytosine reproduction using the enzymes *N*-glycosylase[12] or endonuclease V.[13] If left unrepaired, however, the C-to-U transformation results in G:C→A:T mutation.[14,15] The nitrosative C-to-U process is thought to occur *via* the cytosinediazonium ion and its hydrolysis by direct nucleophilic aromatic substitution.

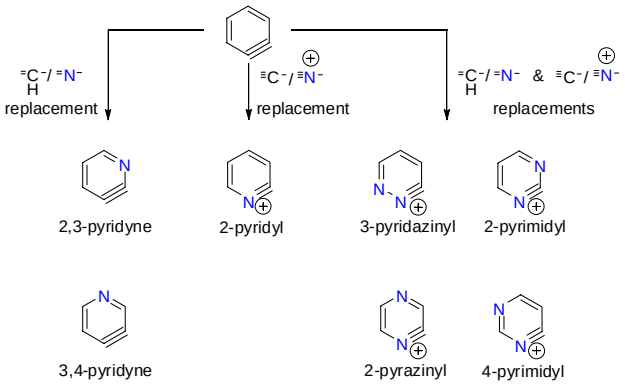

Scheme 1.1. Azarynes and diazarynes formally derived from *o*-benzyne by isoelectronic (=CH– / =N–) or/and (≡C– / ≡N^+–) replacements.

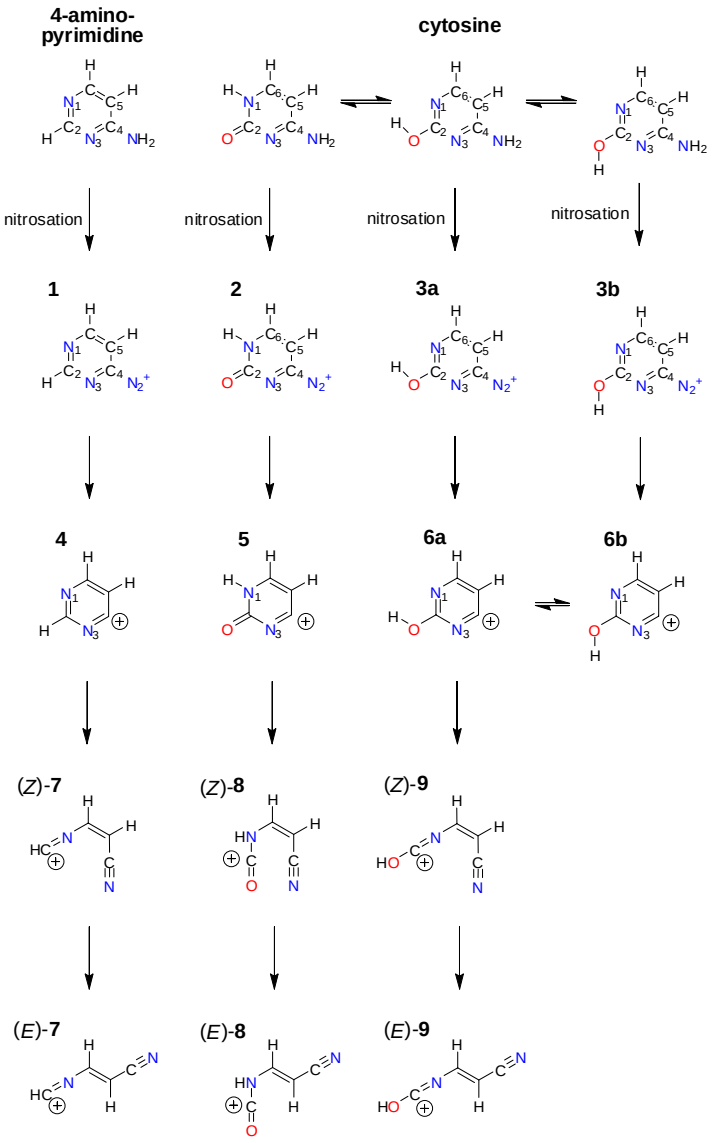

Scheme 1.2. Nitrosation and dediazoniation of 4-aminopyrimidine and of cytosine tautomers leads to 4-pyrimidyl cation **4** and the substituted derivatives **5** and **6**, respectively. The acrylonitriles N≡C–CH=CH–X^+ (X = –NCH, –HNCO, –NCOH) **7** - **9** are acyclic isomers of **4** - **6**.

In this paper, we will show that 4-pyrimidyl cations **4** - **6** are readily accessible from the diazonium ions **1** - **3**, respectively, and we will discuss **4** - **6** to address the question as

to whether these ions are heteroanalogs of phenyl cation, azarynes, or cyclic nitrilium ions (Scheme 1.3). The 4-pyrimidyl cation is usually represented by structures of type **A – D** (but not **E**). Scheme 1.3 shows **5** and **6** to be isoelectronic with **4** and that all three ions could be seen as cationic azarynes. Ions **4** and **6** show more formal similarity considering that quasi-aromatic amide resonance structures are not important for **5**. Ion **5** usually is described as **5B** or it could be an azaryne **5C**. Careful analysis of the structure of **5** suggested to us that this ion is stabilized by hyperconjugation of the electron-deficient carbon center by the β,γ-NC σ–bond and, in the extreme, this description allows for the cyclic nitrilium structure **5E**, *i.e.* dative bonding between the nitrile-N and the carbonyl-C. We will now demonstrate the existence of C2–N3 dative bonding in cations **4** - **6** based on the results of studies of the C2–N3 dissociation reactions of **4** - **6**, of studies of the geometrical isomers of acyclic acrylonitriles **7** - **9** formed, and of analyses of the electron densities of **4** - **9**.

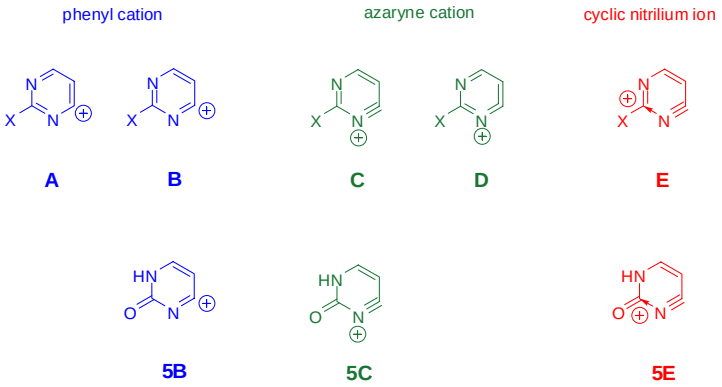

Scheme 1.3. 4-Pyrimidyl cations **4** (X = H), **5**, and **6** (X = OH) formally can be discussed as heteroanalogs of phenyl cation (**A** & **B**), azarynes (**C** & **D**), or cyclic nitrilium ions (**E**).

1.2 Theoretical and Computational Methods

Quantum-Mechanical Methods, Software, and Data Reduction. *Ab initio* calculations[16] were performed with Gaussian03[17] and earlier versions on a 64-processor SGI Altix system. Second-order Møller-Plesset perturbation theory was employed and all electrons were included in the active space of the correlation calculation; MP2(full). The basis set 6-31G** assures flexible description of valence electrons. Vibrational analyses were carried out to obtain thermodynamical data and to ensure that a proper stationary point had been located by the gradient optimization. To account more fully for the effects of electron correlation, single-point calculations were performed using quadratic CI theory considering single and double excitations, QCISD, and including an approximation for the contributions from triple excitations, QCISD(T). The QCI calculations employed the triply-split valence basis set 6-311G** basis set and were based on the MP2(full)/6-31G** structures. Solvent effects were examined with the application of the isodensity polarized continuum model[18] (IPCM) at the QCISD/6-311G**//MP2(full)/6-31G** level. With a view to the relevance of the chemistry discussed to physiology and toxicology, aqueous solvation was modeled (ε = 78.39). The results of the calculations are provided as Supporting Information and these data include total energies E_{tot}, vibrational zero-point energies *VZPE* (kcal mol^{-1}), thermal energies *TE* (kcal mol^{-1}), and molecular entropies *S* (cal K^{-1} mol^{-1}).

Dinitrogen Affinities, Cyclization Energies, Activation Barriers, (*E*)-Preference Energies, and Binding Energies. Relative and reaction energies are reported in Table 1.1 and the values given are ΔE, $\Delta E_0 = \Delta E + \Delta VZPE$, $\Delta H_{298} = \Delta E + \Delta TE$, and $\Delta G_{298} = \Delta H_{298} - 0.29815 \cdot \Delta S$. The MP2(full)/6-31G** thermodynamical data are used in all sets.

Table 1.1. Dinitrogen Affinities, Cyclization Energies, Activation Barriers, (*E*)-Preference Energies, and Electrophile Binding Affinities[a]

Parameter	ΔE	ΔE_0	ΔH_{298}	ΔG_{298}
		MP2(full)/6-31G**		
DA(**1**)	8.33	5.00	5.31	-5.20
DA(ITS-**1**)	1.25	-0.16	-0.12	-9.63
DA(IMC-**1**)	4.58	4.12	3.11	-2.61
DA(**2**)	-2.42	-4.88	-4.72	-14.87
DA(ITS-**2**)	-3.05	-4.63	-4.40	-14.49
DA(IMC-**2**)	5.05	4.65	3.67	-2.29
DA(**3a**)	9.30	6.20	6.49	-4.00
DA(ITS-**3a**)	2.24	0.98	0.98	-8.48
DA(IMC-**3a**)	4.87	4.41	3.44	-2.65
DA(**3b**)	10.28	6.86	7.21	-3.38
DA(ITS-**3b**)	2.20	0.81	0.83	-8.65
DA(IMC-**3b**)	4.72	4.25	3.27	-2.76
CE(**4**)	9.56	11.86	10.80	13.29
CE(**5**)	5.01	6.55	5.62	8.02
CE(**6**)	1.32	3.54	2.12	5.91
E_A(**4** → **10**)	7.25	5.50	5.61	5.35
E_A(**5** → **11**)	2.53	1.39	1.49	1.15
E_A(**6a** → **12a**)	13.88	11.64	12.13	10.97
E_A(**6b** → **12b**)	7.38	5.84	6.09	5.46
E_{rel}(**6b** *vs*. **6a**)	3.00	2.64	2.70	2.59
E_A(**6a** → **6d**)	8.66	7.49	7.36	7.53
E_A(**6b** → **6d**)	5.66	4.85	4.66	4.94
EPE(**7**)	-2.03	-1.93	-2.02	-2.08
EPE(**8**)	-4.39	-4.25	-4.37	-3.91
EPE(**9**)	-2.53	-2.50	-2.54	-2.96
PA(CH_3CN)	193.35	186.46	187.14	179.77
MA(CH_3CN)	102.15	96.84	97.30	85.43
CO-Loss from (*Z*)-**8**	61.36	64.40	58.31	47.30

Deprot. of (*Z*)-**8 - CO**	148.83	148.83	141.56	134.35
	QCISD/6-311G**//MP2(full)/6-31G**			
DA(**1**)	4.17	0.84	1.15	-9.36
DA(ITS-**1**)	0.95	-0.46	-0.42	-9.94
DA(IMC-**1**)	4.76	4.30	3.29	-2.42
DA(**2**)	-4.85	-7.31	-7.15	-17.30
DA(ITS-**2**)	-4.17	-5.75	-5.52	-15.61
DA(IMC-**2**)	4.42	4.02	3.04	-2.92
DA(**3a**)	4.98	1.88	2.17	-8.31
DA(ITS-**3a**)	1.47	0.21	0.21	-9.24
DA(IMC-**3a**)	4.64	4.18	3.21	-2.88
DA(**3b**)	5.34	1.92	2.27	-8.31
DA(ITS-**3b**)	1.04	-0.35	-0.33	-9.81
DA(IMC-**3b**)	4.44	3.97	2.99	-3.04
CE(**4**)	12.48	14.78	13.72	16.21
CE(**5**)	7.50	9.04	8.11	10.52
CE(**6**)	3.26	5.48	4.06	7.85
E_A(**4** $\rightarrow$ **10**)	8.70	6.95	7.06	6.80
E_A(**5** $\rightarrow$ **11**)	3.62	2.48	2.58	2.24
E_A(**6a** $\rightarrow$ **12a**)	16.53	14.29	14.78	13.62
E_A(**6b** $\rightarrow$ **12b**)	10.76	9.21	9.46	8.83
E_{rel}(**6a** *vs*. **6b**)	2.56	2.20	2.26	2.15
E_A(**6a** $\rightarrow$ **6d**)	9.74	8.57	8.45	8.61
E_A(**6b** $\rightarrow$ **6d**)	7.18	6.37	6.18	6.46
EPE(**7**)	-2.03	-1.93	-2.03	-2.08
EPE(**8**)	-3.20	-3.06	-3.18	-2.72
EPE(**9**)	-2.48	-2.45	-2.49	-2.92
PA(CH_3CN)	194.60	187.71	188.39	181.02
MA(CH_3CN)	96.91	91.60	92.06	80.19
CO-Loss from (*Z*)-**8**	32.66	29.19	29.61	18.60
Deprot. of (*Z*)-**8 - CO**	150.58	142.61	143.31	136.10

Table 1.1. *Continued.* (Attach to the right without repeating the "Parameter" Column)

Parameter	ΔE	ΔE_0	ΔH_{298}	ΔG_{298}
	QCISD(T)/6-311G**//MP2(full)/6-31G**			
DA(**1**)	2.94	-0.39	-0.08	-10.59
DA(ITS-**1**)	-0.20	-1.61	-1.57	-11.09
DA(IMC-**1**)	4.32	3.86	2.85	-2.86
DA(**2**)	-4.86	-7.32	-7.16	-17.30
DA(ITS-**2**)	-4.29	-5.87	-5.64	-15.72
DA(IMC-**2**)	4.52	4.12	3.14	-2.82
DA(**3a**)	4.24	1.14	1.43	-9.05
DA(ITS-**3a**)	0.67	-0.59	-0.59	-10.04
DA(IMC-**3a**)	4.32	3.86	2.89	-3.19
DA(**3b**)	4.54	1.12	1.47	-9.11
DA(ITS-**3b**)	0.23	-1.16	-1.14	-10.62
DA(IMC-**3b**)	4.09	3.62	2.64	-3.39
CE(**4**)	8.55	10.85	9.79	12.28
CE(**5**)	5.21	6.75	5.82	8.23
CE(**6**)	-0.02	2.20	0.78	4.57
E_A(**4** $\rightarrow$ **10**)	8.59	6.84	6.95	6.69
E_A(**5** $\rightarrow$ **11**)	3.44	2.30	2.40	2.06
E_A(**6a** $\rightarrow$ **12a**)	16.18	13.94	14.43	13.28
E_A(**6b** $\rightarrow$ **12b**)	9.77	8.22	8.48	7.85
E_{rel}(**6a** *vs.* **6b**)	2.44	2.08	2.14	2.03
E_A(**6a** $\rightarrow$ **6d**)	9.22	8.05	7.92	8.09
E_A(**6b** $\rightarrow$ **6d**)	6.77	5.97	5.78	6.05
EPE(**7**)	-1.97	-1.87	-1.96	-2.02
EPE(**8**)	-3.49	-3.35	-3.47	-3.01
EPE(**9**)	-2.46	-2.43	-2.47	-2.90
PA(CH_3CN)	217.74	210.85	211.54	204.16
MA(CH_3CN)	122.10	116.79	117.25	105.38
CO-Loss from (*Z*)-**8**	58.06	54.69	55.01	44.00
Deprot. of (*Z*)-**8** - **CO**	151.89	143.92	144.62	137.41
	IPCM(QCISD/6-311G**//MP2(full)/6-31G**)			
DA(**1**)	4.64	1.31	1.62	-8.89

DA(ITS-**1**)	-0.88	-2.29	-2.25	-11.76
DA(IMC-**1**)	0.75	0.29	-0.72	-6.44
DA(**2**)	-3.08	-5.54	-5.38	-15.53
DA(ITS-**2**)	-4.84	-6.42	-6.19	-16.27
DA(IMC-**2**)	0.56	0.16	-0.82	-6.79
DA(**3a**)	10.35	7.25	7.54	-2.95
DA(ITS-**3a**)	4.25	2.99	2.99	-6.46
DA(IMC-**3a**)	5.88	5.42	4.45	-1.64
DA(**3b**)	4.57	1.15	1.50	-9.08
DA(ITS-**3b**)	-1.83	-3.22	-3.20	-12.68
DA(IMC-**3b**)	5.91	5.44	4.46	-1.57
CE(**4**)	22.36	24.66	23.61	26.09
CE(**5**)	14.72	16.26	15.33	17.73
CE(**6**)	13.88	16.10	14.68	18.47
E_A(**4** → **10**)	8.09	6.33	6.45	6.19
E_A(**5** → **11**)	3.88	2.74	2.84	2.50
E_A(**6a** → **12a**)	13.71	11.47	11.96	10.80
E_A(**6b** → **12b**)	12.49	10.94	11.20	10.57
E_{rel}(**6a** *vs*. **6b**)	0.64	0.28	0.35	0.24
E_A(**6a** → **6d**)	7.37	6.21	6.08	6.25
E_A(**6b** → **6d**)	6.73	5.92	5.73	6.01
EPE(**7**)	-0.75	-0.65	-0.74	-0.80
EPE(**8**)	1.25	1.39	1.27	1.72
EPE(**9**)	-7.47	-7.44	-7.48	-7.91
PA(CH_3CN)	256.45	249.56	250.25	242.87
MA(CH_3CN)	63.31	58.00	58.46	46.59
CO-Loss from (*Z*)-**8**	51.51	54.98	48.46	37.46
Deprot. of (*Z*)-**8** - **CO**	212.03	220.00	204.76	197.55

The dinitrogen affinities *DA* (eq. 1) characterize the stabilities of diazonium ions, of their respective ion-molecule complexes (IMC), and of the isomerization transitions state (ITS) structures between these minima. The endocyclic N→C dative bond strengths are characterized by the cyclization energies *CE* of the (*Z*)-alkenes N≡C–CH=CH–X^+ and

CE is defined as the energy difference between the acyclic and the cyclic (*Z*)-isomers via eq. 2. The activation barriers for the ring opening reaction are provided by eq. 3. The configurational preference of 1,2-disubstituted alkenes X–CH=CH–Y are described by the (*E*)-preference energy *EPE*(X,Y) defined by eq. 4. Finally, proton and methyl cation affinities of nitriles are defined as the negative reaction energy of the appropriate association reaction (eq. 5).

$$DA = E([RN_2]^+) - E(R^+) - E(N_2) \quad \text{(eq. 1)}$$

$$CE = {}^{cyclic}E_{(Z)} - {}^{acyclic}E_{(Z)} \quad \text{(eq. 2)}$$

$$E_A = {}^{TS}E_{(Z)} - {}^{cyclic}E_{(Z)} \quad \text{(eq. 3)}$$

$$TPE = E_{(Z)} - E_{(E)} \quad \text{(eq. 4)}$$

$$PA = E([RCNH]^+) - E(RCN) - E(H^+) \quad \text{(eq. 5.1)}$$

$$MA = E([RCNCH_3]^+) - E(RCN) - E(CH_3^+) \quad \text{(eq. 5.2)}$$

Electron Density Analysis. In the natural bond order method (NBO),[19] the molecular orbitals are transformed into a set of maximally localized molecular orbitals (natural orbitals) and the natural populations of these orbitals produce charges that agree well with expectations based on the ionization energies of atoms. This method was employed to analyze the correlated electron density distributions computed at the MP2(full)/6-31G** level.

1.3 Results and Discussion

Nitrosative Deamination of 4-Aminopyrimidines. We found only one report on the stabilities of diazonium ions of derivatives of 4-aminopyrimidine.[20] The pyrimidine-4-diazonium ions were described as stable (abstract: "is stable and gives very little nitrogen

at room temperature"; summary: "diazonium compound [*sic*] of 4-aminopyrimidine derivatives [*sic*] was stable") and few details were given. The nitrosative deamination of 4-aminopyrimidine has been studied in cold aqueous acidic solution and resulted in a 94:6 product mixture of 4-pyrimidone and 4-pyrimidin-4-ol, respectively, with a combined yield of 48.5%.[21]

Cytosine deamination has been studied, but it appears that no study accounted quantitatively for all of the cytosine and its reaction products and, at this time, the palette of known reaction products might not be complete. For example, in a study of the deamination of 2'-deoxycytidine and 2'-deoxycytidine 5'-monophosphate (dC and dCMP) by NO at pH = 7.4, the ratio between unreacted cytosine and slowly formed uridine (dU, dUMP) was reported as about 9:1, and no information was given as to how much material was unaccounted for by the time this ratio was determined by HPLC analysis.

Facile Dediazonation. The nitrosative C-to-U process is thought to occur via the transient cytosinediazonium ion.. Our previous theoretical study of **2** and **3** was based on RHF/6-31G* structures and single-point energy calculations at the levels MP2/6-31G* and MP3/6-31G*. It was found that the classical diazonium ion **2** (**5**←N≡N) is merely a shallow minimum and 2.4 (1.1) kcal/mol *less* stable than free **5** and N_2 at the MP2//RHF (MP3//RHF) level and that an electrostatic complex IMC-**2** (**2**···N≡N) is bound by only 4.9 (4.3) kcal/mol. A classical diazonium ion structure was preferred by the HO-tautomer **3a** (**6a**←N≡N) with a dinitrogen affinity of 9.4 (10.8) kcal/mol relative to **6a** and N_2. As with IMC-**2**, there exists a second minimum IMC-**3a** (**6a**···N≡N) and this ion-molecule complex is bound by 3.5 (3.5) kcal/mol.

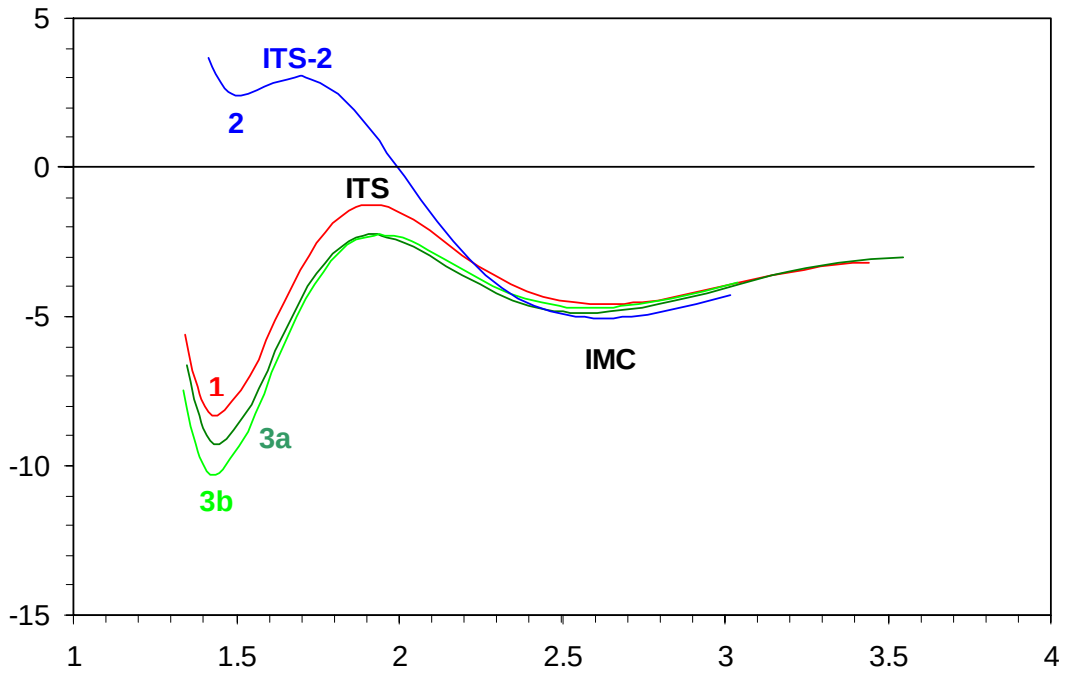

Figure 1.1. The MP2(full)/6-31G** energy profiles of the dissociations of diazonium ions **1** - **3** are shown relative to the energy of the respective pyrimidylium ion **4** - **6** and free N_2 and as a function of the C–N_2 distance.

Improved hard- and software now have allowed for higher-level studies of the dissociation reactions and the examination of solvent effects. The MP2(full)/6-31G** dissociation profiles of **1**, **2**, **3a** and **3b** are shown in Figure 1.1 and pertinent dinitrogen affinities are listed in Table 1.1. The earlier and the current dediazonation profiles of **2** and **3a** agree very well. Conformation **3a** was considered earlier because of its relevance in the guanine-cytosine base pair (GC). The alternative conformation **3b** is about 3 kcal/mol thermodynamically less stable than **3a** while it is kinetically slightly more stable toward dediazoniation. Figure 1.1 shows that the dissociation characteristics of the pyrimidine-4-diazonium **1** and of its 2-hydroxyderivatives **3a** and **3b** are similar. The

shapes of the dissociation curves persist at the QCISD//MP2 and QCISD(T)//MP2 levels but the diazonium ion structures are destabilized substantially. Ions **1**, **3a** and **3b** are destabilized so much that they become less stable (**1**) or energetically comparable (**3**) to the respective IMC complexes. Thermal energies favor IMC over diazonium structures and the QCI//MP2-derived E_0 and H_{298} values show IMC preference for **1**, **2**, and **3**. While[22] Dediazoniation reactions are well-known for being remarkably independent of the solvent[23,24] and, indeed, the computed solvent corrections to dinitrogen affinities are modest and show no discernable general trend (Table 1.1). For **2** the solvent further weakens the cation-N_2 interaction and even the IMC structure is predicted to be unbound. Hence, all of these calculations provide compelling evidence that the nitrosative deaminations of 4-aminopyrimidine and of the tautomers of cytosine all essentially produce a free cation, *i.e.* **4**, **5** or **6**.

Features of Typical Nitrilium Ions. Protons, carbenium ions, and other electrophiles readily add to nitriles and form nitrilium ions.[25-28] We performed electron density analyses at the MP2(full)/6-31G** level of free, protonated and methylated acetonitrile to provide a reference for the discussion of **4** - **6**.

The shortness of the CN bond is a common and characteristic feature of nitrilium ions; the CN bonds in the cations R–C≡N→E^+ (H^+: 1.158 Å; Me^+: 1.160 Å) are shorter than in acetonitrile itself (1.178 Å). The computed proton and methyl cation binding energies of acetonitrile are 193.4 and 102.2 kcal/mol, respectively, and the respective Gibbs free enthalpies are 179.8 and 85.4 kcal/mol. These bonds are roughly twice as strong as the respective bonds in protonated dinitrogen (118.2 kcal/mol[29]) and methyldiazonium ion (44.1 kcal/mol[30,31c]).

The cyano group of $H_3C–C{\equiv}N$ is slightly charged, q(CN) = -0.05, and it is polar with about one third of (-)- or (+)-charge on N and C, respectively. The charge relaxation associated with the binding of acetonitrile to an electrophile E^+ involves polarization and charge transfer. Placement of acetonitrile in the electric field of a (+)-point charge increases the charge on the cyano group slightly, q(CN) = -0.15, and the major effect is a substantial CN-polarization, q(N) = -0.80 and q(C) = +0.65. Bond formation to H^+ or CH_3^+ has similar effects in that some of acetonitrile's *N*-density is transferred but the N atom remains *negatively* charged. In fact, the cyano-C and the CH_3 group are slightly *more* positive in $R–C{\equiv}N{\rightarrow}E^+$ because the charge transfer $N{\rightarrow}E^+$ is offset by increased internal CN-polarization. Theoretical[31-34] and experimental[32,35] studies showed that $N{\equiv}N{\rightarrow}E^+$ dative bond formation leaves N_α negative and proceeds with little charge transfer. The main difference between $N{\equiv}N$ *vs*. $R–C{\equiv}N$ coordination to an electrophile lies with the amount of charge transfer: there is much more charge transfer in the nitrilium ions and the term "nitrilium ion" actually is appropriate.

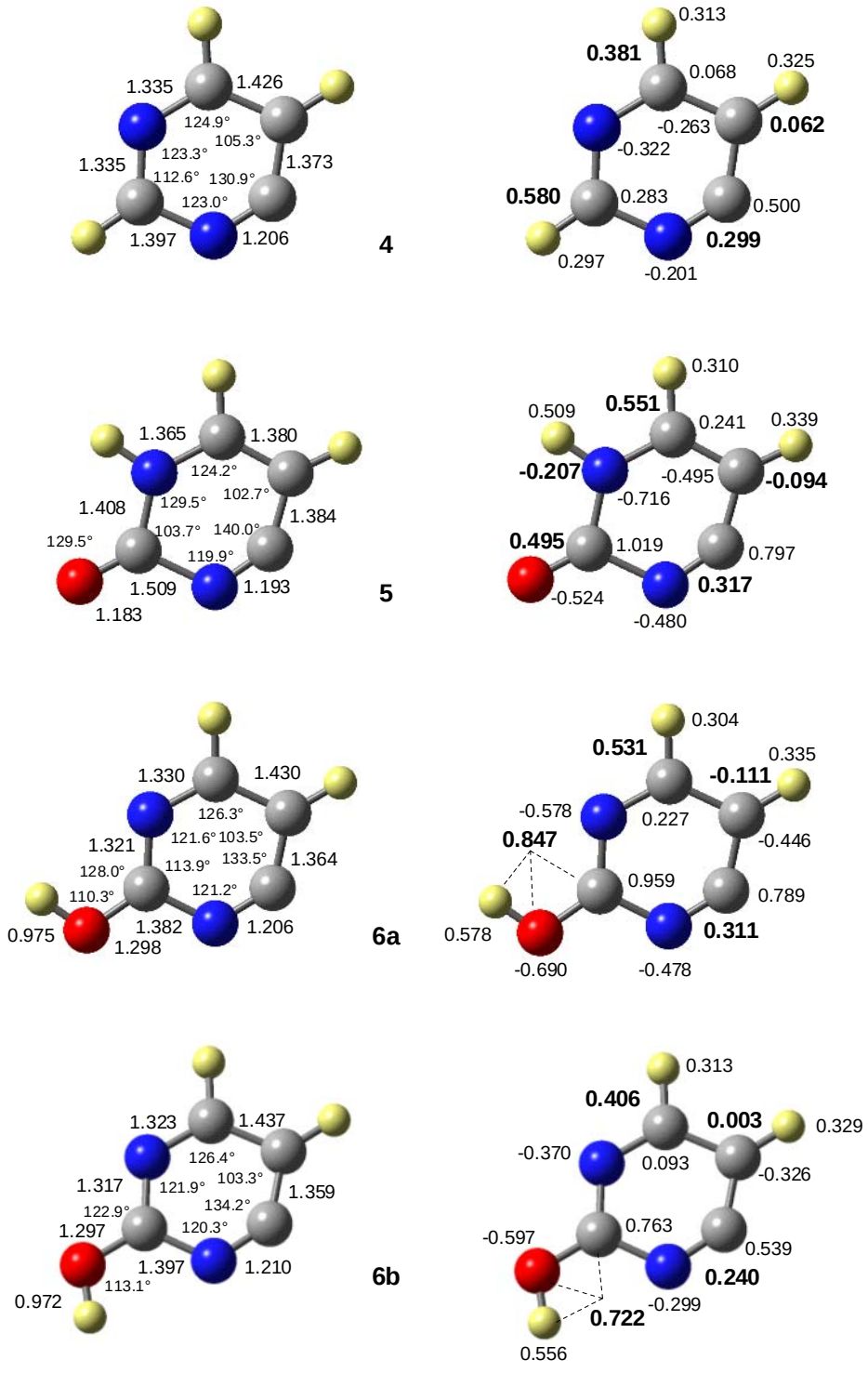

Figure 1.2. Major structural parameters (left) and natural populations (right) of the computed MP2(full)/6-31G** structures of cations **4** - **6**.

Endocyclic Nitrilium Ions and Highly Distorted Rings. The structures of **4** - **6** are highly distorted with in-ring angles varying between 100˚ and 140˚ and bond lengths alternating greatly (Figure 1.2). Each cation exhibits an extremely short N3–C4 bond length (1.193 - 1.198 Å) which is indicative of a C≡N triple bond (1.17 Å). Eberlin et al. argued for the azaryne resonance form based on the short CN bonds computed for the 2-pyridyl and 4-pyrimidyl cations.[36] By analogy one might then postulate **4C** - **6C** as the dominant contributors to the electronic structures of ions **4** - **6**. However, the C2–N3 bonds provide another important structural indicator, and this indicator is less compatible with **C**-type structures. The *d*(C2–N3) values in **4** and **6** are in the range 1.382 - 1.397 Å, respectively, and **5** displays an extremely long bond of 1.509 Å.

The population analysis reveals alternating positive and negative charges (Figure 1.2, right). ; The (+)-charge does *not* reside on the N3 atom in **4** - **6**; the N3-charges are *negative* (**4**: -0.20; **5**: -0.48; **6a**: -0.48; **6b**: -0.30) and **4C** - **6C** therefore cannot be dominant. In fact, only about one third of the charge is on the CN fragment of **4** - **6** (**4**: 0.30; **5**: 0.32; **6a**: 0.31; **6b**: 0.24). The large amount of (+)-charge associated with C4 (**4**: 0.50; **5**: 0.80; **6a**: 0.79; **6b**: 0.54) directs attention to the phenyl cation forms, but **4b** - **6b** fail to explain the short N1–C6 bond. However, there is considerable cationic character on the C2-side of N3 in the cations. The charge on C2 is 0.28 in **4** and it is small, while the C2-charges of 5 and 6 are very large (**5**: 1.02; **6a**: 0.96; **6b**: 0.76). The C2-atom of **4** carries an H-atom and hydrogens play an important role in stabilizing cations by sharing positive charge,[37] whereas the O-atoms at C2 deprive the C2-atoms in **5** and **6** of electron density. To grasp the bigger picture, it is advantageous to consider the charges of the C(2)–H, C(2)–O and C(2)–OH fragments and they are 0.58 (**4**), 0.50 (**5**), 0.85 (**6a**), and 0.72 (**6b**). The sum of the fragment charges on the C(2)X and the CN groups are 0.0.88

(**4**), 0.82 (**5**), 1.16 (**6a**), and 0.96 (**6b**) and these sums are close to unity. Hence, most of the (+)-charge *is* located on these fragments and it is for this reasons that the bonding situation is best decribed as dative bonding from the nitrile-N3 to the electron-deficient C2, the **E**-resonance forms.

Ions **4 – 6** feature the structural and electronic characteristics of acetonitrilium ion, and they are best represented as cyclic nitrilium ions. Cyclic nitrilium ions are not uncommon of course; they are intermediates in Beckmann rearrangements [38] and intramolecular Ritter reactions,[39] and salts of cyclic nitrilium have been prepared.[40] Ions **4** - **6** are uncommon nitrilium ions only in the sense that the acceptor is unsaturated and conjugated to the donor. The acceptor in nitrilium ion in **4** and **6** is a nitrilium ion itself ($Y–C^+=N–R$ ↔ $Y–C\equiv N^+–R$), and the acceptor is an acylium ion in **5** ($O=C^+–NH–R$ ↔ $O=C=NH^+–R$). The N1–C2 bonds in **4** and **6** are shorter than in **5** (vide supra) and the N3→C2 dative bonding model provides a straightforward explanation in that acylium ions are weaker electrophiles.[41]

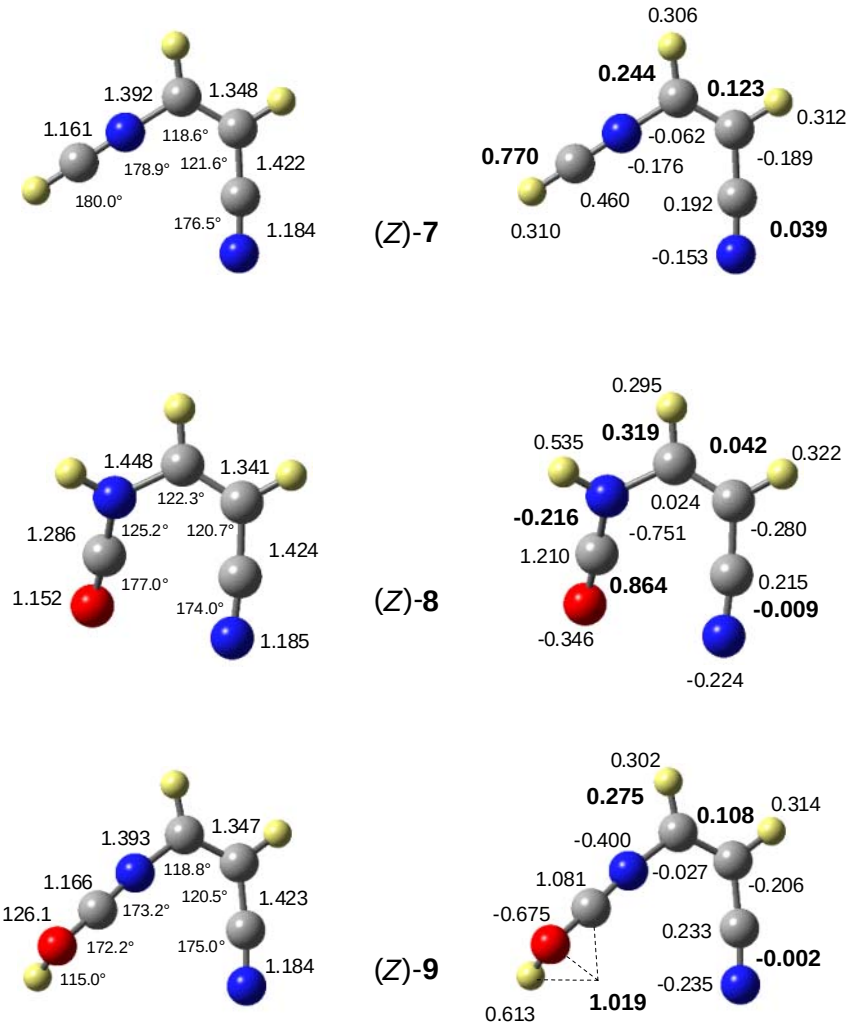

Figure 1.3. Major structural parameters (left) and natural populations (right) of the computed MP2(full)/6-31G** structures of acyclic and (*Z*)-configured cations **7** - **9**.

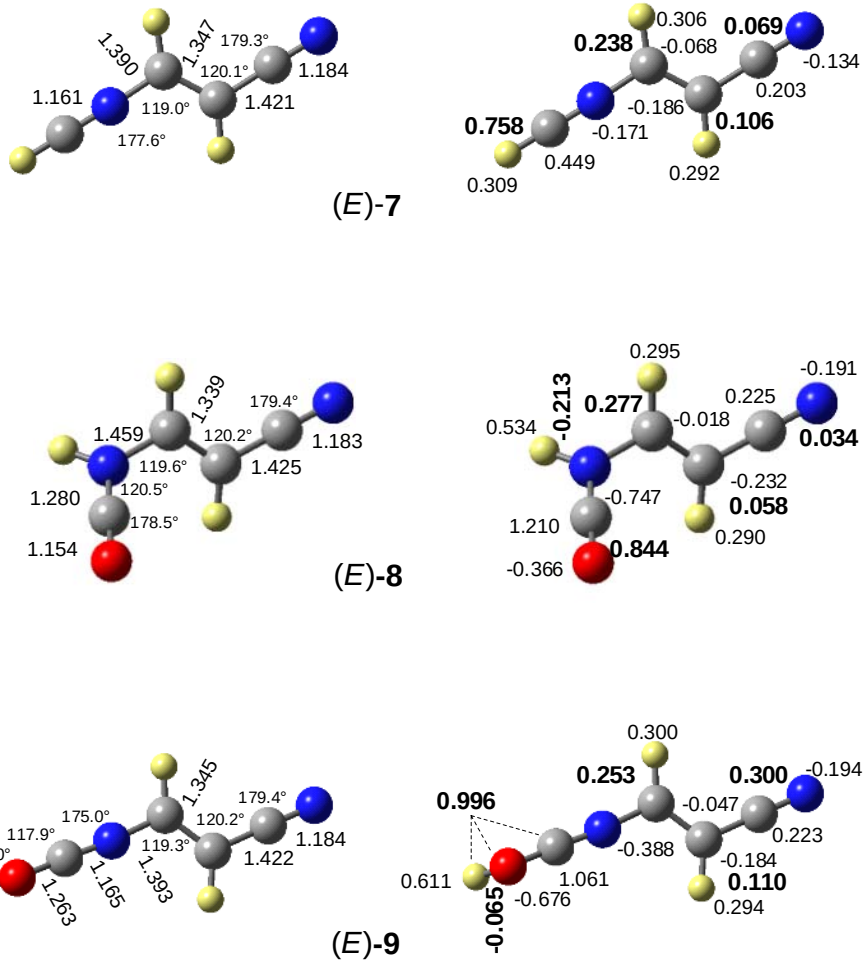

Figure 1.4. Major structural parameters (left) and natural populations (right) of the computed MP2(full)/6-31G** structures of acyclic and (*E*)-configured cations **7** - **9**.

Stability and Accessibility of Acyclic Structures. Recognizing the C2–N3 bonds as dative bonds, one immediately wonders just how weak the bonding might be? The dative bonding model essentially considers **4** - **6** as acrylonitriles of type N≡C–CH=CH–X^+ (X = –NCH, –HNCO, –NCOH) and, consequently, we studied the (*Z*)- and (*E*)-isomers of alkenes **7** - **9** (Figures 3 and 4). Ion **7**, *N*-methylidyne ethenaminium, has been discussed as a fragment in the mass spectra of pyridine,[42] pyrimidine,[43] and cytosine.[44] Ion **8** may form isomers with regard to the C–N single bond[45] and we focus on the conformation

most relevant to cyclization. Ions **8** and **9** formally result from *N*- and O-protonation of 3-isocyanatoacrylonitrile OCN–CH=CH–CN. *N*-protonation of isocyanates is well-known to produce carbamyl cations characterized by an NC double bond and a CO triple bond.[46] In ion **9**, the isocyanate-N is sp-hybridized, the CN bond is extremely short and essentially a CN triple bond. Ion **9** essentially is planar except for the position of the hydroxyl-H.[47]

The cyclization energies for (*Z*)-**7 -** (*Z*)-**9** all are *positive*, that is, the acyclic (*Z*)-isomers of **7 – 9** are preferred over the heterocyclic structures **4** - **6**! At the level of optimization, the cyclization of (*Z*)-**7** to **4** is endergonic by ΔG_{298} = 13.3 kcal/mol. The cyclizations of (*Z*)-**8** and (*Z*)-**9** to **5** and **6a**, respectively, remain endergonic with ΔG_{298} values of 8.0 and 5.9 kcal/mol, respectively. The QCISD(T) data confirm the preference for the acyclic structures and their sequence, and the agreement between the MP2 and QCISD(T) data is excellent. The IPCM calculations show that the absolute preference for the acyclic ions is *enhanced* in aqueous solution while the difference between the cyclization energies of tautomers (*Z*)-**8** and (*Z*)-**9** is diminished.

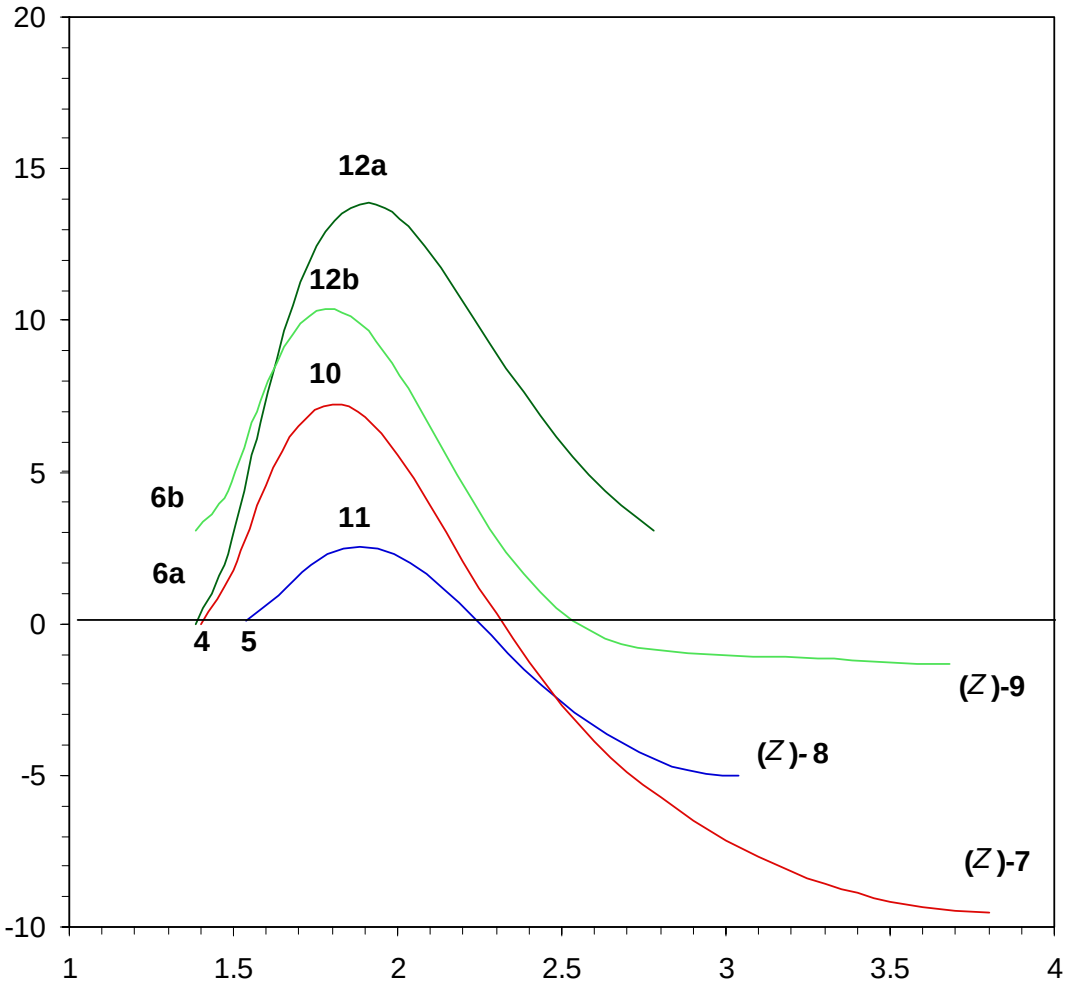

Figure 1.5. The ring-opening reactions of ions **4** - **6** are exothermic and kinetically facile. The MP2(full)/6-31G** energy profiles are shown relative to the energy of the most stable cyclic ion and as a function of the C2–N3 distance starting at the value of the cyclic ion and ending at the value of the respective (*Z*)-configured ion.

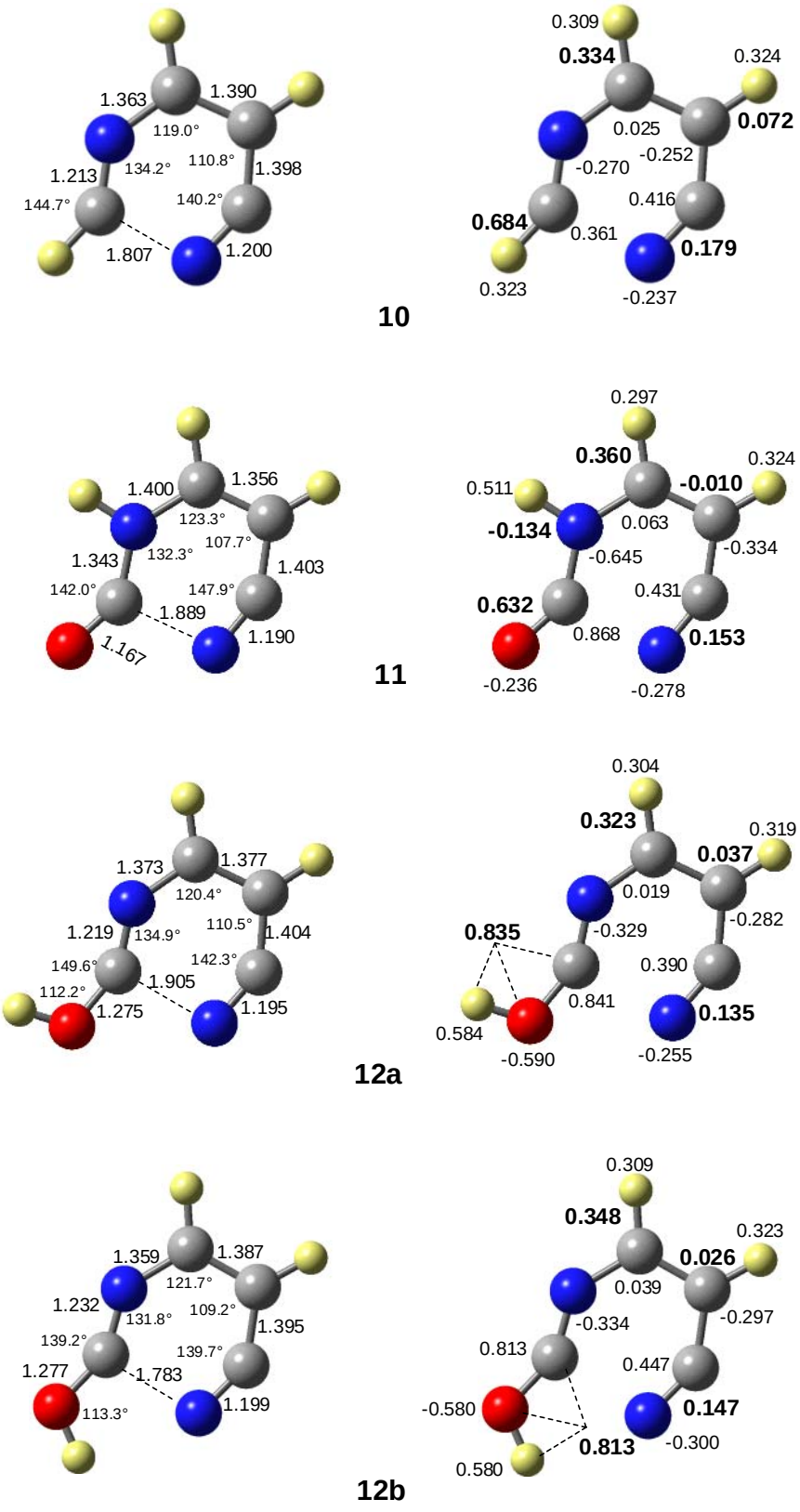

Figure 1.6. Transition state structures **10 – 12** for the ring-openings of ions **4** - **6**.

The intrinsic reaction paths and the transition state structures between the heterocyclic and the acyclic (*Z*)-cations are shown in Figures 5 and 6. In the context of deamination chemistry, the activation barriers for the ring-openings are most pertinent and these are listed in Table 1.1. There are two path to (*Z*)-**9** starting from **6a** and **6b** and the less stable isomer **6b** features the lower barrier to ring-opening. The interconversion between **6a** and **6b** involves rotation via transition state structure **6d** with a barrier of less than 10 kcal/mol (rather than O-inversion via **6c**, a second-order saddle point structure). There is very little hindrance to pyrimidine ring-opening in all cases! At the level of optimization the free energies of activation are 5.4 (**4** → **10**), 1.2 (**5** → **11**), 11.0 (**6a** → **12a**) and 5.5 (**6b** → **12b**) kcal/mol, respectively. The QCISD(T) data give slightly higher barriers and the effect of solvation on the activation barrier to ring-opening is small and the free energies become are 6.2 (**4** → **10**), 2.5 (**5** → **11**), 10.8 (**6a** → **12a**) and 10.6 (**6b** → **12b**) kcal/mol, respectively. Hence, the electronic structures of the transition state structures ressemble the heterocyclic ions and major electronic relaxations occur only *after* the CN bond has been elongated beyond its distance in the transition state structure.

The (*E*)-isomers of alkanes **7 – 9** allow for the least direct steric interactions between the vicinal functional groups and their energies provide the level of reference in Scheme 1.4. All (*E*)-preference energies are *negative* and the (*Z*)-isomers are preferred. The (*E*)-preference energy for **7** is ΔG_{298} = -2.0 kcal/mol at all the levels used and the values for **8** and **9** are markedly more negative (Table 1.1). This preference can be understood because the (*Z*)-isomers allow for through-space electrostatic attraction between the cyano group and the positively charged 3-substituent. It is less obvious why the *EPE* data vary for the free ions as they do and, in particular, as to why (*E*)-**8** would be

preferred in solution. In any case, Scheme 1.4 illustrates that the heterocycles all are significantly less stable than either one of the acyclic alternatives.

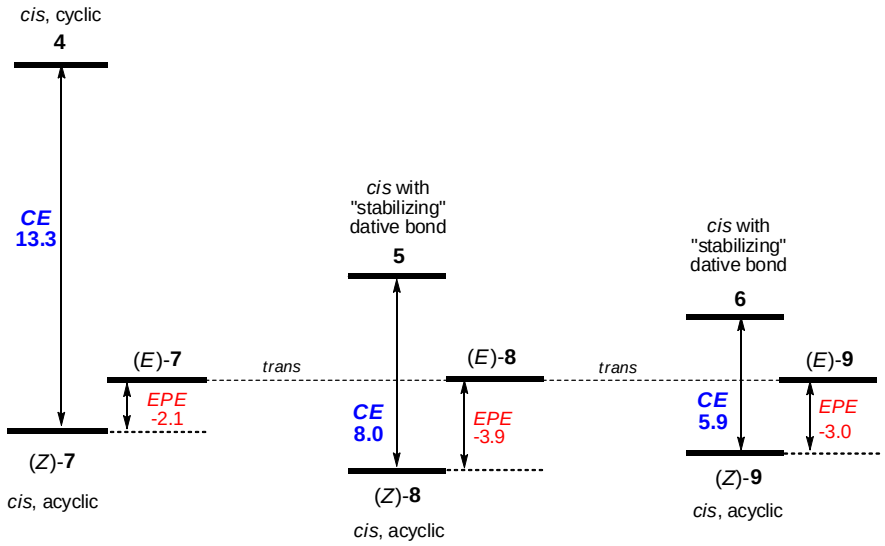

Scheme 1.4. Schematic illustrations of the situations in **4** - **6** drawn to vertical scale using the MP2(full)/6-31G** Gibbs free energies.

Cyclization and Electronic Relaxation. Natural charges of **7** - **9** are given in Figures 3 and 4 and selected fragment charges are summarized in Table 1.2 to conceptualize the bonding in ions **4** - **6**. The fragment charges are given of the heterocyclic system and of the (Z)- and (*E*)-isomers are given in the first three data columns, and their differences are given in last three data columns. These data are given from top to bottom for the acceptors, the CN donors, and their sum. The charge changes in the last set are less than 0.1 and justifies the consideration of the donor-acceptor bond formation as a local event.

Table 1.2. Charge Relaxation in Acrylonitriles NC–CH=CH–X^+.

Group	Mols.	Natural Charge			Change of Natural Charge		
		Cyclic	*Z*-acyc.	*E*-acyc.	Cyclic *vs.* *Z*-acyc.	Cyclic *vs.* *E*-acyc.	*Z*-acyc. *vs.* *E*-acyc.
X^+	**4**, **7**	0.258	0.594	0.587	-0.336	-0.329	-0.007
	5, **8**	0.288	0.648	0.631	-0.360	-0.343	-0.017
	6, **9**	0.269	0.619	0.608	-0.350	-0.339	-0.011
CN	**4**, **7**	0.299	0.039	0.069	0.260	0.230	0.030
	5, **8**	0.317	-0.009	0.034	0.326	0.283	0.043
	6, **9**	0.277	-0.002	0.029	0.279	0.306	0.031
X^+ + CN	**4**, **7**	0.557	0.633	0.621	-0.076	-0.065	-0.012
	5, **8**	0.605	0.639	0.665	-0.034	-0.060	0.026
	6, **9**	0.546	0.617	0.637	-0.071	-0.091	0.020

Table 1.2 shows nicely that the differences between the acyclic isomers are minor (< 0.05) and the discussion can focus on the charge relaxation associated with the cyclization of the (*Z*)-acyclic ions. In support of the dative bond hypothesis it is found: Cyclization leads to a significant charge transfer from the nitrile group to the acceptor group in every case. The CN groups are hardly charged (< 0.1) in the acrylonitriles *in spite of* the proximate cationic center. The (+)-charge in **8** and **9** is mostly localized on the X groups (HNCO in **8**; NCOH in **9**) and the (*Z*)-structures benefit—much more than the (*E*)-structures—from charge-induced polarization of the nitrile group. These data support the idea that this through-space interaction is responsible for the (*Z*)-preferences of **7** - **9**. In the heterocycles **4** - **6**, on the other hand, the CN groups are rather positive (0.28 - 0.34) and highly polarized—as in $H_3C–C{\equiv}N{\rightarrow}^+CH_3$—and the charges of the acceptor groups are decreased by 0.19 to 0.36.

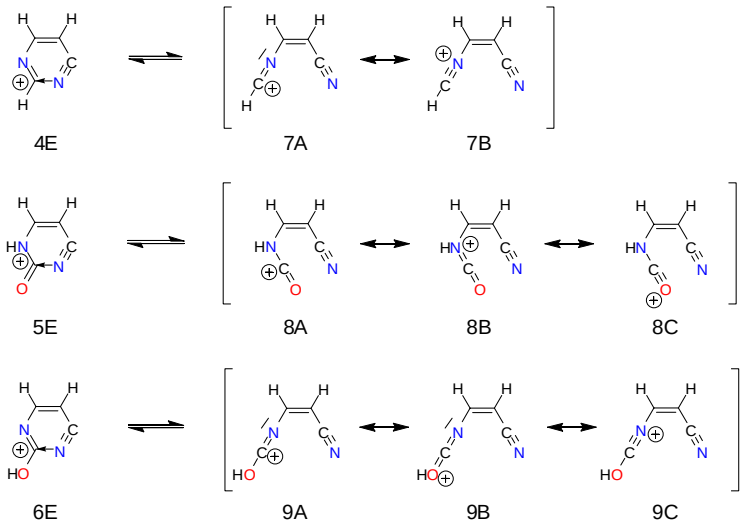

Scheme 1.5. Stabilization mechanisms in acyclic ions **7** - **9** *vs*. dative bond formation and cyclization.

In **8A** and **9A**, the formal (+)-charge is assigned to the C2 atom that engages in dative bond formation upon cyclization (Scheme 1.5). These C atoms are in fact highly charged in **8** and **9** and their charges are reduced only slightly upon cyclization (Figures 2 and 3). Yet, the bonding situations of C2 in **8** or **9**, respectively, greatly differ from those in **5** or **6**. In **8** and **9**, the charge is associated with a {- + -}-quadrupolar cumulene:[48] C2 is sp-hybridized, the CO and CN bonds are very short, and the heteroatoms are *negatively* charged. **8B**,**C** and **9B**,**C** are useful in that they indicate the cumulene π-systems (**B**) and the triple bond character of one of the C–Het bonds (**C**). To benefit from the high positive C-charge, electron density does not need to be transferred to that electron-deficient center and it suffices to move electron density closer.[31a,b] As ring formation progresses from **8** (**9**) to **4** (**6**), C2 changes hybridization, the CN bond lengthens by 0.122 (0.155) Å, the CO bond lengthens by 0.031 (0.037) Å, and the negative charges on the

heteroatoms increase,[49] and thus *ring formation comes at a cost.* For dative bonding to occur, the stabilization mechanisms of the electron-deficient carbons in **8** and **9** (cumulene π-system, CX triple bond) have to be reduced or cancelled.

One might be inclined to assume that cation affinities of neutral nucleophiles are positive. Yet, this clearly is not generally true. The addition of a neutral Lewis base to a cationic Lewis acid may become endothermic if the cation benefits from effective internal stabilization and Lewis Acid-Lewis Base adduct formation would disrupt this mode of stabilization. We recently showed that phenyl→CH_2 π-dative bonding in benzyl cation is more effective than N≡N→C σ-dative bond formation and a classical "benzyldiazonium ion" does not exist.[32,50] The present cases are examples of borderline cases where dative bond formation still can occur—the ring structures are minima—even though the processes are endothermic.

Implications for Nitrosative Cytosine and Cytidine Deamination. The theoretical studies of **1** - **3** show that the dediazoniation of 4-aminopyrimidinediazonium ion and of both tautomers of cytosinediazonium ion are facile, in gas phase and in aqueous solution, and any nucleophilic substitution would be S_N1-like.[51] The results show further that ions **4** - **6** will undergo ring-opening to the thermodynamically favored acyclic cations and, moreover, that the kinetic barriers to ring-opening are easily crossed even at low temperatures. Hence, in reactions that form any of the ions **4** - **6**, the ring-opened ions (*Z*)-**7** – (*Z*)-**9** must be considered as viable reactive intermediates. This result requires a paradigm shift in that any mechanistic explanation of the products of nitrosative cytosine deamination has to explain why the ring might *not* open—rather than explaining why it might open—and the present study seriously puts in question whether uracil is the only product.

If the R-group is ribose, amide-iminol tautomerization is no longer possible, and **5** and its acyclic (*Z*)- and (*E*)-isomers **8** are the appropriate models for the deamination of cytidine, its nucleotides CMP, CDP, and CTP, and their 2'-deoxy derivatives (Scheme 7). The ubiquitous nucleophile water might react with **8** by substitution or addition. Substitution would lead to deglycation and (*Z*)-3-isocyanatoacrylonitrile. Unsaturated isocyanates[52] are toxic[53] and 3-isocyanatoacrylonitrile can form adducts and cross-links.[54,55] Alternatively, **8** can form (*Z*)-3-aminoacrylonitrile by diffusion controlled carbamic acid formation[56] and subsequent decarboxylation.[57] The push-pull (*Z*)-3-aminoacrylonitrile is susceptible to base-[58,59] and acid-catalyzed[60] nucleophilic addition to the C=C and C≡N bonds and this chemistry also might lead to DNA adducts. Decarbonylation of (*Z*)-**8** has been observed in the gas phase[42-44] and we computed the decarbonylation and subsequent deprotonation of (*Z*)-**8** (Table 1.1). As can be seen, the decarbonylation requires significant activation in the gas phase (ΔG_{298} = 44.0 kcal/mol) and in aqueous solution (ΔG_{298} = 37.5 kcal/mol) and this process is not likely to compete with diffusion-controlled hydrolysis.

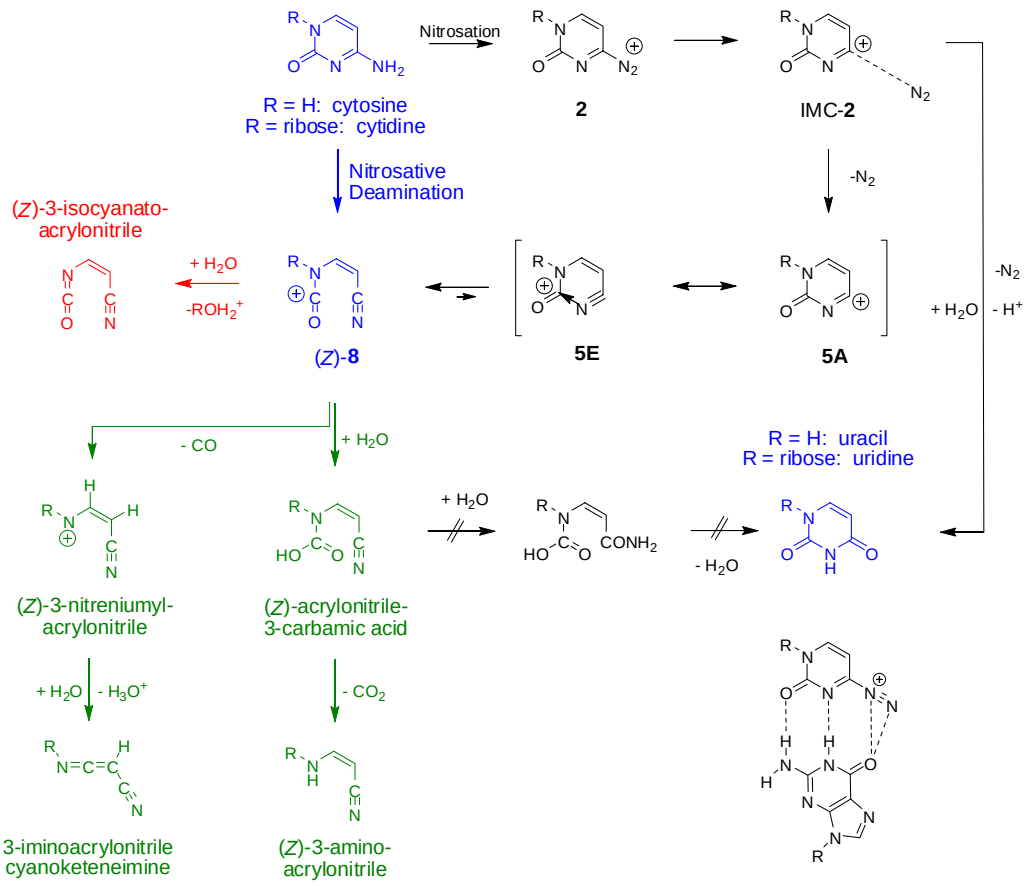

Scheme 1.6. Mechanism for the nitrosative deamination of the DNA base cytosine, its nucleoside cytidine, its nucleotides CMP, CDP, and CTP, and their respective 2'-deoxy derivatives.

We have explored with experimentation and theoretical study whether (*Z*)-acrylonitrile-3-carbamic acid might recyclize and found such a path to be unlikely.[61] Consequently, at the present time it is an open question as to why uridine is formed in the nitrosative cytosine deamination. One possible answer might have to do with guanine catalysis of the cytosine deamination; hydrogen bonding in the guanine adducts of **2** and **3** might alter the mechanim of dediazoniation and this possibility is now being explored.

We have studied the cytosine catalysis of the guanine deamination and in that case the hydrogen-bonding state greatly affects the course of the reaction.

1.4 Conclusions

The present study shows that ions **4** - **6** have similar electronic properties, that none of them is heteroaromatic, and that these ions are neither phenyl cations nor azaryne cations. The study firmly establishes that **4** - **6** are cyclic nitrilium ions. Ions **4** - **6** and acetonitrile adducts Me–C≡N→E^+ share the same structural and electronic characteristics and, moreover, the similaries are compelling of the structural and electronic relaxations which are associated with dative bond formations between Me–C≡N and E^+ and the cyclizations of the (*Z*)-acrylonitriles **7** - **9**. Explanations have been provided for the (*Z*)-preferences of **7** - **9** and for their higher stability relative to the heterocycles **4** - **6**. The most important and significant result is the non-intuitive discovery that ions **4** - **6** undergo thermodynamically slightly favored and kinetically facile pyrimidine ring-opening.

There is a significant difference in the processes that led to the suggestion of pyrimidine ring-opening in the deaminations of guanine[62] as opposed to adenine[63] and cytosine. Dediazoniation of a free guaninediazonium ion is *accompanied* by ring-opening and *cannot* result in a cyclic phenyl cation-type intermediate. Moreover, experimental observations by Suzuki,[64] Dedon,[65] and Shuker[66] required ring-opening and the mechanisms are now well understood.[67,68,69] In contrast, to date no experiments were reported that required the consideration of the ring-opened ions **8** and **9**.

The discovery of the propensity of ions **5** and **6** for cycloreversion is the result of bonding analysis alone. While theory often is recruited to explain new and unexpected outcomes of experiments, here the theoretical results suggest new experiments to probe

the ring-openings of **5** and **6**, and the chemistries of **8** and **9**, respectively. The record on studies of nitrosative cytosine deamination is dominated by qualitative studies and lacking in a quantitative accounting of all cytosine. A complete understanding of cytidine deamination is necessary to appreciate its metabolic and toxicological consequences. It is likely that the observed product palette is incomplete and some of the unidentified reaction products might be deleterious and perhaps even more so than the known uridine formation.

1.5 References

(1) (a) Stoermer, R.; Kahlert, B. *Ber. Dtsch. Chem. Ges.* **1902**, *35,* 1633-1640. (b) Komppa, G.; Weckmann, S. *J. Prakt. Chem.* **1933**, *138,* 109-127.

(2) (a) Wittig, G.; Pieper, G.; Fuhrmann, G. *Ber. Dtsch. Chem. Ges.* **1940**, *73,* 1193-1197. (b) Wittig, G. *Angew. Chem.* **1957**, *69,* 245-251.

(3) Hoffman, R. W. *Dehydrobenzene and Cycloalkanes.* Academic Press: New York, 1967.

(4) (a) Chapman, O. L.; Mattes, K.; McIntosh, C. L.; Pacansky, J.; Calder, G. V.; Orr, G. *J. Am. Chem. Soc.* **1973**, *95,* 6134-6135. (b) Chapman, O. L.; Chang, C.-C.; Kolc, J.; Rosenquist, N. R.; Tomioka, H. *J. Am. Chem. Soc.* **1975**, *97,* 6586-6588. (c) Wentrup, C.; Blanch, R.; Briehl, H.; Gross, G. *J. Am. Chem. Soc.* **1988**, *110,* 1874-1880. (d) Dunkin, I. R.; MacDonald, J. G. *J. Chem. Soc. Chem. Commum.* **1979**, 722-723. (e) Nam, H.-H.; Leori, G. E. *J. Mol. Struct.* **1987**, *157,* 301-304. (f) Simon, J. G. G.; Munzel, N.; Schweig, A. *Chem. Phys. Letters* **1990**, *170*, 187-192. (g) Radziszewski, J. G.; Hess, B. A.; Zahradnik, Jr. R. *J. Am. Chem. Soc.* **1992**, *114,* 52-57. (h) Jiao, H.; Schleyer, P. v. R.; Beno, B. R.; Houk, K. N.; Warmuth, R. *Angew. Chem. Int. Ed. Engl.* **1997**, *36,* 2761-2764. (i) Warmuth, R. *Angew. Chem. Int. Ed. Engl.* **1997**, *36,* 1347-1350.

(5) (a) Kauffmann, T. *Angew. Chem.* **1965**, *77,* 557-571. (b) Kauffmann, T.; Wirthwein, R. *Angew. Chem. Int. Ed. Engl.* **1971**, *10,* 20-33.

(6) Hart, H. *Chemistry of Triple-Bonded Functional Groups* **1994**, *2*, 1017-1134.

(7) Pellissier, H.; Santelli, M. *Tetrahedron* **2003**, *59*, 701-730.

(8) Glaser, R.; Rayat, S.; Lewis, M.; Son, M.-S.; Meyer, S. *J. Am. Chem. Soc.* **1999**, *121,* 6108-6119.

(9) Wink, D. A.; Kasprzak, K. S.; Maragos, C. M.; Elespuru, R. K.; Misra, M.; Dunams, T. M.; Cebula, T. A.; Koch, W. H.; Andrews, A. W.; Allen, J. S.; Keefer, L. K. *Science* **1991**, *254,* 1001-1003.

(10) Caulfield, J. L.; Wishnok, J. S.; Tannenbaum, S. R. *J. Biol. Chem.* **1998**, *273,* 12689-12695.

(11) (a) Wyszynski, M.; Gabbara, S.; Bhagwat, A. S. *Proc. Natl. Acad. Sci. USA* **1994**, *91*, 1574-1578. (b) Yebra, M. J.; Bhagwat, A. S. *Biochem.* **1995**, *34*, 14752-14757. (c) Sharath, A. N.; Weinhold, E.; Bhagwat, A. S. *Biochem*. **2000**, *39*, 14611-14616.

(12) (a) Lindahl, T. *Proc. Natl. Acad. Sci. USA* **1974**, *71,* 3649-3653. (b) Tye, B. K.; Chien, J.; Lehman, I. R.; Duncan, B. K.; Warner, H. R. *Proc. Natl. Acad. Sci. USA* **1978**, *75,* 233-237. (c) Wallace, S. S. *Environ. Mol. Mutagen.* **1988**, *12*, 431-477.

(13) Schouten, K. A.; Weiss, B. *Mut. Res. DNA Repair* **1999**, *435*, 245-254.

(14) (a) Bridges, B. A. *Science* **1999**, *284*, 62-63. (b) Loeb, L. A.; Cheng, K. C. *Mutat. Res.* **1990**, *238,* 297-304. (c) Duncan, B. K.; Miller, J. H. *Nature* **1980**, *287,* 560-561.

(15) Suzuki, T.; Nakamura, T.; Yamada, M.; Ide, H.; Kanaori, K.; Tajima, K.; Morii, T.; Makino, K. *Biochemistry* **1999**, *38*, 7151-7158.

(16) (a) Hehre, W. J.; Random, L.; Schleyer, P. v. R.; Pople, J. A. *Ab Initio Molecular Orbital Theory;* John Wiley & Sons: New York, **1986**. (b) Cramer, C. J. *Essentials of Computational Chemistry: Theories and Models*; John Wiley & Sons: New York, **2002**.

(17) Gaussian 03, Revision C.02, Frisch, M. J. et al., Gaussian, Inc., Wallingford CT, 2004.

(18) Foresman, J. B.; Keith, T. A.; Wiberg, K. B.; Snoonian, J.; Frisch, M. J. *J. Phys. Chem.* **1996**, *100*, 16098-16104.

(19) (a) Glendening, E. D.; Reed, A. E.; Carpenter, J. E.; Weinhold, F. *NBO Version 3.1*. (b) Glendening, E. D.; Weinhold, F. *J. Comput. Chem.* **1998**, *19,* 628-646.

(20) Takagi, S.; Suzuki, T.; Imaeda, K. *Yakugaku Zasshi* **1951**, *71,* 82-84.

(21) Majumdar, P., Ph.D. Dissertation, University of Missouri-Columbia, 2007.

(22) Gao, J.; Garcia-Viloca, M.; Poulsen, T. D.; Mo, Y. *Adv. Phys. Org. Chem.* **2003**, *38*, 161-181.

(23) (a) Glaser, R.; Horan, C. J.; Lewis, M.; Zollinger, H. *J. Org. Chem.* **1999**, *64*, 902-913. (b) Glaser, R.; Horan, C. J.; Zollinger, H. *Angew. Chem.* **1997**, *109*, 2324-2328. *Angew. Chem. Int. Ed. Engl.* **1997**, *36*, 2210-2213.

(24) Wu, Z.; Glaser, R. *J. Am. Chem. Soc.* **2004**, *126*, 10632-10639.

(25) Wincel, H.; Fokkens, R. H.; Nibbering, N. M. M. *Int. J. Mass Spect. Ion Proc.* **1989**, *88*, 241-256.

(26) de Lijser, H. J. P.; Arnold, D. R. *J. Phys. Chem.* **1998**, *102*, 5592-5598.

(27) (a) HCN/HCN/SO_3: Fiacco, D. L.; Hunt, S. W.; Leopold, K. R. *J. Phys. Chem. A* **2000**, *104*, 8323-8328. (b) HCN/SO_3 and CH_3CN/SO_3: Burns, W. A.; Phillips, J. A.; Canagaratna, M.; Goodfriend, H.; Leopold, K. R. *J. Phys. Chem. A* **1999**, *103*, 7445-7453. (c) HCN/BF_3: Reeve, S. W.; Burns, W. A.; Lovas, F. J.; Suenram, R. D.; Leopold, K. R. *J. Phys. Chem.* **1993**, *97*, 10630-10637.

(28) Scott, F. A.; Butler, R. N. *Azacarbonium Ions*, Chapter 30 in *Carbonium Ions*, Vol. 4, Olah, G. A., Schleyer, P. v. R., Eds. Wiley Interscience: New York, 1973, 1643.

(29) Lias, S. G.; Liebman, J. F.; Levin, R. D. *J. Phys. Chem. Ref. Data* **1984**, *13*, 695-808.

(30) Glukhovtsev, M. N.; Szulejko, J. E.; McMahon, T. B.; Gauld, J. W.; Scott, A. P.; Smith, B. J.; Pross, A.; Radom, L. *J. Chem. Phys.* **1994**, *98*, 13099-13101.

(31) (a) Glaser, R.; Horan, C. J. *J. Org. Chem.* **1995**, *60*, 7518-7528. (b) Horan, C. J.; Glaser, R. *J. Phys. Chem.* **1994**, *98*, 3989-3992. (c) Glaser, R.; Choy, G. S.-C. *J. Am. Chem. Soc*. **1993**, *115*, 2340-2347. (d) Glaser, R.; Choy, G. S.-C.; Horan, C. J. *J. Org. Chem.* **1992**, *57*, 995-999. (e) Glaser, R.; Choy, G. S.-C.; Hall, M. K. *J. Am. Chem. Soc.* **1991**, *113*, 1109-1120. (f) Glaser, R. *J. Comput. Chem*. **1990**, *11*, 663-679. (g) Glaser, R. *J. Phys. Chem.* **1989**, *93*, 7993-8003. (h) Glaser, R. *J. Am. Chem. Soc.* **1987**, *109*, 4237-4243.

(32) Glaser, R.; Farmer, D. *Chem. Eur. J.* **1997**, *3*, 1244-1253.

(33) (a) Glaser, R.; Horan, C. J.; Haney, P. E. *J. Phys. Chem.* **1993**, *97*, 1835-1844. (b) Glaser, R.; Horan, C. L.; Choy, G. S.-C.; Harris, B. L. *J. Phys. Chem.* **1992**, *96*, 3689-3697.

(34) (a) Glaser, R.; Horan, C. J. *Can. J. Chem.* **1996**, *74*, 1200-1214. (b) Horan, C. L.; Barnes, C. L.; Glaser, R. *Chem. Ber*. **1993**, *126*, 243-249. (c) Glaser, R.; Mummert, C. L.; Horan, C. J.; Barnes, C. L. *J. Phys. Org. Chem.* **1993**, *6*, 201-214. (d) Horan, C. J.; Haney, P. E.; Barnes, C. L.; Glaser, R. *Acta Cryst.* **1993**, *C49*, 1525-1528. (e) Horan, C. J.; Barnes, C. L.; Glaser, R. *Acta Cryst.* **1993**, *C49*, 507-

509. (f) Glaser, R.; Horan, C.; Nelson, E.; Hall, M. K. Incipient Nucleophilic *J. Org. Chem.* **1992**, *57*, 215-228.

(35) Chen, G. S.; Glaser, R.; Barnes, C. L. *Chem. Commun*. **1993**, 1530-1532. (b) Glaser, R.; Chen, G. S.; Barnes, C. L. *Angew. Chem. Int. Ed. Engl.* **1992**, *31*, 740-743.

(36) (a) Carvalho, M.; Gozzo, F. C.; Mendes, M. A.; Sparrapan, R.; Kascheres, C.; Eberlin, M. N. *Chem. Eur. J.* **1998**, *4*, 1161-1168. (b) Gozzo, F. C.; Eberlin, M. N. *J. Org. Chem.* **1999**, *64*, 2188-2193. (c) Sparrapan, R.; Mendes, M. A.; Carvalho, M.; Eberlin, M. N. *Chem. Eur. J.* **2000**, *6*, 321-326.

(37) (a) Bader, R. F. W. *Can. J. Chem.* **1986**, *64,* 1036-1045. (b) Wiberg, K. B.; Schleyer, P. v. R.; Streitwieser, A. *Can. J. Chem.* **1996**, *74,* 892-900. (c) Glaser, R.; Horan, C.; Nelson, E.; Kirk Hall, M. K. *J. Org. Chem.* **1992**, *57*, 215-228.

(38) (a) Li, D.; Shi, F.; Guo, S.; Deng, Y. *Tetrahedron Lett.* **2005**, *46*, 671-674. (b) De Luca, L.; Giacomelli, G.; Porcheddu, A. *J. Org. Chem.* **2002**, *67*, 6272-6274.

(39) (a) Penner, M.; Schweizer, F *Carbohydrate Res.* **2007**, *342*, 7-15. (b) Rosenberg, M. G.; Haslinger, U.; Brinker, U. H. *J. Org. Chem.* **2002**, 67, 450-6. (c) Van Emelen, K.; De Wit, T.; Hoornaert, G. J.; Compernolle, F. *Org. Lett.* **2000**, *2*, 3083-3086.

(40) Hitzler, M. G.; Lutz, M.; Shrestha-Dawadi, P. B.; Jochims, J. C. *Liebigs Ann.* **1996**, 247-257.

(41) Olah, G. A. *Angew. Chem. Int. Ed. Engl.* **1993**, *32,* 767-788.

(42) Bews, J. R.; Glidewell, C. *Theochem* **1983**, *91*, 353-371.

(43) Turecek, F.; Wolken, J. K.; Sadilek, M. *Eur. Mass Spectr*. **1998**, *4*, 321-332.

(44) Qian, M.; Wu, H.; Majumdar, P.; Yang, S.; Leigh, N.; Glaser, R. *J. Am. Soc. Mass Spect.*, accepted.

(45) Glaser, R.; Wu, H.; Saint-Paul, F. v. *J. Mol. Model.* **2006**, *12*, 731-737.

(46) Olah, G. A.; Germain, A., White, A. M. *Carbonium Ions,* Vol. 5, Olah, G. A.; Schleyer, P. v. R., Eds. Wiley Intercience: New York, 1976, p. 2049.

(47) Two planar structures **9'** and **9"** were located and they are transition state structures for enantiomerization. See Supporting Information.

(48) (a) Glaser, R.; Lewis, M.; Wu, Z. *J. Phys. Chem. A* **2002**, *106*, 7950-7957. (b) Lewis, M.; Wu, Z.; Glaser, R. *J. Phys. Chem. A* **2000**, *104*, 11355-11361.

(49) (a) Lewis, M.; Glaser, R. *J. Am. Chem. Soc.* **1998**, *120*, 8541-8542. (b) Lewis, M.; Glaser, R. *Chem. Eur. J.* **2002**, *8*, 1934-1944.

(50) Partial bonding between neutral donors and acceptors, see: (a) Leopold, K. R.; Canagaratna, M.; Phillips, J. A. *Acc. Chem. Res.* **1997**, *30*, 57-64. (b) *Partially Bonded Molecules and Their Transition to the Crystalline State*. Leopold, K. R., in *Advances in Molecular Structure Research,* Vol. 2, Hargittai, M.; Hargittai, I.; Eds. JAI Press: 1996, p. 103.

(51) Wu, Z.; Glaser, R. *J. Am. Chem. Soc.* **2004**, *126*, 10632-10639.

(52) Badawi, H. M.; Förner, W.; Al-Saadi, A. *J. Mol. Str. THEOCHEM* **2001**, *535*, 183-197.

(53) (a) Nakashima, K.; Takeshita, T.; Morimoto, K. *Env. Health and Prevent. Med.* **2002**, *7*, 1-6. (b) Karol, M. H.; Jin, R. *Chem. Res. Tox.* **1991**, *4*, 503-509.

(54) Schwetlick, K.; Noack, R.; Stebner, F. *J. Chem. Soc. Perkin Trans 2,* **1994**, 599-608.

(55) Tiger, R. P.; Levina, M. A.; Entelis, S. G.; Andreev, M. A. *Kinetics & Catalysis* **2002***, 43*, 662-666.

(56) Raspoet, G.; Nguyen, M. T.; McGarraghy, M.; Hegarty, A. F. *J. Org. Chem.* **1998**, *63*, 6867-6877.

(57) (a) Satchell, D. P. N.; Satchell, R. S. *Chem. Soc. Rev.* **1975**, *4,* 231-250. (b) Saunders, J. H.; Frisch, K. C. *Polyurethanes, Chemistry and Technology.* Interscience: New York, 1962.

(58) Yamamoto, T.; Hirasawa, S.; Muraoka, M. *Bull. Chem. Soc. Jpn.* **1985**, *58*, 771-772.

(59) (a) Alberola, A.; Antolin, L. F.; Gonzalez, A. M.; Laguna, M. A.; Pulido, F. J. *J. Heterocyclic Chem.* **1986***, 23*, 1035-1038. (b) Cocco, M. T.; Congiu, C.; Onnis, V. *J. Heterocyclic Chem.* **1995**, *32*, 1679-1682.

(60) Wu, H.; Glaser, R. *Chem. Res. Toxicol.* **2005**, *18*, 111-114.

(61) Rayat, S.; Qian, M.; Glaser, R. *Chem. Res. Toxicol.* **2005**, *18,* 1211-1218.

(62) Glaser, R.; Son, M.-S. *J. Am. Chem. Soc.* **1996**, *118,* 10942-10943.

(63) Hodgen, B.; Rayat, S.; Glaser, R. *Org. Lett.* **2003**, *5*, 4077-4080.

(64) (a) Suzuki, T.; Yamaoka, R.; Nishi, M.; Ide, H.; Makino, K. *J. Am. Chem. Soc.* **1996**, *118*, 2515-2516. (b) Suzuki, T.; Kanaori, K.; Tajima, K.; Makino, K. *Nucleic Acids Symp. Ser.* **1997**, *37*, 313-314. (c) Suzuki, T.; Yamada, M.; Kanaori, K.; Tajima, K.; Makino, K. *Nucleic Acids Symp. Ser.* **1998**, *39*, 177-178. (d) Suzuki, T.; Ide, H.; Yamada, M.; Endo, N.; Kanaori, K.; Tajima, K.; Morii, T.; Makino, K. *Nucleic Acids Research* **2000**, *28*, 544-551.

(65) Dong, M.; Wang, C.; Deen, W. M.; Dedon, P. C. *Chem. Res. Toxicol.* **2003***, 16,*

1044-1055.

(66) (a) Lucas, L. T.; Gatehouse, D.; Shuker, D. E. G. *J. Biol. Chem.* **1999**, *274*, 18319-18326. (b) Lucas, L. T.; Gatehouse, D.; Jones, G. D. D.; Shuker, D. E. G. *Chem. Res. Toxicol*. **2001**, *14*, 158-164.

(67) (a) Rayat, S.; Majumdar, P.; Tipton, P.; Glaser, R. *J. Am. Chem. Soc.* **2004**, *126*, 9960-9968. (b) Rayat, S.; Wu, Z.; Glaser, R. *Chem. Res. Toxicol.* **2004**, *17*, 1157-1169. (c) Rayat, S.; Glaser, R. *J. Org. Chem.* **2003**, *68*, 9882-9892.

(68) (a) Qian, M.; Glaser, R. *J. Am. Chem. Soc.* **2004**, *126*, 2274-2275. (b) Qian, M.; Glaser, R. *J. Am. Chem. Soc.* **2005**, *127*, 880-887.

(69) (a) Glaser, R.; Wu, H.; Lewis, M. *J. Am. Chem. Soc.* **2005**, *127*, 7346-7358. **2005**. (b) Glaser, R.; Lewis, M. *Org. Lett.* **1999**, *1*, 273-276.

CHAPTER 2. Ammonia Elimination from Protonated Nucleobases and Related Synthetic Substrates

2.1 Introduction

Nitric oxide (NO) and nitrous acid (HNO_2) cause DNA base deamination and interstrand cross-link formation [1, 2]. This chemistry has been studied extensively because of the dietary and environmental exposure of humans to these substances [3, 4, 5]. Toxicological studies of deamination became more significant when it was recognized that endogenous nitric oxide [6, 7] causes nitrosation [8, 9] and that this process is accelerated by chronic inflammatory diseases [10, 11]. It has been known for a long time that deamination of adenine **1**, guanine **2**, and cytosine **3** (Scheme 2.1) results in the formation of hypoxanthine, xanthine, and uracil, respectively, and these products are thought to result from DNA base diazonium ions **4** – **6**, respectively, by direct nucleophilic dediazoniation. The discovery of oxanine formation [12, 13, 14] in the nitrosative deamination of guanine challenged the generality and completeness of this mechanism. Our theoretical studies revealed that unimolecular dediazoniation of guaninediazonium ion **5** is accompanied or immediately followed by pyrimidine ring-opening [15, 16] and that cytosine promotes the process by deprotonation [17, 18]. The resulting 5-cyanoimino-4-oxomethylene-4,5-dihydroimidazole is a highly reactive intermediate and undergoes acid-catalyzed 1,4-addition via the cyano-*N* or imino-*N* protonated 5-cyanoimino-4-oxomethylene-4,5-dihydroimidazoles, **9** and **10**, respectively [19]. Labeling studies support this reaction mechanism for oxanine formation [20].

Moreover, we synthesized 5-cyanoamino-4-imidazolecarboxamide and studied its cyclization [21] and cross-link formation chemistry [22]. The unimolecular dediazoniation of the diazonium ions of adenine and cytosine can proceed without ring-opening but the cations **7** and **11** formed in this way are predicted to undergo facile ring-opening [23] to ions **8** and **12**, respectively (Scheme 2.1).

We reported the results of ab initio studies (MP2/6-31G*) on the electronic structures of ions **9** and **10** and of their common conjugate base and solvent effects were considered by way of a continuum model [19]. The characteristic features of the ions persist in solution, but solvation does have a marked consequence on the site of and the propensity for protonation. While cyano-*N* protonation is preferred in gas phase, imino-*N* protonation is preferred in polar condensed phase. While protonation is fast and exergonic in the gas phase, it is endergonic in polar condensed phase. It is an immediate consequence of this computational result that the direct observation of cations **9** and **10** is possible only in the gas phase.

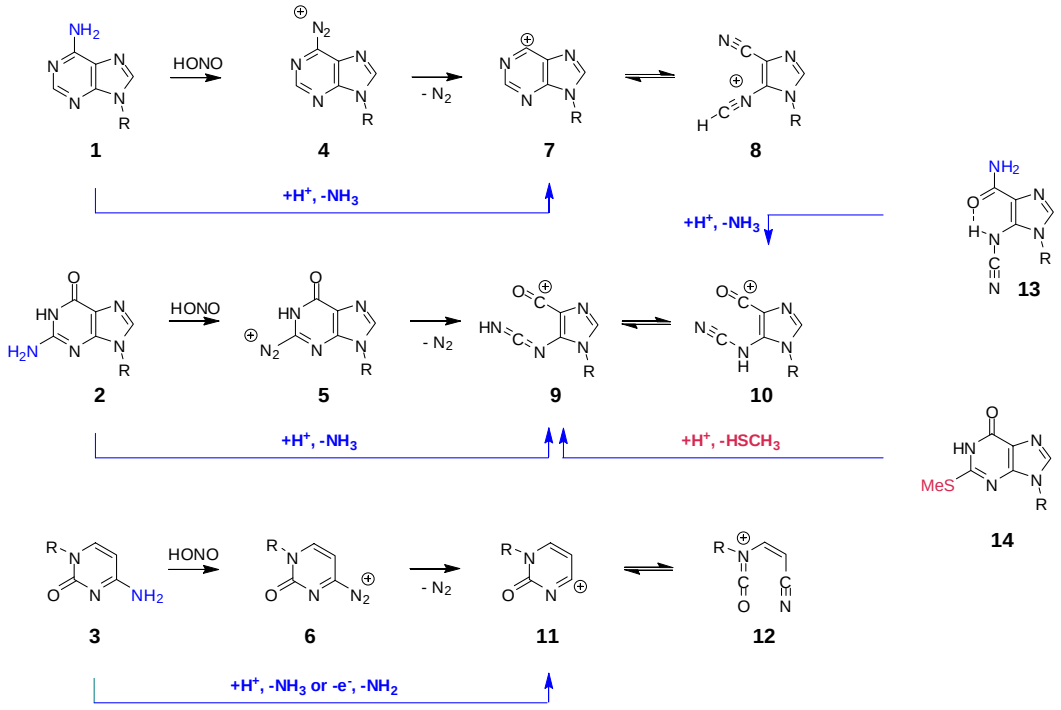

Scheme 2.1. Nucleoside and nucleobase deamination by nitrosation and by proton-catalyzed ammonia elimination.

In this context, it has been our aim to provide experimental evidence (a) for the existence of these ions **8** - **10** and **12** and (b) for their formation by dediazoniation of the diazonium ions of the nucleobases **1h**, **2h** and **3h**. With the present study we address the first of these goals. The impetus for this study was provided by the realization that the ions produced by dediazoniation of the putative nucleobase diazonium ions can be prepared in the gas phase via a sequence of protonation and ammonia elimination (Scheme 2.1). Hence, we have studied NH_3 elimination form the conjugate acids of the nucleobases **1h** - **3h** and the models **13h** and **14h**. We report the results of a gas phase study of deamination of the protonated nucleosides adenosine **1r** (**1**, R = ribose), guanosine **2r** (**2**, R = ribose) and deoxycytidine **3d** (**3**, R = deoxyribose). The study of the nucleosides is equivalent to the study of the nucleobases **1h** - **3h** themselves because

of the deglycation in the ESI experiments (vide infra) and the study of the nucleosides is advantageous because of their solubility. We also examined the potential formations of **9** and/or **10** from precursors **13e** (ether R = $CH_2OCH_2CH_2OH$), 1-[(2-hydroxy-ethoxy)methyl]-5-cyanoamino-imidazole-4-carboxamide, and **14e**, 9-[(2-hydroxyethoxy)-methyl]-2-(methylthio)hypoxanthine. The proton affinities of N-, O-, and S-sites were computed for aniline, for the nucleobases 9*H*-adenine, 1*H*,9*H*-guanine, and 1*H*-cytosine, for the (*Z*,*Z*)- and (*E*,*Z*)-rotamers of cyanoamine **13h**\ and for the (*Z*)- and (*E*)-rotamers of 2-thiomethyl-(1*H*,9*H*)-guanine **14h** (Scheme 2.2) to begin the discussion of the gas-phase ion chemistry and several relevant reaction paths also have been computed. The MS analyses in conjunction with the computational assessment of pertinent gas-phase reactions provide compelling evidence for pyrimidine ring-opened species.

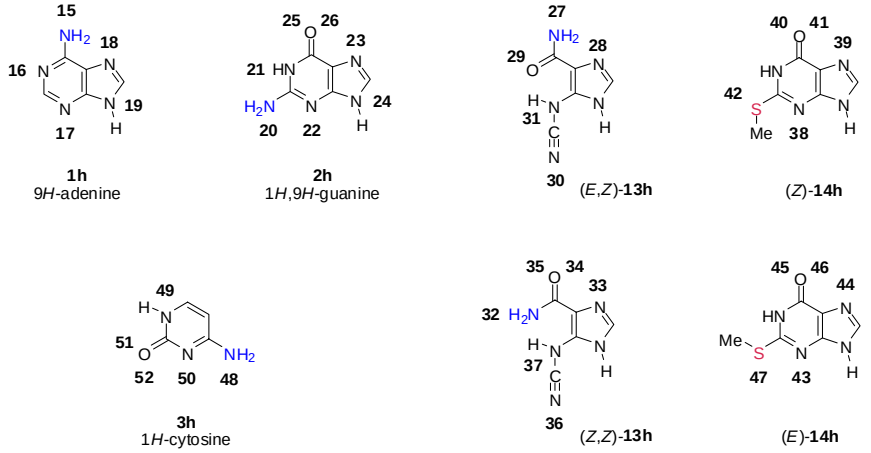

Scheme 2.2. Conjugate acids resulting from protonation of **1h**, **2h**, **3h**, **13h** and **14h** are numbered according to the protonation sites indicated.

2.2 Experimental and Computational Section

Mass analyses were performed on a Thermo Finnigan TSQ7000 triple-quadrupole mass spectrometer equipped with an AP12 source and Performance Pack. For all experiments, the heated capillary was maintained at 250 °C and the electrospray voltage was 4.5 kV. Voltages for in-source collision-induced dissociation and collision-induced dissociation [24] (CID) in the collision cell were optimized for each sample (Table 2.1). Other instrument parameters were optimized as part of biweekly maintenance and tuning. LC experiments employed a system that included a P4000 pump, AS3000 auto-sampler and UV6000 photodiode array detector.

Table 2.1. Voltages for in-source and in-collision cell CID

Analyte	Voltage		Figure
	in-source CID	collision-cell CID	
Adenosine, **1r**		40	1a
Guanosine, **2r**		30	1b
Cytidine, **3d**		0	1c
[**1h** + H]$^+$, *m/z* 136	30	50	2a
[**8**]$^+$, *m/z* 119	30	35	2b
[**16**]$^+$, *m/z* 109	60	30	2c
[**2r** + H - 132]$^+$, *m/z* 152	20	50	4a
[**9**]$^+$, *m/z* 135	40	50	4b
[**25**]$^+$, *m/z* 110	50	50	4c
[**13r** + H]$^+$, *m/z* 226		20	7a
[**13h** + H]$^+$, *m/z* 152	30	5	7b
[**14r** + H]$^+$, *m/z* 257		35	7c
[**12h** + H]$^+$. *m/z* 112	30	50	10

For each of the three nucleosides, direct infusion MS experiments showed that the protonated nucleoside is the overwhelmingly dominant ion produced. In-source CID was used to promote deglycation of the nucleosides and to maximize the production of the

corresponding protonated nucleobases. Parent ion scans for the protonated nucleobases produced by in-source CID demonstrate that they arise only from the corresponding nucleosides.

The nucleobases were further fragmented using CID in the collision cell of the mass spectrometer to yield the spectra shown. The overall information derived from the MS/MS experiments is equivalent to an MS/MS/MS experiment for each nucleoside. In some cases, in-source CID was used to deglycosylate the nucleoside and also fragment the nucleobase, giving access to ions further along some of the major degradation pathways and allowing positive identification of the fragments along those pathways.

Adenosine, guanosine and deoxycytidine were purchased from Sigma and used without further purification. Samples were prepared by dissolving 1 mg nucleoside in 1 ml of 1% acetic acid solution. The preparations of the cyanoamine **13** and the thioether **14** have been described previously [21]. The LC-MS studies were performed with a Waters XTerra^{TM} analytical column (C18, 5 μm, 4.5×250 mm) using a solvent gradient (solvents A and B are 0.1% formic acid and acetonitrile, 1% B at 1 min, 10% B at 3 min, 40% B at 20 min, 1% B at 22 min) at a flow rate of 1.0 ml/min while monitoring at λ = 254 nm.

Table 2.2. Calculated proton affinities of aniline, the nucleobases cytosine, adenine, and guanine, the (*E*,*Z*)- and (*Z*,*Z*)-rotamers of cyanoamine **13h**, and the (*Z*)- and (*E*)-rotamers of thioether **14h**[a]

Protonation Site	Aniline	Cyt.	Ade.	Gua.	**13h** (*E*,*Z*)	**13h** (*Z*,*Z*)	**14h** (*Z*)	**14h** (*E*)
expt.	874[b]	976.4[c]	978.0[c]	981.4[c]				
NH_2	**879.9**	819.9	848.5	793.2	831.3	894.1		

N1	874.6[d]	**943.8**	813.6[d]				
N3	**955.4**	**937.5**	887.2			874.1	891.6
N7		909.9	**959.8**	876.2	**923.9**	**944.9**	**946.5**
N9		755.9	766.0				
C2–O, N1	921.6						
C2–O, N3	**956.9**						
C6–O, N1			900.7			895.9	890.2
C6–O, N7			**936.3**		914.4	927.7	925.1
C6–O, NH_2				868.0	872.2		
NCN, cyano				**924.5**	890.2		
NCN, amino				849.4	827.7		
S						760.7	

[a] Proton affinities (ΔH) in kJ/mol computed at B3LYP/6-31++G**. Data for guanine reported in ref. 37.

[b] Exp. value for aniline from refs. 41 and 42.

[c] Exp. values for nucleosides from ref. 39.

[d] These protonated systems are ring-opened structures; see supporting information.

The structures of the nucleobases and the models, of their conjugate acids, and of various intermediates and transition states along relevant reaction paths were determined with density functional theory (DFT) [25]. The hybrid method B3LYP was employed in conjunction with the 6-31++G** basis set, B3LYP/6-31++G**, and the calculations were performed with *Gaussian03* [26] on a 64-processer SGI Altix system. Structures were optimized and vibrational analysis was performed for each structure to confirm that the structure was in fact stationary, to confirm the character of the stationary structure, and to determine thermochemical data. Total energies E, vibrational zero-point energies $VZPE$, thermal energies TE, and entropies S are tabulated in Supporting Information and Cartesian coordinates of all optimized structures are provided there as well. These data allow for the determination of relative and reaction energies ΔE, enthalpies $\Delta H_0 = \Delta(E+VZPE)$ and $\Delta H_{298} = \Delta(E+TE)$, and free energies $\Delta G = \Delta(E+TE-298.15 \cdot S)$. Unless

otherwise noted, we report ΔH_{298} values in kJ/mol, and proton affinities are listed in Table 2.2.

2.3 Results and Discussion

Initial Expulsion of Nitrile or Ammonia

The mass spectra of the nucleobases have been studied using electron-impact ionization many years ago [27]. The EI study of adenine showed that the major fragmentation path involves successive loss of HCN molecules. Studies of labeled adenines [28, 29] demonstrated that the HCN eliminated first is the one that contained the N1 atom and the loss of the NH_2 group was *not* observed. For guanine, the initial expulsion of neutral cyanamide (H_2NCN) is the dominant fragmentation (from the pyrimidine's N1–C2–NH_2 fragment) and some NH_2 group elimination was observed as well. For cytosine [30], NH_2 elimination was observed and it is followed by loss of HCN. Initial decarbonylation of the molecular ion also was observed and the peaks at *m/z* 69, 68 and 67 were explained by retro Diels-Alder reactions eliminating first ·N=C=O, HNCO, or H and HNCO, respectively, and subsequent HCN loss. Alternatively, the *m/z* 95 peak might be due to **11h** (**11**, R = H) *and* **12h** and the peak *m/z* 68 could be explained as the result of elimination of HCN or HNC from **12h** and the formation of protonated isocyanatoethyne. Hence, the observation of *m/z* 68 might present a first indication for the possible existence of **12**.

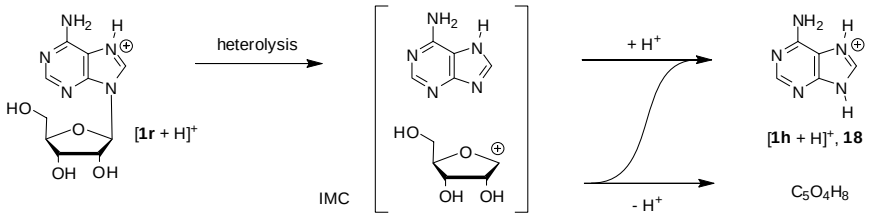

Scheme 2.3. Conversion of protonated nucleosides to protonated nucleobases.

ESI and Deglycation

Electrospray ionization (ESI) mass spectrometry of the nucleosides is employed in the diagnosis of purine and pyrimidine metabolic disorders [31]. Fryčák et al. reported in 2002 that the dominant fragmentations of the nucleoside molecular ions consist of the collision-induced dissociations of the glycosidic C–N bonds and leads to the replacement of the sugar moiety by a hydrogen atom, as had been suggested by McCloskey [32], and the process is shown in Scheme 2.3 for the conversion of adenosine **1r** (**1**, R = ribose) to adenine **1h** (**1**, R = H) [31]. The N7-protonation is shown as an example and the resulting positive ion forms an ion-molecule complex (IMC) by heterolysis of the glycosidic C–N bond and the intermittent neutral purine is protonated by the oxocarbenium sugar moiety. The spectra in Figure 2.1 demonstrate these deglycation reactions for **1r**, **2r**, and **3d**. McCloskey et al. studied the CID spectra of protonated adenine [33] and protonated guanine [34], and Tureček et al. [35] explored the dissociation mechanisms of protonated adenine in detail.

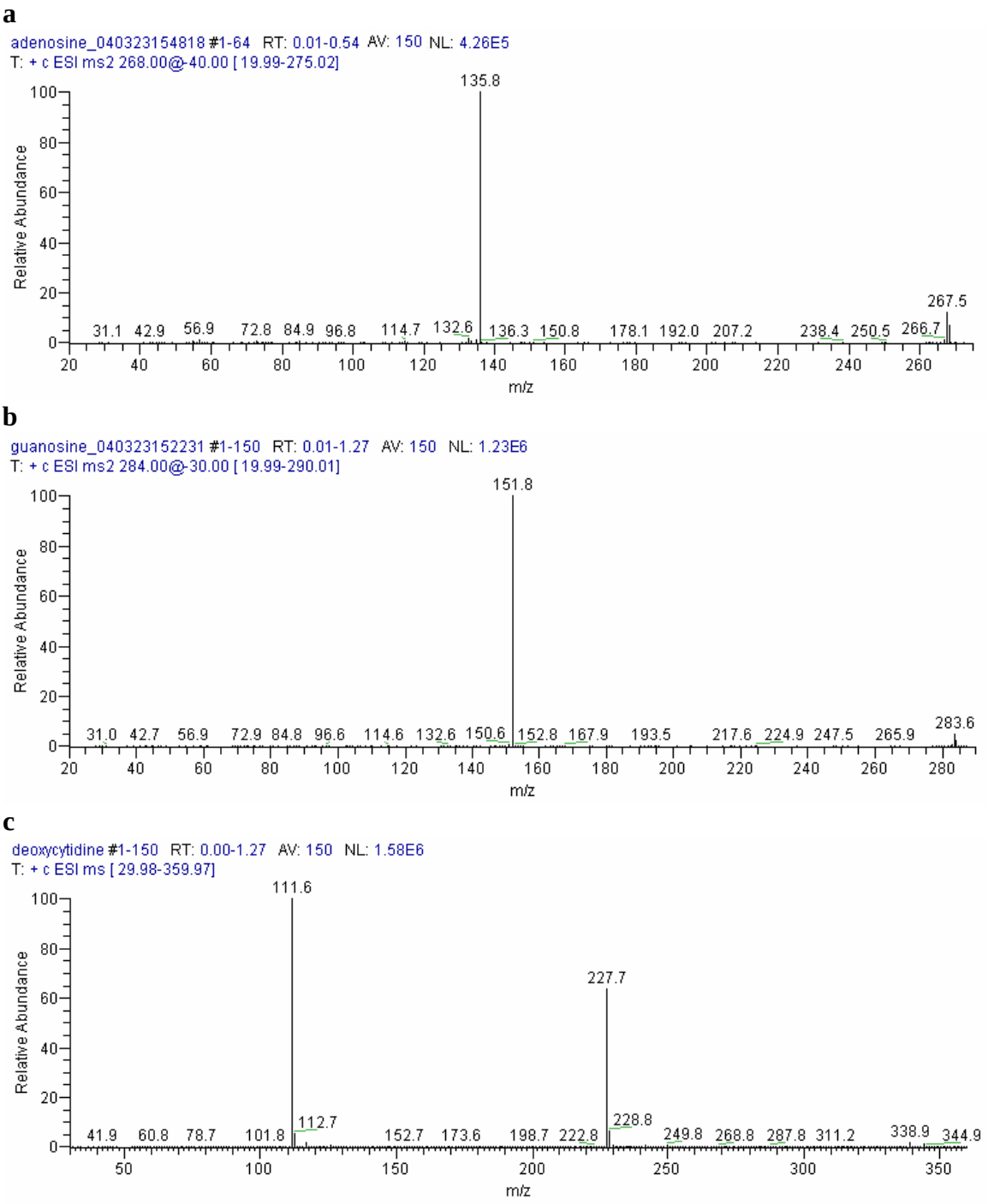

Figure 2.1. Product-ion spectra of (a) protonated adenosine [**1r** + H]$^+$, *m/z* 268, and (b) protonated guanosine [**2r** + H]$^+$, *m/z* 284. (c) The mass spectrum of deoxycytidine features [**3d** + H]$^+$, *m/z* 228, and [**3h** + H]$^+$, *m/z* 112.

Site of Protonation and Mode of Initial Fragmentation

The computed proton affinities (Table 2.2) show that the theoretical level employed presents an acceptable compromise between desired accuracy and computational demand [36]; the computed proton affinities are within five percent of the experimental values.

There is general agreement with earlier theoretical studies of the purine bases [35 - 39] and of cytosine [40]. The measured proton affinity of aniline is 874 kJ/mol (208.8 [41] and 209.5 kcal/mol [42]) and experimental [43] and theoretical [44] studies showed almost equal propensity for protonation at the amino-N- and the *para*-C-atoms. The proton affinities of the amino group of the nucleobases are lower than for aniline and, moreover, amino group protonation cannot compete with the alternatives (Table 2.2). Guanine prefers imidazole ring protonation with carbonyl-O protonation being a close second, adenine prefers pyrimidine ring protonations, and for cytosine the proton affinities for N3- and O-protonation are similar.

The amino group is *not* the best protonation site for the nucleobases or the model compunds, and have to discuss how the amino group can serve as the dissociative protonation site [45] or consider alternative mechanisms for ammonia elimination. Some guidance is provided by the emerging understanding of H_3N elimination from peptides [46]. The "mobile proton model" holds that intramolecular proton migration to various protonation sites can occur before fragmentation. The presence of basic amino acids might impede the proton mobility [47], and in such cases the actual mechanisms of ammonia elimination can be more complex [48, 49].

ESI-MS/MS of Adenosine

The mass spectrum of electrosprayed adenosine gave two peaks as shown in Figure 2.1: *m/z* 268 [**1r** + H]$^+$ is protonated adenosine and *m/z* 136 [**1h** + H]$^+$ results by cleavage of the glycosidic C–N bond. Mass selection for *m/z* 136 and application of CID results in the spectrum of Figure 2.2, the mechanisms of the fragmentation of the quasi-molecular ion *m/z* 136 are outlined in Scheme 2.4, and molecular models of relevant intermediates and transition state structures are shown in Figure 2.3.

a

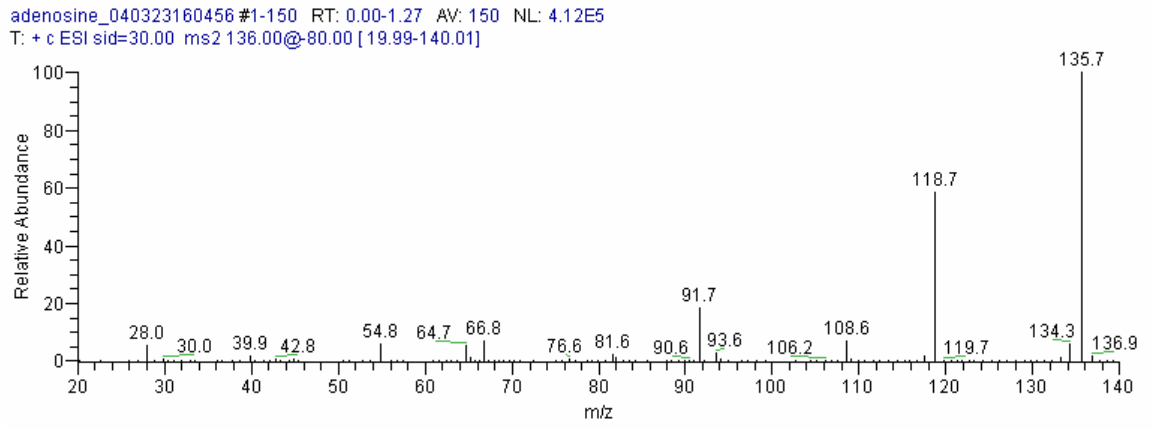

b

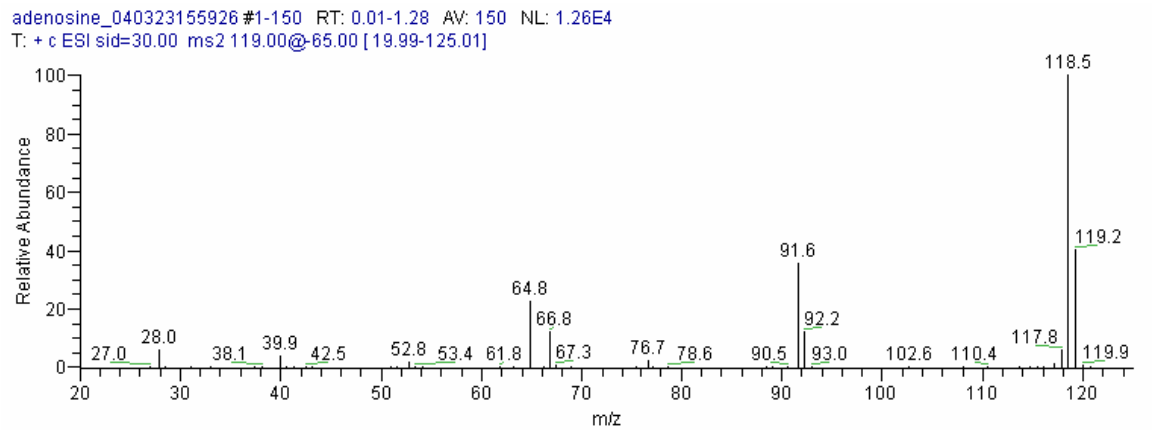

c

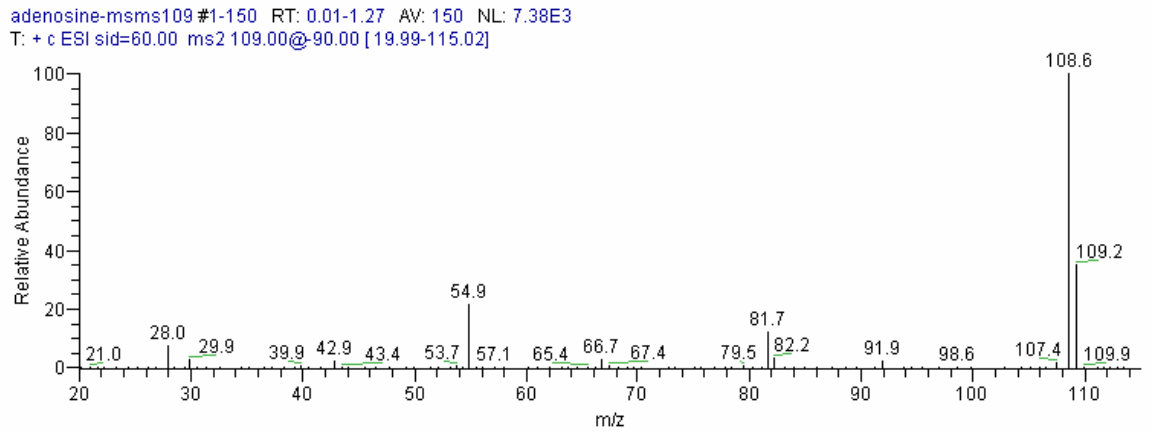

Figure 2.2. Product-ion spectra of (a) [**1h** + H]$^+$, *m/z* 136, (b) **8'**, *m/z* 119, and (c) **16**, *m/z* 109. All of these precursor ions were produced by in-source fragmentation of [**1r** + H]$^+$ at increasing energies.

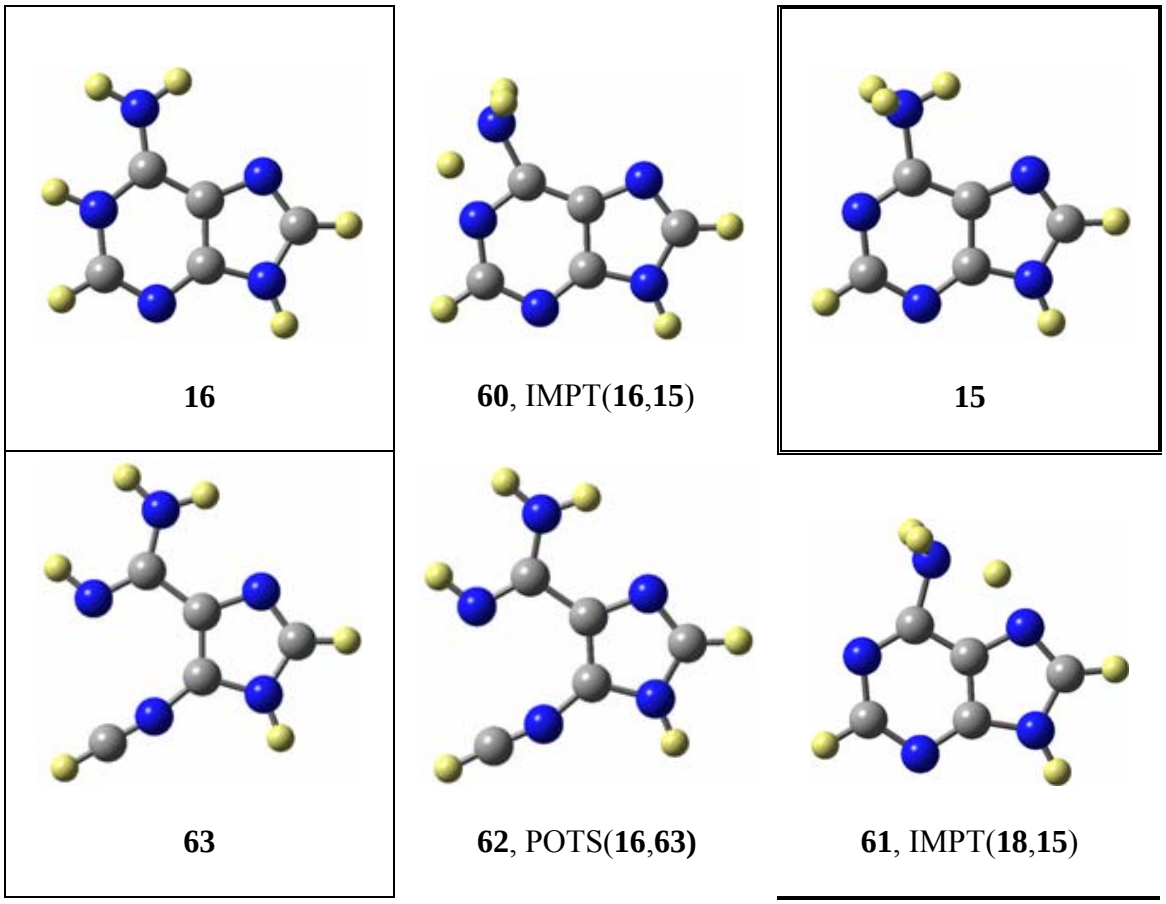

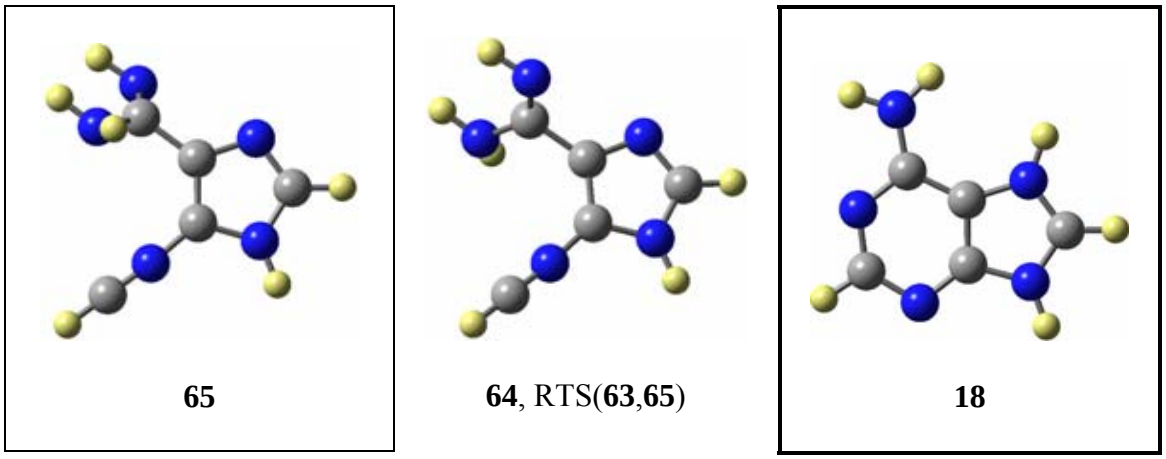

Figure 2.3. Intramolecular proton transfer allows for the conversions of N1- and N7-protonated tautomer **16** and **18** to the ammonium tautomer **15** (double-outlined). Pyrimidine ring-opening of N1-protonated adenine may lead to amidines **63** and **65** but these paths are not competitive.

The minor pathways for fragmentation of ion [**1h** + H]$^+$ involve initial loss of HCN or NH_2CN and these are the fragmentations observed in EI-MS. The MS/MS analysis of ion **53** (Figure 2.2c) shows the formations of ions **54** (*m/z* 82) and **55** (*m/z* 55) by successive losses of three HCN and resulting in the formation of **56** (*m/z* 28), protonated HCN. Initial elimination of cyanoamine leads to **57** (*m/z* 94) and another HCN (or HNC) elimination cascade from **57** via **58** (*m/z* 58) to **59** (*m/z* 59).

Amino protonation is less likely than protonation at N1, N3, or N7 of adenine **1h** (Table 2.2) and ammonium ion **16** would have to be generated by proton transfer within [**1h** + H^+]. Proton transfers from **16** and **18** to **15** via transition state structures **60** and **61**, respectively, requires activation enthalpies of 189.9 and 162.4 kJ/mol, respectively.

Whether NH_3 elimination via **15** is observed depends on whether **16** is stable with regard to pyrimidine ring-opening and formation of **63** or **65**. One can envision the

formation of **8h** by direct NH_3 elimination from **63** (consider resonance form **63-B**) or via tautomer **67** by NH_3 elimination from **66** or **68** after internal proton transfer. All these options depend on the accessibility of **63** and **65**. Indeed, **63** and **65** are minima on the potential energy surface, **63** is preferred over **65** by ΔE = 60.4 kJ/mol, and the rotational barrier for the conversion of **63** to **65** via transition state structure **64** is ΔE = 60.7 kJ/mol. As soon as thermal energies are considered, this activation barrier vanishes, and **65** becomes the transition state structure for the rotational automerization of **63** with an activation enthalpy of ΔH_{298} = 59.6 kJ/mol.

Table 2.3. Calculated relative energies and activation barriers[a]

Parameter	ΔE	ΔH_0	ΔH_{298}	ΔG_{298}
E_{act}(**16** → **60**‡)	203.72	191.07	189.86	191.74
E_{act}(**17** → **61**‡)	175.40	164.26	162.42	164.50
E_{act}(**16** → **62**‡)	279.83	263.29	266.26	259.51
E_{rel}(**63** *vs.* **16**)	279.64	263.57	268.67	256.76
E_{act}(**63** → **64**‡)	60.67	59.54	57.24	48.90
E_{rel}(**63** *vs.* **65**)	60.42	59.75	59.55	58.97
E_{act}(**23** → **74**‡)	303.46	293.24	294.54	290.16
E_{rel}(**75** *vs.* **23**)	131.27	119.88	123.81	112.97
E_{act}(**75** → **76**‡)	32.02	30.85	29.43	32.15
E_{rel}(**77** *vs.* **75**)	7.96	7.62	7.41	7.96
E_{act}(**77** → **78**‡)	84.79	73.45	72.36	74.70
E_{rel}(**79** *vs.* **77**)	39.14	39.10	39.81	38.51
E_{act}(**23** → **80**‡)	268.54	251.04	251.29	249.31
E_{rel}(**81** *vs.* **23**)	22.18	20.63	21.30	20.04
E_{act}(**81** → **82**‡)	220.27	209.13	207.08	210.68
E_{rel}(**83** *vs.* **81**)	126.85	128.98	128.36	129.01
E_{act}(**81** → **84**‡)	235.28	224.23	222.30	225.54
E_{rel}(**85** *vs.* **81**)	156.34	157.43	157.39	156.49
E_{act}(**23** → **86**‡)	215.12	204.06	202.39	205.24
E_{rel}(**87** *vs.* **23**)	124.47	126.56	126.73	124.12

E_{rel}(**22** *vs*. **23**)	75.60	71.33	72.79	69.90
E_{rel}(**22** *vs*. **81**)	53.41	50.69	51.49	49.85
E_{act}(**22** → **88**‡)	243.33	232.11	230.19	233.57
E_{rel}(**89** *vs*. **22**)	167.90	167.90	168.32	166.18
E_{act}(**22** → **91**‡)	172.77	165.90	166.07	163.47
E_{rel}(**92** *vs*. **22**)	150.79	148.36	148.48	144.88
E_{act}(**22** → **90**‡)	195.97	185.88	183.28	187.95
E_{rel}(**20** *vs*. **22**)	91.37	137.22	94.05	96.01
E_{rel}(**21** *vs*. **23**)	152.19	142.68	146.45	136.28
E_{act}(**21** → **93**‡)	239.08	225.89	224.97	224.73
E_{rel}(**94** *vs*. **21**)	126.37	127.21	127.59	125.98
E_{rel}(**13h**, (*Z*,*Z*) *vs*. (*E*,*Z*))	60.55	60.42	60.42	60.07
E_{act}(**103** → **104**‡)	50.06	44.66	39.34	38.30
E_{rel}(**105** *vs*. **103**)	27.12	24.86	25.87	23.27
E_{act}(**105** → **106**‡)	183.54	170.68	170.27	170.58
E_{rel}(**107** *vs*. **105**)	38.57	38.91	39.49	37.68
E_{act}(**103** → **108**‡)	77.23	76.06	**74.72**	76.71
E_{rel}(**109** *vs*. **103**)	-0.92	-1.00	-0.88	-1.46
E_{act}(**109** → **110**‡)	54.20	43.14	42.22	43.87
E_{rel}(**111** *vs*. **109**)	1.84	1.38	1.92	0.51
E_{act}(**111** → **112**‡)	44.76	43.51	42.04	44.76
E_{rel}(**113** *vs*. **111**)	42.87	41.53	42.20	39.41
E_{act}(**113** → **114**‡)	71.75	60.44	58.89	62.88
E_{rel}(**107** *vs*. **113**)	21.91	21.86	22.12	22.49
E_{rel}(**118** *vs*. **107**)	29.82	29.90	29.40	30.67
E_{rel}(**118** *vs*. **103**)	95.51	93.67	94.76	91.63
E_{act}(**28** → **121**‡)	95.40	85.52	83.59	89.47
E_{rel}(**27** *vs*. **28**)	40.66	42.71	42.46	44.99
E_{act}(**33** → **122**‡)	57.68	47.25	45.16	50.24
E_{rel}(**123** *vs*. **33**)	41.50	42.68	41.71	45.00
E_{rel}(**28** vs. **103**)	46.28	47.16	48.41	43.21
E_{rel}(**33** vs. **103**)	57.84	60.22	61.02	58.11
E_{act}(**39** → **128**‡)	267.85	250.14	250.52	247.38
E_{rel}((*Z*)-**129** *vs*. **39**)	33.97	32.92	31.12	35.40

E_{act}((*Z*)-**129** → **130**‡)	15.22	15.14	13.13	17.96
E_{rel}((*E*)-**129** *vs*. (*Z*)-**129**)	-1.11	-1.24	-1.11	-1.74
E_{act}((*Z*)-**129** → **131**‡)	231.37	214.45	214.03	215.04
E_{rel}((*E*)-**132** *vs*. (*Z*)-**129**)	179.15	169.27	169.98	168.13
E_{act}((*E*)-**129** → **133**‡)	212.53	195.41	194.78	196.67
E_{rel}((*E*)-**134** *vs*. (*E*)-**129**)	171.44	161.69	162.19	159.80
E_{rel}((*Z*)-**134** *vs*. (*E*)-**134**)	15.04	14.37	14.70	12.75
E_{act}((*Z*)-**39** → **135**‡)	293.51	281.58	283.84	277.92
E_{rel}(**136** *vs*. (*Z*)-**39**)	122.22	109.32	114.22	99.48
E_{act}((*Z*)-**39** → **137**‡)				
E_{act}(**50**→ **138**‡)	241.60	227.99	227.07	228.31
E_{rel}(**48** *vs*. **50**)	141.80	141.38	142.09	139.41
E_{act}(**50**→ **139**‡)	364.07	349.34	352.02	343.21
E_{rel}(**140** *vs*. **50**)	230.92	226.65	227.32	224.54
E_{act}(**50**→ **141**‡)				
E_{rel}(**142** *vs*. **50**)				
E_{act}(**142** → **143**‡)				
E_{rel}(**144** *vs*. **142**)				

[a] All data in kJ/mol and determined at B3LYP/6-31++G**.

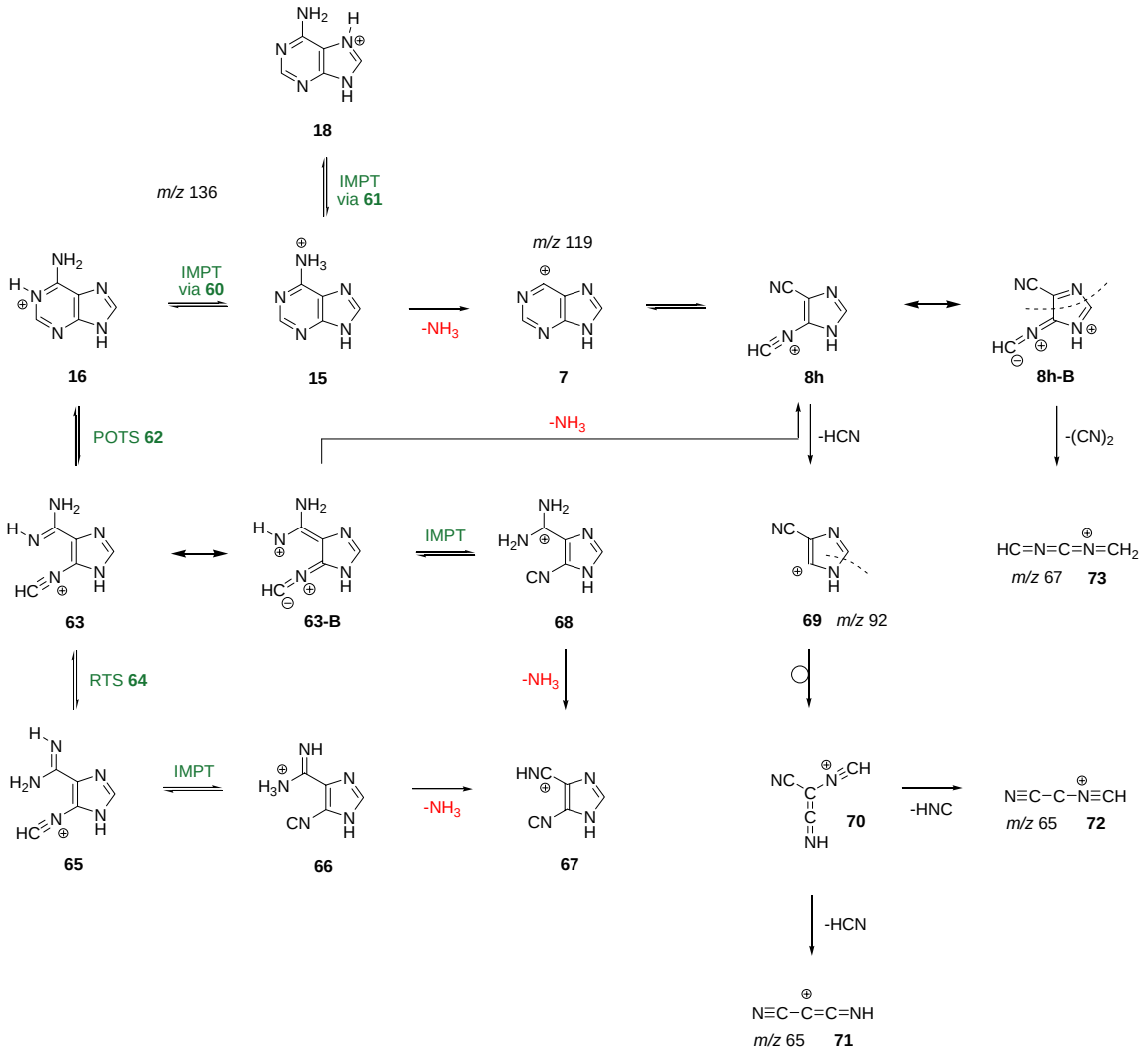

Scheme 2.4. Fragmentation paths of protonated adenine beginning with NH_3 elimination.

There is hardly any barrier for the back-reaction of **63** via transition state structure **62** to **16**, and it is this feature that is the hallmark of a pseudopericyclic reaction [50]. Most importantly, the relative energy of **63** with regard to **16** is 268.7 kJ/mol and too high for any of the paths involving **63** to compete with the path via ammonium ion **15**.

The potential energy surface analysis suggests that the major fragmentation cascade begins with internal proton transfer in [**1h** + H^+] to form **15** and subsequent fast ammonia elimination to yield **8h** with *m/z* 119 (Figure 2.2a). The subsequent HCN (or HNC)

elimination can be explained conveniently from **8h** and, hence, the observation of **69** with *m/z* 92 provides evidence for the existence of the pyrimidine ring-opened ion **8h**. Ion **69** then can rearrange to **70** on its way to ions *m/z* 65, protonated dicyanocarbene **71** and/or its mono-isonitrile isomer **72** (Figure 2.2b).

We found that ion *m/z* 119 also leads to fragments *m/z* 67 and 40 (Figure 2.2b). The $H_3C_3N_2^+$ ion occurs as **58** in the decomposition path that begins with NH_2CN elimination and an ion with this formula also can form along the major path. Considering resonance form **8h-B** we propose that *m/z* 67 might be the result of dicyanogen (ethanedinitrile) elimination to form the protonated cumulene **73**.

ESI-MS of Guanosine

The mass spectrum of electrosprayed guanosine gave a product peak at *m/z* 152 after cleavage of the glycosidic CN bond (Figure 2.1). Figure 2.4 shows the product-ion spectra obtained by CID of $[\mathbf{2h} + H]^+$, *m/z* 152, and its two most abundant fragments *m/z* 135 and *m/z* 110 resulting from NH_3 and cyanamide elimination. We considered seven possible paths (Scheme 2.5) and relevant stationary structures are shown in Figures 5 and 6.

a.

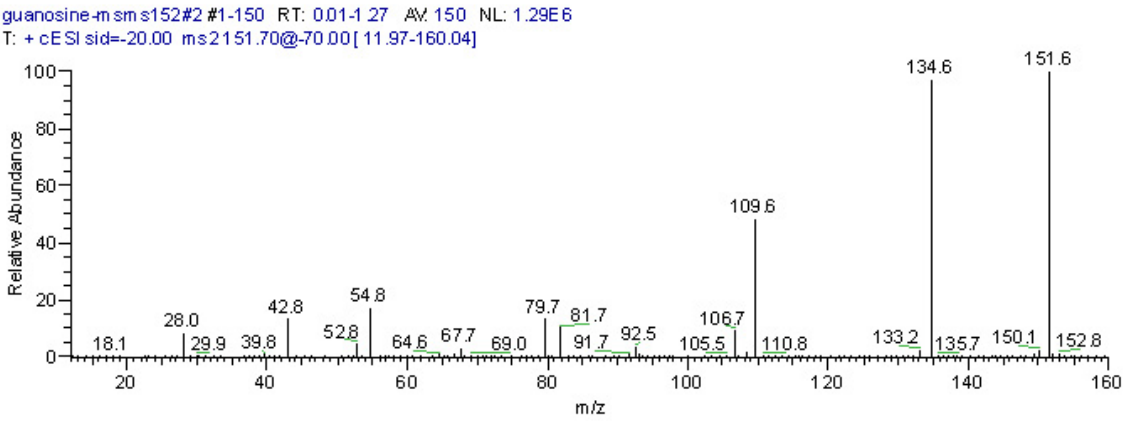

b

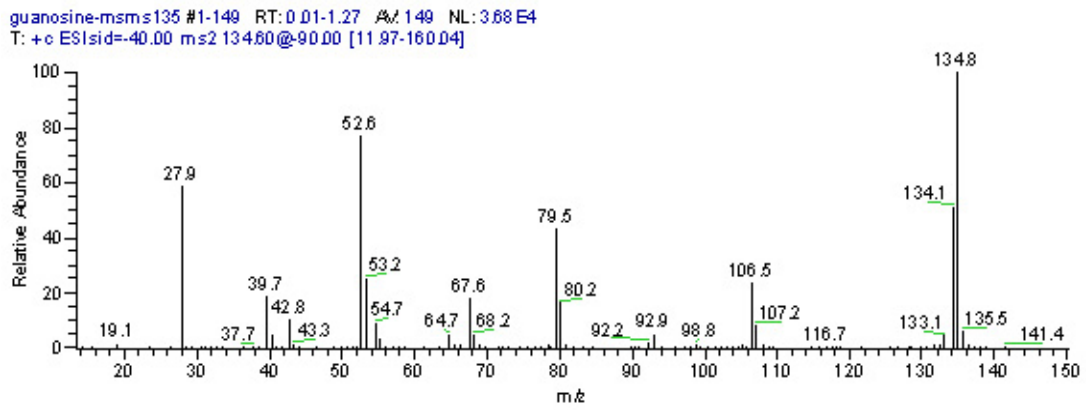

c

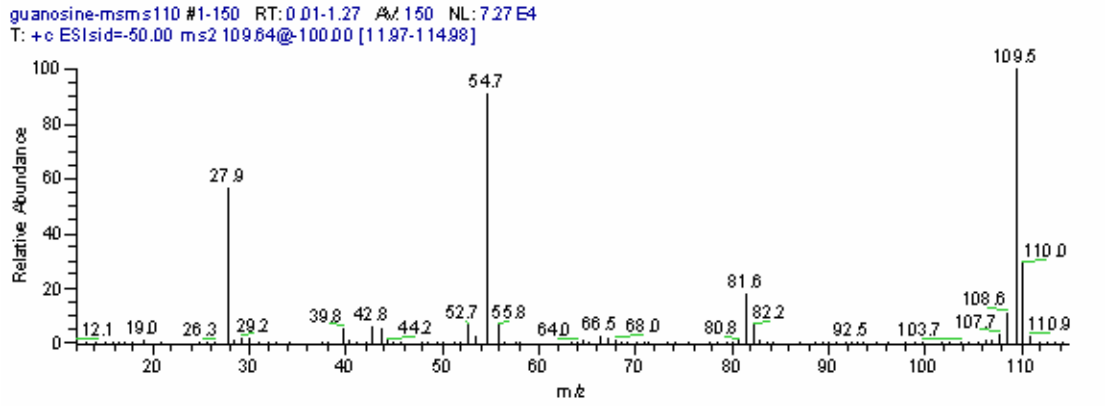

Figure 2.4. Product-ion spectra of (a) [**2h** + H]$^+$, *m/z* 152, (b) **9'**, *m/z* 135, and (c) **98**, *m/z* 110. All precursors were produced by in-source fragmentation of [2**r** + H]$^+$ at increasing energies.

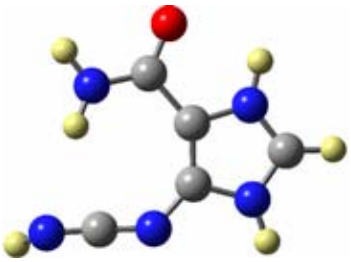

75

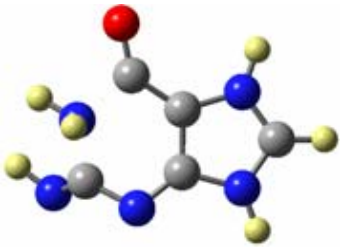

on path **74** → **75**

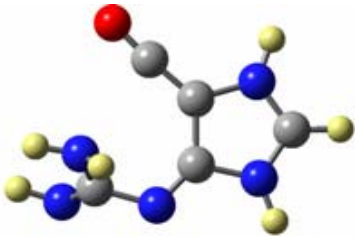

74, RTS(**23**,**75**)

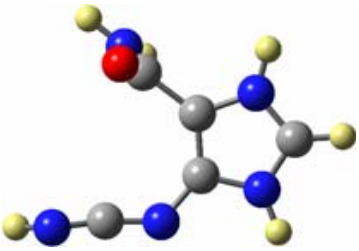

76, RTS(**75**,**77**)

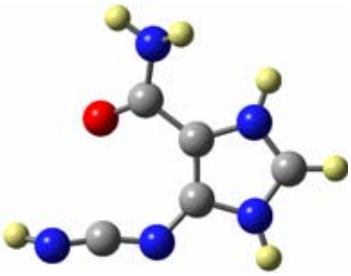

77

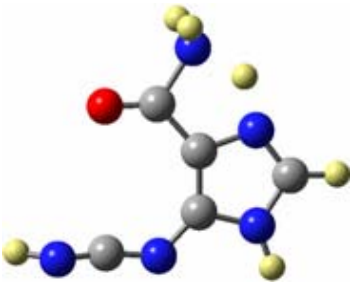

78, IMPT(**77**,**79**)

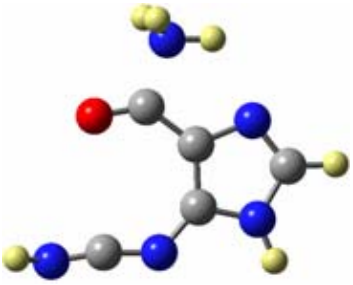

79

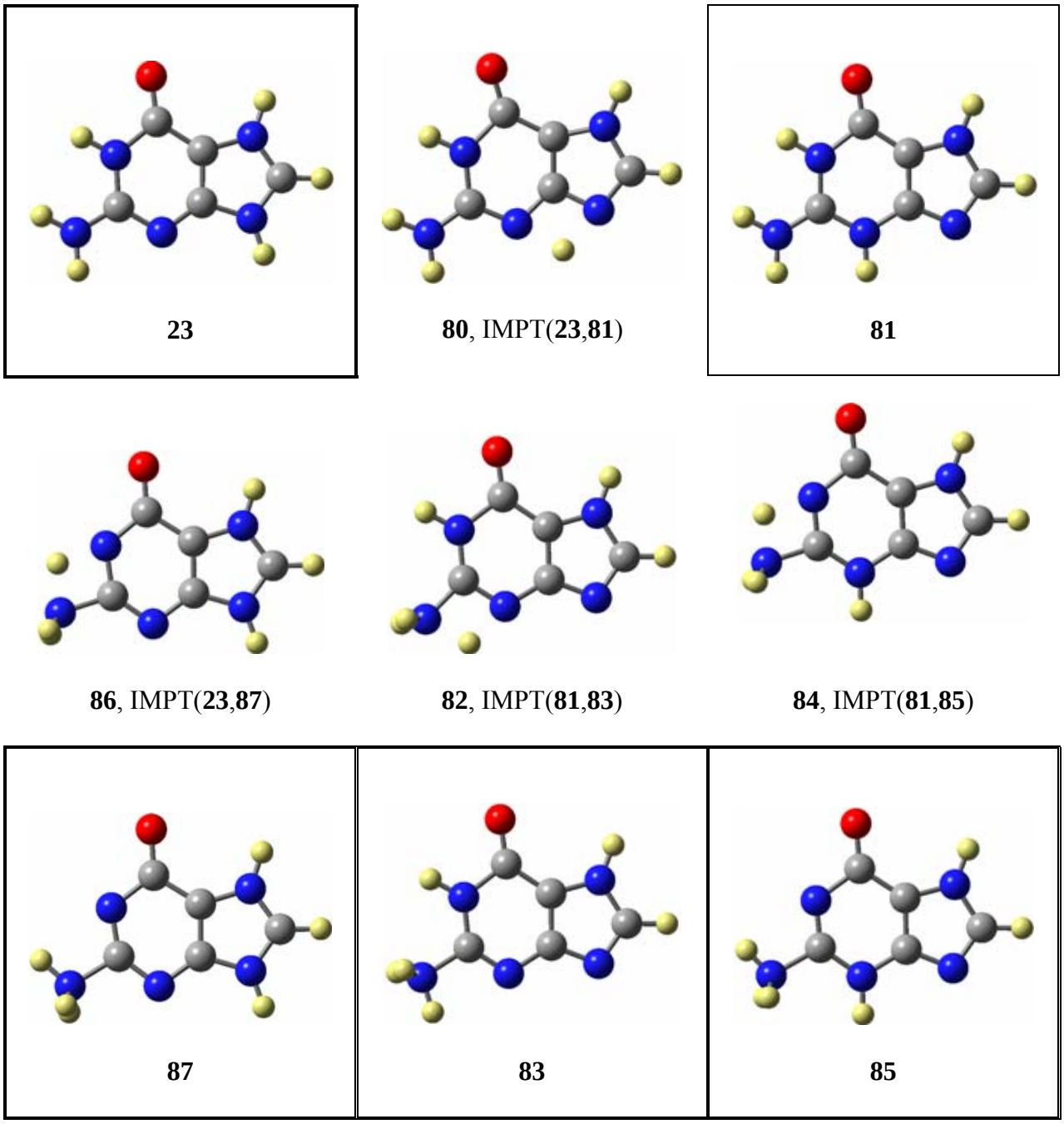

Figure 2.5. N7-Protonated guanine **23** (bold single-outlined) is the most stable structure of [**2h** + H]$^+$. The paths are shown for the formations of isomeric ammonium ion precursors **77** and **81** (single-outlined) and of their ammonium ions **79**, **83**, **85**, and **87** (double-outlined).

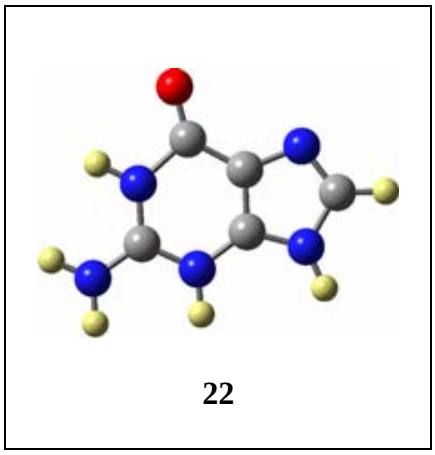

22

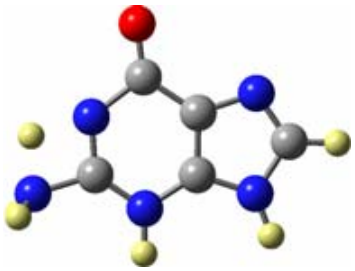

88, IMPT(**22**,**87**)

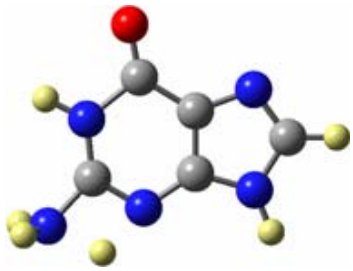

90, IMPT(**22**,**20**)

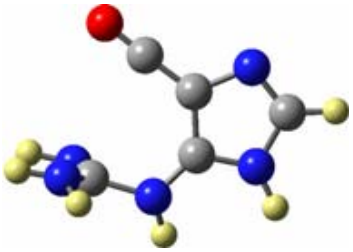

91, IMPT(**22**,**92**)

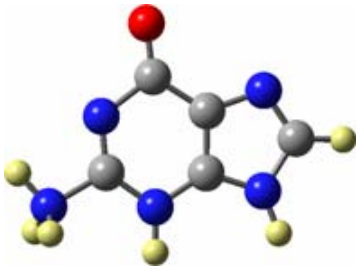

89

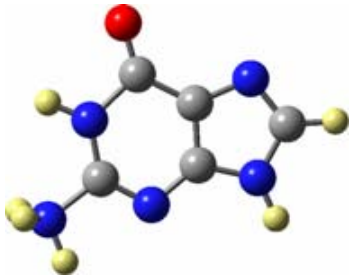

20

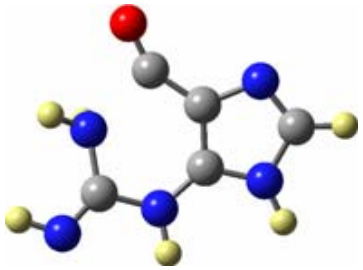

92

Figure 2.6. The N3- and N1-protonated guanines 2**2** and **21** (single-outlined) are potential intermediates in the fragmentation of [**2h** + H]$^+$, and they are ammonium ion precursors on the paths to the ammonium ions **30**, **89**, and **94** ((double-outlined).

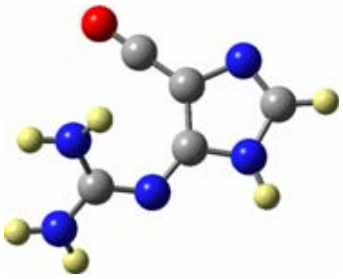

21

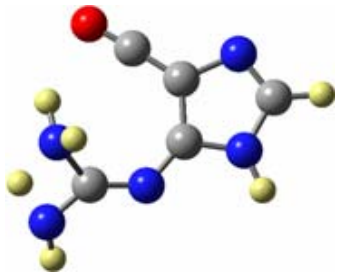

93, IMPT(**21**,**94**)

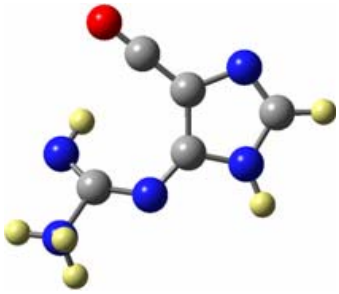

94

Figure 2.6. (Continued. Attach to the right of the Figure on the previous page.)

The N7-protonated tautomer **23** is the most stable and most abundant ion of [**2h** + H]$^+$. We first considered the pyrimidine ring-opening of **23** to amidine **74** by pseudopericycloreversion. We found that an amidine like **74** does not correspond to a

minimum on the potential energy surface and, instead, rotation about the C2–N3 bond via transition state structure **74** results in amino-group transfer along the down path from **74** to **75**. The activation barrier for the reaction **23** → **74**‡ → **75** is ΔH_{298} = 294.5 kJ/mol and, should **75** be accessible, one could envision the facile formation of **9'** via **77** and **79**. Next, we considered two paths that begin with initial proton transfer to **81**; the computed activation barrier for the reaction **23** → **80**‡ → **81** is ΔH_{act} = 251.3 kJ/mol and some 40 kJ/mol lower than the path via **74**. The back-reaction of **81** is less likely than are the intramolecular proton transfer reactions **81** → **82**‡ → **83** (ΔH_{act} = 207.1) and **81** → **84**‡ → **85** (ΔH_{act} = 222.3 kJ/mol). Ammonium ions **83** and **85** are substrates for the formations of **9'** and **10'**.

The initial proton transfer **23** → **81** was considered because we thought that NH_3 elimination required electrophilic catalysis, that is, the availability of an acidic H atom for 1,2-elimination. Eventually, we wondered whether the N1-hydrogen in **23** might not be acidic enough for the reaction **23** → **86**‡ → **87**. In fact, resonance form **23-C** makes perfect sense: the zwitterion-like π-polarization effectively helps to stabilize the charge in the σ-system caused by N7-protonation. Indeed, reaction **23** → **86**‡ → **87** requires an activation barrier of only ΔH_{act} = 202.4 kJ/mol.

Ion **23** is the most stable tautomer of [**2h** + H]$^{+}$ and it can be formed directly from [**2r** + H]$^{+}$. The initial formation of tautomers **21** and **22** cannot be excluded and their isomerizations to **23** should be fast in the hot ion [**2h** + H]$^{+}$. Nevertheless, the isomerization **23** → **20**, 2**3** → **21**, and **23** → **22** could be relevant for the discussion of the fragmentation pattern. The conversion of **23** to **20** is likely to proceed via **81** and **22** in that sequence. But suppose that **22** were accessible from **23** without going through **81**,

such a path **23** → **22** would become interesting only if **22** were to offer a reaction channel for NH_3 elimination with a barrier that was at least 72.8 kJ/mol lower than for the reaction **23** → **87**. The conversion of **23** to **21** is likely to proceed via **26** and **25**. Since **21** is 146.5 kJ/mol less stable than **23**, the path **23** → **21** becomes interesting if **21** were to offer any reaction channel for NH_3 elimination with a barrier that were at least that much lower than for the reaction **23** → **87**. Neither of these options seemed likely, but they were explored (Figure 2.6) and we computed the reactions **22** → **88**‡ → **89** (ΔH_{act} = 230.2), **22** → **90**‡ → **20** (ΔH_{act} = 183.3 kJ/mol), **22** → **91**‡ → **92** (ΔH_{act} = 166.1 kJ/mol), and **21** → **93**‡ → **94** (ΔH_{act} = 225.7). The situations with **22** → **91**‡ → **92** and **23** → **74**‡ → **75** provide for an interesting comparison and an acyclic amidine does not exist in either case. Hence, there are two paths from **22** and one path from **21** to ammonium ions, and the computed activation barriers show that these paths do not offer alternative, low-energy channels to ammonium ions.

Hence, the reaction **23** → **86**‡ → **87** with activation barrier ΔH_{act} = 202.4 kJ/mol provides the most easily accessible ammonium ion of [**2h** + H]$^{+}$ and ammonia elimination yields **95**, a tautomer of carbodiimides **9** and **9'** and cyanoimines **10** and **10'**. In the gas-phase the activation barrier for the isomerization between the prototypical carbodiimide and cyanamide is over 330 kJ/mol [51]. We will The tautomerization of **95** to **10'** also is not possible is unable to compete with is not likely to compete with decarbonylation and 1,2-hydrogen shift to **96** (*m/z* 107). In any case, another HCN from ion *m/z* 107 results in **97** (*m/z* 80) and **97** can loose another HCN (or HNC) to form **98** (*m/z* 53, $C_2N_2H^+$) or it can eliminate dicyanogen to form **56** (*m/z* 28, H_2CN^+).

The initial cyanamide expulsion is the dominant mode of guanosine decomposition in EI-MS, the process leads to the *m/z* 110 ion, and its product-ion spectrum is shown in Figure 2.4c. It appears most likely that **23** itself is the most suitable precursor for the NH_2CN elimination. Our PES exploration of the reaction **23** → **74**‡ → **75** suggested that one amino-H in a **74**-like structures would be well-positioned to transfer to N3, that is, for carbodiimide elimination via transitions state structure **99** leading to **100** (Scheme 2.5). The prominent peaks with *m/z* values of 82, 55, and 28 further suggest decarbonylation to **101**, and HCN (or HNC) eliminations to **102** and **56**.

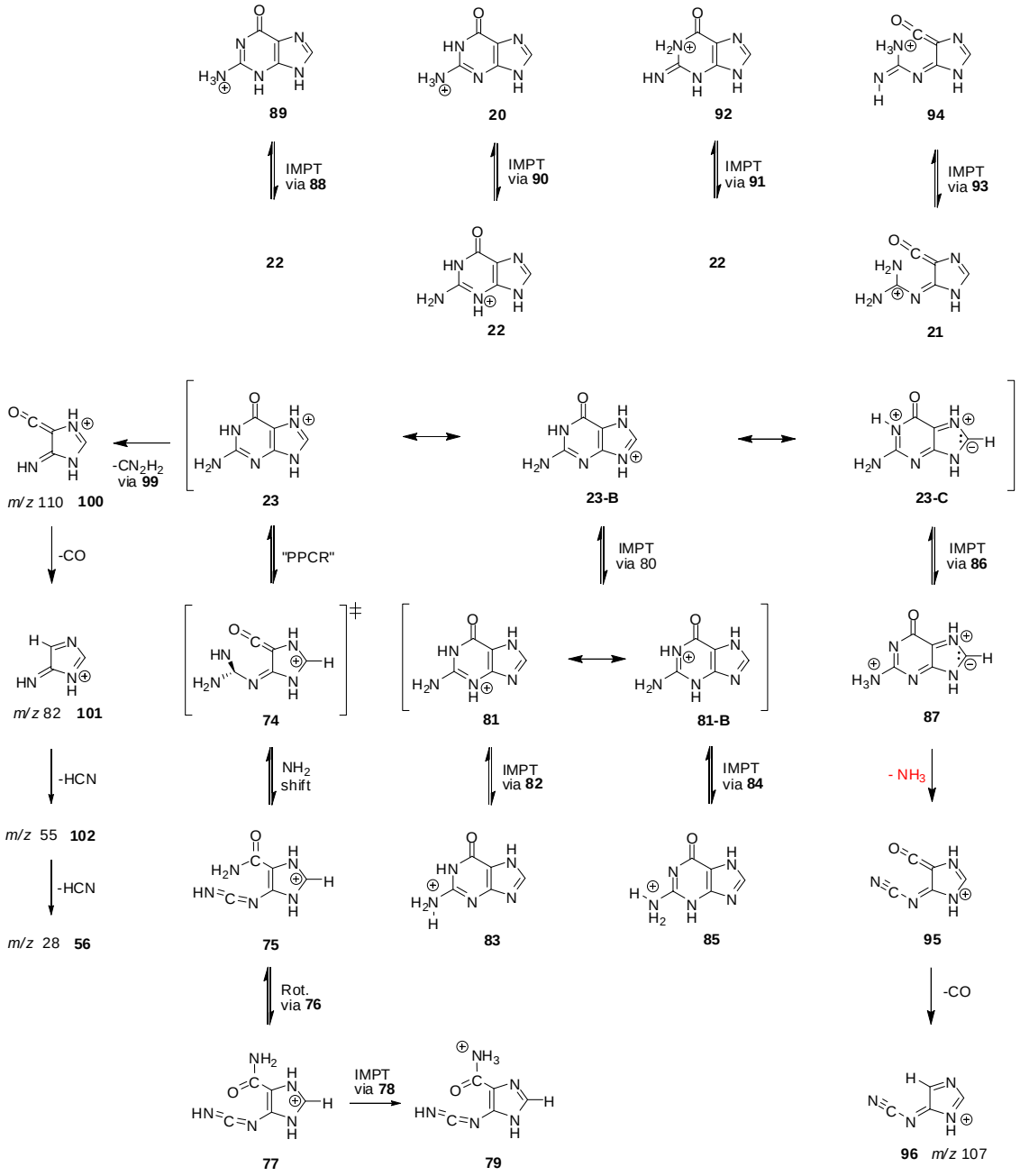

Scheme 2.5. Fragmentation paths of protonated guanine [**2h** + H]$^+$.

*ESI-MS Spectrometry of 5-Cyanoamino-Imidazole-4-Carboxamide **13e***

We synthesized cyanoamine **13e** (**13**, ether R = $CH_2OCH_2CH_2OH$) and studied its cyclization reaction and cross-link formation chemistry [21, 22]. The product-ion spectra of [**13e** + H]$^+$, *m/z* 226, and [**13h** + H]$^+$, *m/z* 152, are reported in Figure 2.7. As with

Figure 2.1, the spectrum in Figure 2.7a shows the replacement of the R-group by an H-atom to form [**13h** + H]$^+$, *m/z* 152.

a

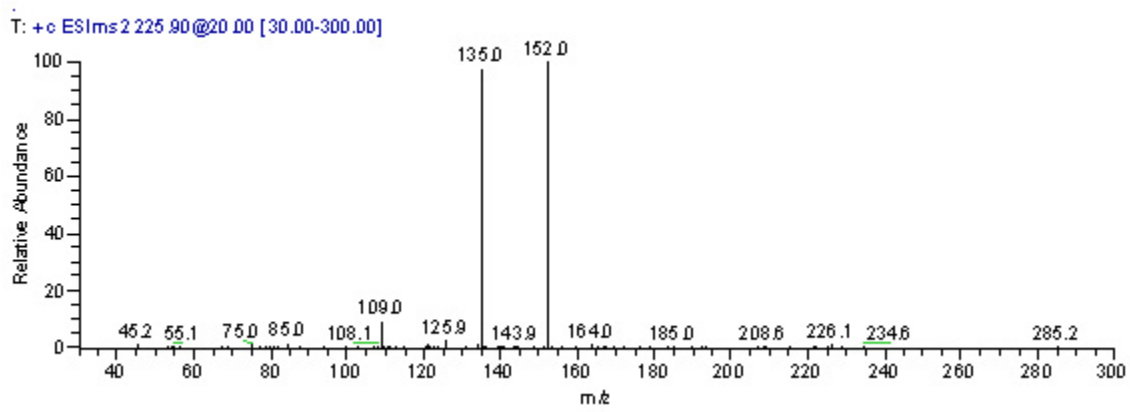

b

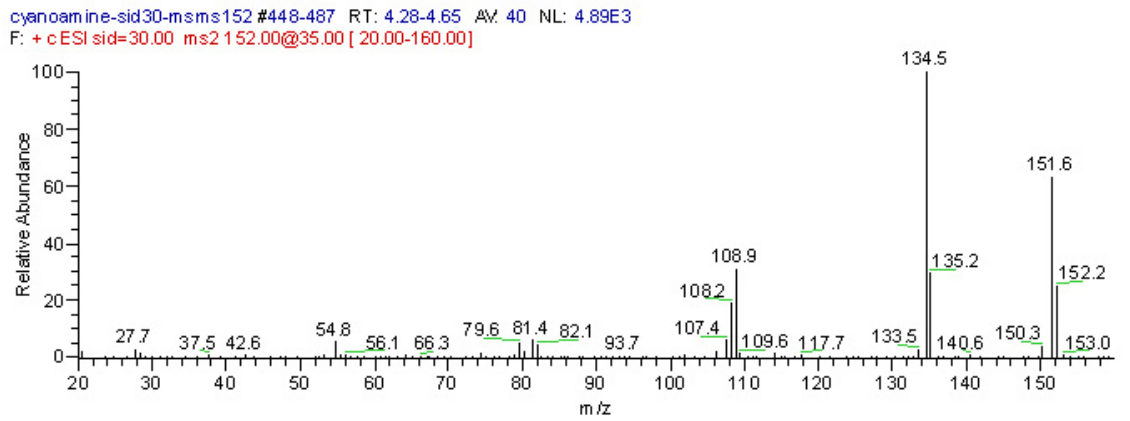

c

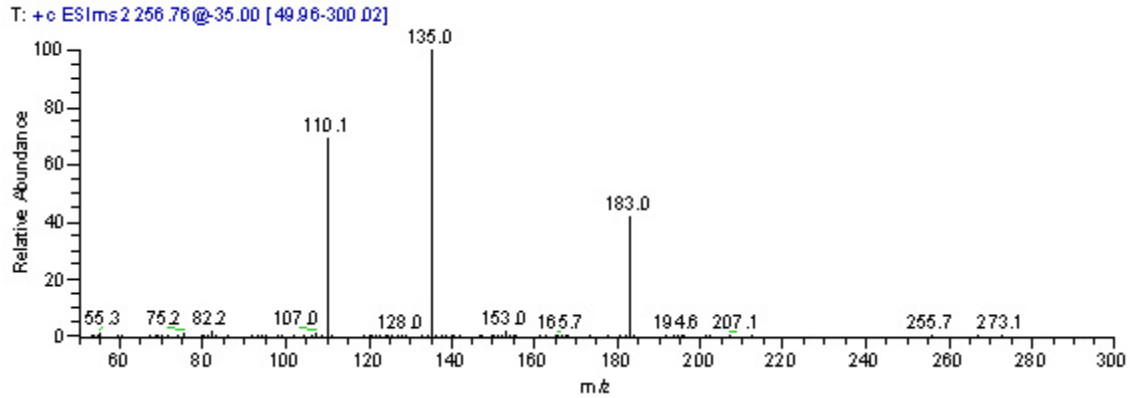

Figure 2.7. (a) Product-ion spectrum of [**13r** + H]$^+$, *m/z* 226. (b) Product-ion spectrum of [**13h** + H]$^+$, *m/z* 152, produced by in-source fragmentation of [**13r** + H]$^+$. (c) Product-ion spectrum of [**14r** + H]$^+$, *m/z* 257.

Ion [**13h** + H]$^+$ eliminates ammonia as in the case of [**2h** + H]$^+$. In contrast to [**2h** + H]$^+$, however, [**13h** + H]$^+$ does *not decarbonylate* and the ion loses CN instead to form *m/z* 109. The potential energy surfaces of **13** and [**13** + H$^+$] are somewhat complex because of the possibility for rotamers (about both exocyclic bonds) and tautomerism (cyanoamine *vs*. carbodiimide) and a complete discussion will be presented elsewhere. For the present purpose it is important to know that the neutral (*E*,*Z*)-rotamer of **13h** is preferred over any of the carbodiimides and that the (*E*,*Z*)-rotamer is preferred by ΔH_{rel} = 60.3 kJ/mol over (*Z*,*Z*)-**13h**. Studies of amides suggest that NH_3 elimination occurs only from the ammonium ion [52]. Yet, neither carbonyl-O nor amino-N protonation can compete with nitrilium or imidazolium ion formation (Table 2.2). Hence, we considered possible paths to ammonium ion formation from nitrilium and imidazolium ions (Scheme 2.6) and relevant stationary structures are shown in Figure 2.8.

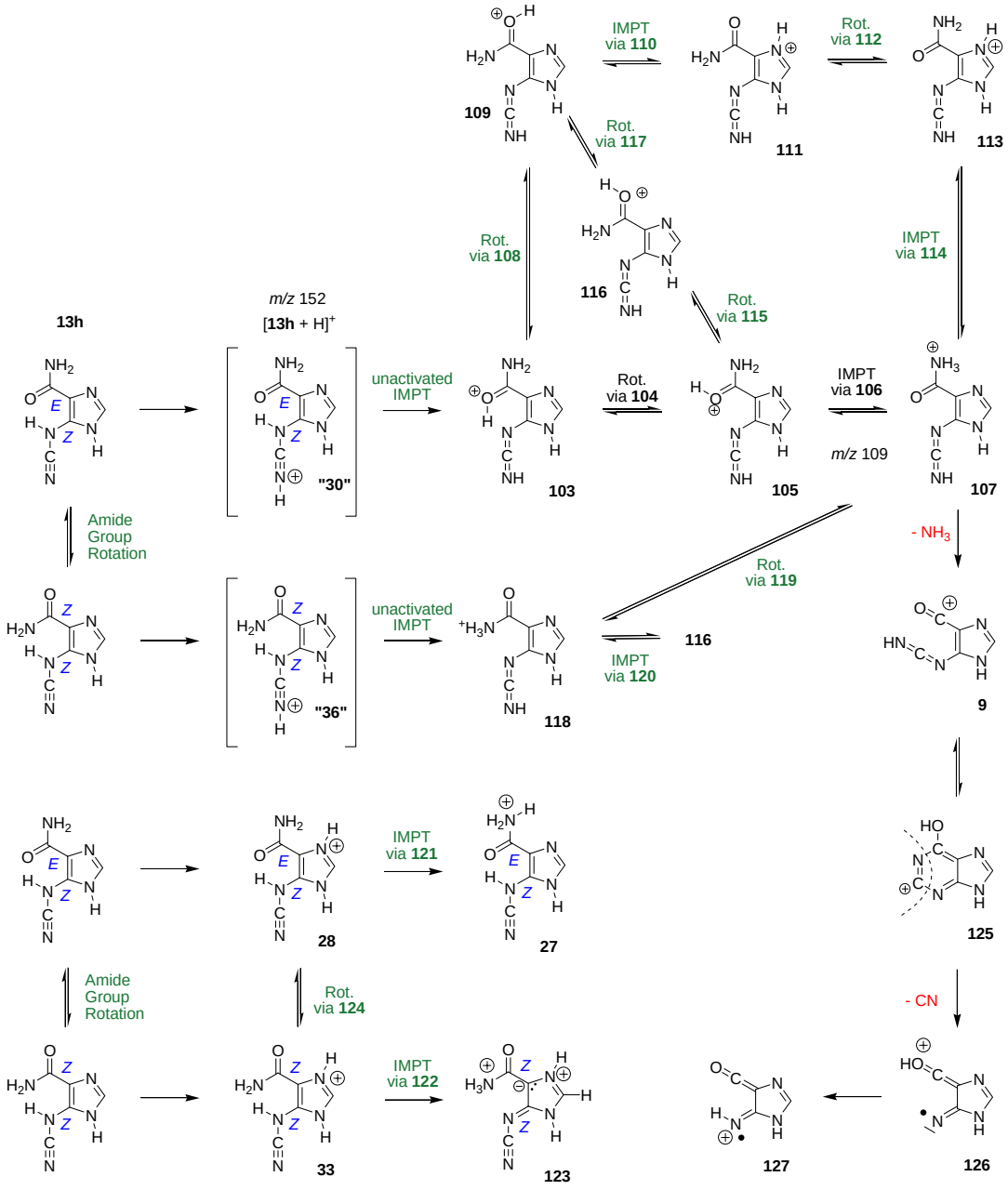

Scheme 2.6. Fragmentation of protonated 5-cyanoaminoimidazole-4-carboxamide [**13h** + H]$^+$.

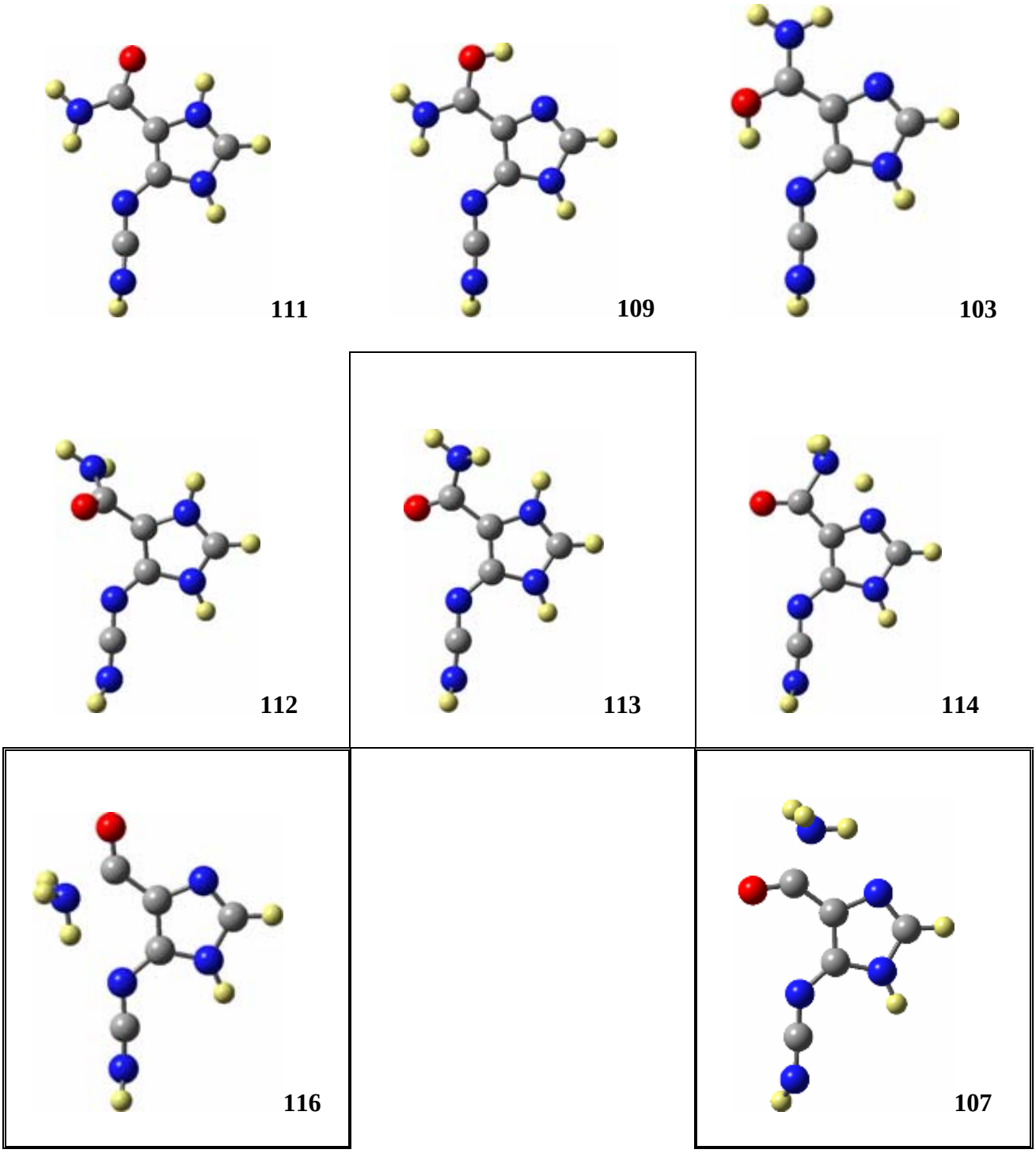

Figure 2.8. Paths to ammonium ions from nitrilium and imidazolium ions formed by protonation of (*E*,*Z*)- and (*Z*,*Z*)-**13h**.

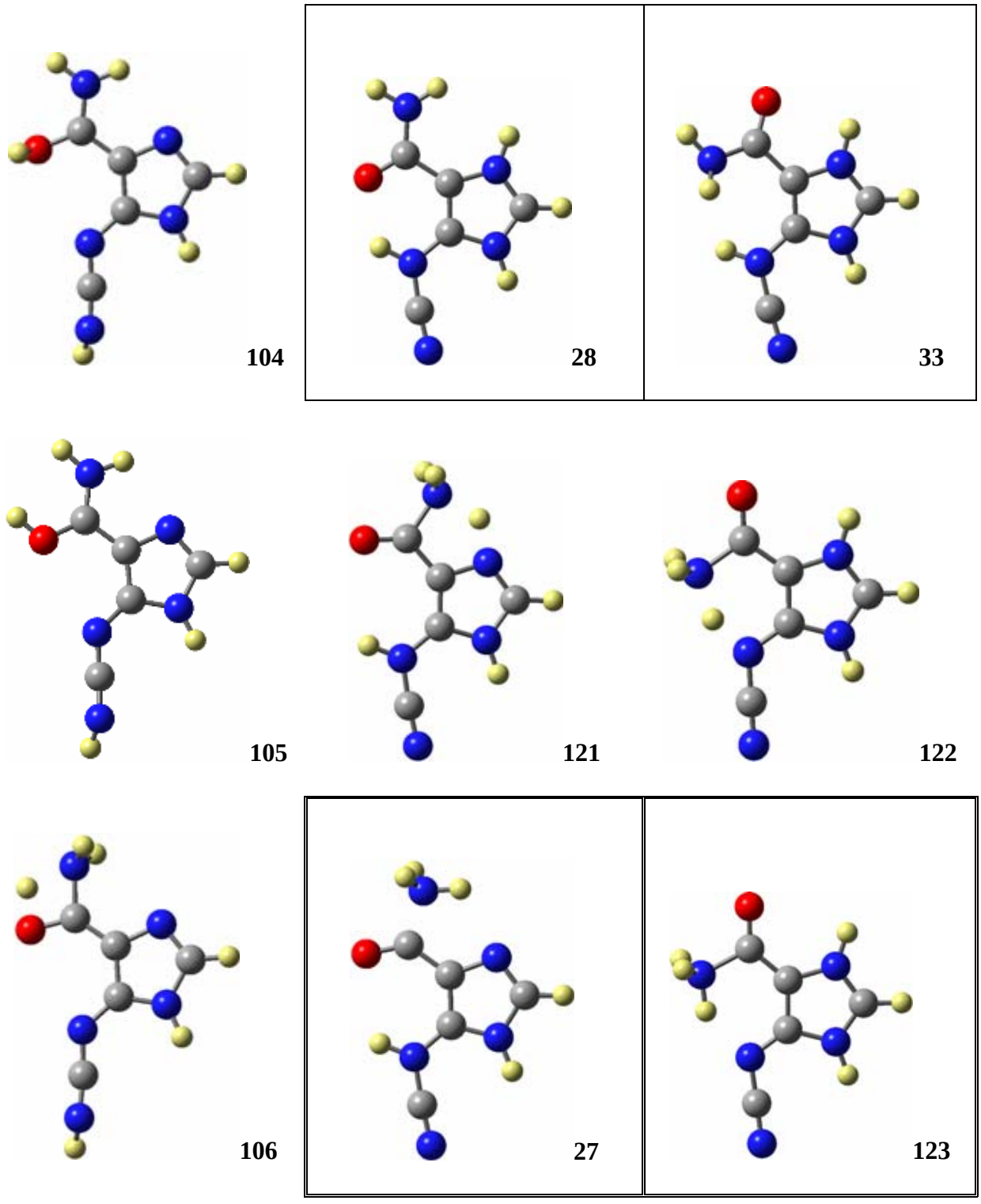

Figure 2.8. (Continued. This is the right half of Figure 2.8.)

Cyano-*N* protonation is by far the best option for cyanoamine (*E*,*Z*)-**13h** and ion **9** becomes accessible by NH_3 elimination from ammonium ions **107**. Cyano-*N* protonation of (*E*,*Z*)-**13h** does not form a stable nitrilium ion **30** but the O-protonated carbodiimide species **103** is formed instead. Its rotamer **105** is easily accessible via rotational transition state structure **104** (ΔH_{act} = 39.3 kJ/mol) but the H-shift from the OH-donor **105** → **106**‡ → **107** requires an activation energy of ΔH_{act} = 170.3 kJ/mol. Another path from **103** to **107** via **109** and **111** involves a series of rotations and offers the great advantage of forming the ammonium ion by H-shift from the NH-donor **113** of ΔH_{act} = 58.9 kJ/mol. The highest rotational barrier along this path is ΔH_{act} = 74.7 kJ/mol for the isomerization **103** → **108**‡ → **109** (and this isomerization could be accomplished in three steps with lower activation barriers via intermediates **105** and **116**). There are many paths from **103** to **107** and it is clear that at least some of them are kinetically facile.

As with the formation of **103** from (*E*,*Z*)-**13h**, ion **118** would be easily available by cyano-N protonation of (*Z*,*Z*)-**13h**. In the absence of (*Z*,*Z*)-**13h**, however, **118** would have to be produced from **116** by H-shift via **120** or by isomerization of **107** via rotational transition state structure **119**. It is clear that at least the latter path is accessible but, hellas, none of this matters because **118** is less stable than **107** by ΔH_{rel} = 29.4 kJ/mol.

The direct formation of **28** by N7-protonation of (*E*,*Z*)-**13h** would offer the advantage that ammonium ion **27** is accessible via transition state structure **121** with activation energy ΔH_{act} = 83.6 kJ/mol. Direct protonation of (*Z*,*Z*)-**13h** favors the formation of imidazolium ion **33** (Table 2.2) and ammonium ion **123** is then accessible by the H-shift **33** → **122**‡ → **123** with an activation energy of only ΔH_{act} = 41.7 kJ/mol. Yet, in the MS experiment, **28** and **33** have to be formed from **103** and these ions are 48.4 and 61.0

kJ/mol less stable, respectively, than **103**. These relative energies together with the computed barriers to form **27** and **123** show that there are no lower-energy alternatives to the formation of ammonium ion **107**.

The potential energy surface of protonated 5-cyanoimino-4-oxomethylene- and 4-cyanoimino-5-oxomethylene-dihydroimidazole is complicated [53] and we have already seen that it includes rotamers of **9** and **9'**, rotamers of **10** and **10'**, and rotamers of **95**. In addition, geometrical isomers of O-protonated species also are possible and it becomes relevant that O-protonation leads to bicyclic ions **125** and **125'**. Cation **9** prefers the *E*-conformation about the C–(N_2CH) bond and the equilibration (*Z*)-**9** ⇄ (*E*)-**9** is facile [19]. Hence, intramolecular H-shift from N in (*E*)-**9** to the O in **125** should be fast. The accessibility of **125** provides a rational for CN elimination from **9** or **126**.

*ESI-MS Spectrometry of 2-Methylthiohypoxanthine **14h***

Thioether **14e** (**14**, with ether R = $CH_2OCH_2CH_2OH$) is a side-product in the synthesis of cyanoamine **13e** and presents as a possible precursor for ions **9** and **10**. The product-ion spectrum of [**14h** + H]$^+$ shown in Figure 2.7 is similar to that of the respective guanosine analog [**2h** + H]$^+$ of Figure 2.4; its fragmentation is described in Scheme 2.7, and relevant stationary structures are shown in Figure 2.9.

The proton affinities of H_2S and MeSH are 744.8±10.0 kJ/mol [54] and 774.0±4.2 kJ/mol [55], respectively. The computed affinities for S-protonation of **14h** fall into that range (Table 2.2). As with guanine, N7-protonation is preferred and we discuss the fragmentation options of the N7-protonated ion [**14h** + H]$^+$, **39** (Scheme 2.7). The major

characteristics of the fragmentation of ion [**14h** + H]$^+$ are analogous to scenario for [**2h** + H]$^+$.

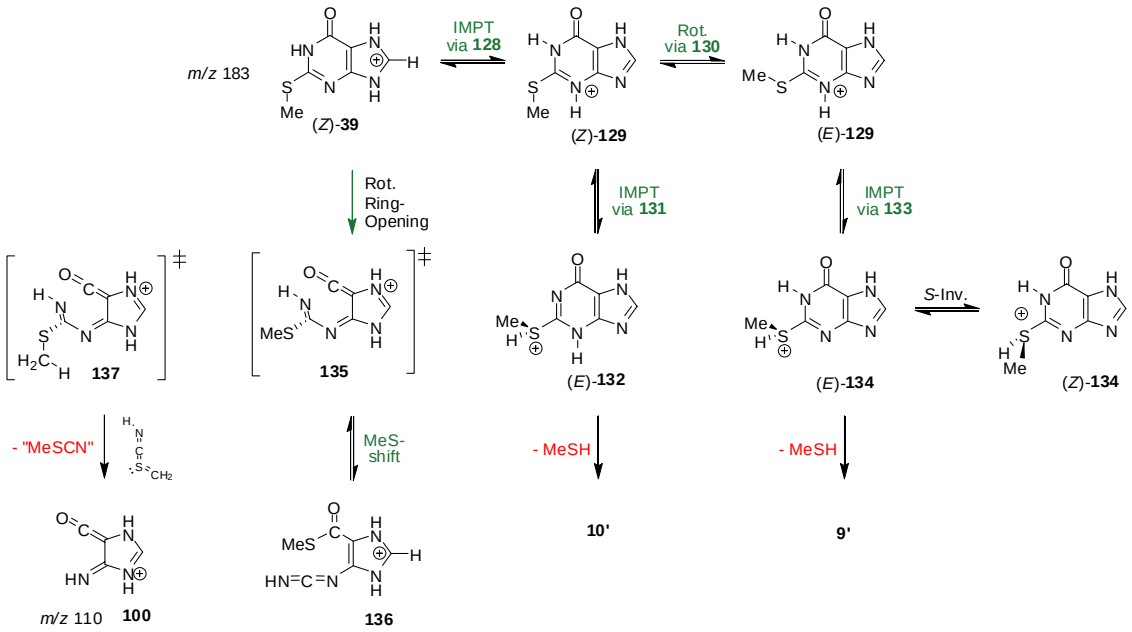

Scheme 2.7. Major fragmentation paths of protonated thioether **14h**.

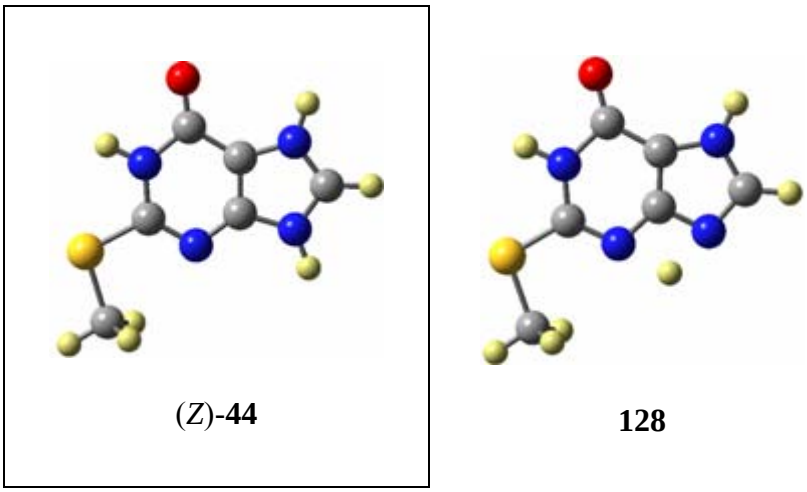

137 **135**

136

Figure 2.9. Paths to ammonium ions by protonated (*E*)-and (*Z*)-**14h.**

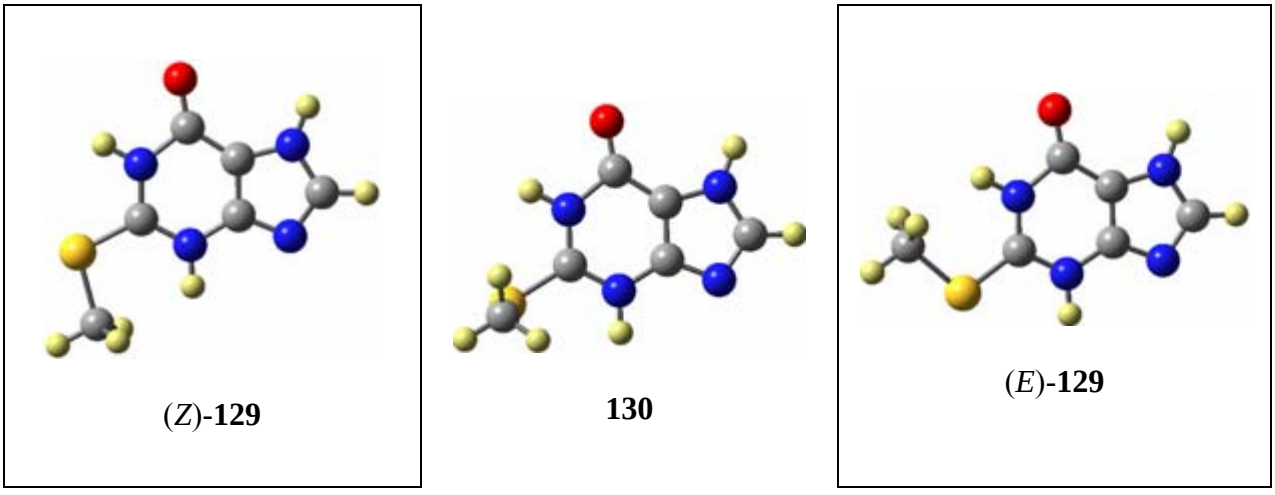

(*Z*)-**129** **130** (*E*)-**129**

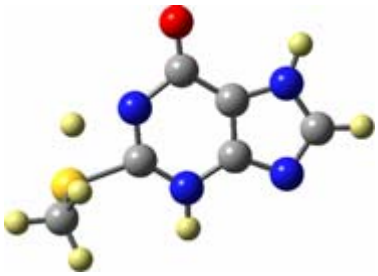

131

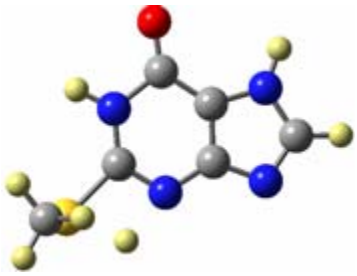

133

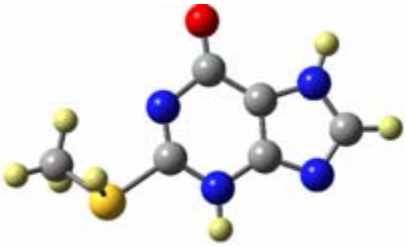

(*E*)-**132**

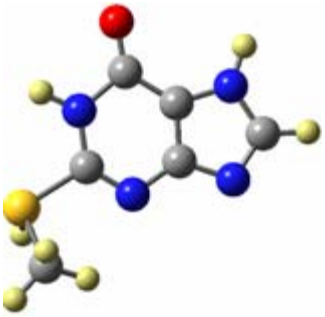

(*Z*)-**134**

(*E*)-**134**

Figure 2.9. (Continued. This is the right half of Scheme 2.7.)

The initially formed ion **39** occurs in conformation (*Z*)-**39** only and its conversion to (*Z*)-**129** via transition state structure **128** requires ΔH_{act} = 250.5 kJ/mol. Once (*Z*)-**129** is reached, its slightly more stable rotamer (*Z*)-**129** also is easily accessible via rotational transition state **130**. The reaction (*E*)-**129** → **133**‡ → (*E*)-**134** requires an activation barrier of ΔH_{act} = 194.8 kJ/mol and (*Z*)-**134** then becomes accessible by facile S-inversion. In the case of 132, (*E*)-**132** is the only existing rotamer and it is formed reaction (*Z*)-**129** → **131**‡ → (*E*)-**132** with an activation barrier of ΔH_{act} = 214.0 kJ/mol.

As with protonated guanine, we explored whether a ring-opened structure of type **135** might exist as a minimum and found that such a structure serves as the transition state structure for the formation of **136**. The ascent to **135** requires ΔH_{act} = 283.8 kJ/mol and significantly more activation that the formation of **129**. It remains to be explored whether a transition state structure **137** can be located for the expulsion of H_2C=SCNH, an isomer of methyl isocyanate.

The computational analysis suggests that **134** is the most easily accessible precursor for MeSH elimination and, hence, ion [**14h** + H - MeSH]$^+$ most likely leads to structure **9**' via the least-energy path. Yet, structure **10'** cannot be dismissed because every (*Z*)-**129** formed contains enough energy to overcome any of the barriers on the paths to **9'** or **10'**.

The discussions of the fragmentations of [**2h** + H]$^+$ and [**13h** + H]$^+$ (Schemes 5 & 6) suggest that the preference of [**2h** + H]$^+$ for CO elimination from **95** as opposed to the preference of [**13h** + H]$^+$ for CN elimination from **9** are consequences of the hydrogen pattern. The loss of CO requires the proximity of an NH site so that the incipient carbene can stabilize itself (*i.e.* **95** → **96** in Scheme 2.5, [56]). But the absence of decarbonylation in the fragmentation of [**14h** + H]$^+$ shows that an NH in the proximity of the putative carbene site is not all that is required to lower the barrier to decarbonylation sufficiently. Carbonylation only occurs from **95** where the proximate NH is part the imidazolium system.

ESI-MS of Deoxycytidine

The mass spectrum of electrosprayed deoxycytidine in Figure 2.1 shows two peaks: the quasi-molecular ion [**3d** + H]$^+$ and the fragment [**3h** + H]$^+$, *m/z* 112, in which the sugar

was replaced by hydrogen. The fragmentation of [**3h** + H]$^+$ was studied by MS/MS and the spectrum of Figure 2.9 is rationalized in Scheme 2.8 with the help of the computational results (Figure 2.10).

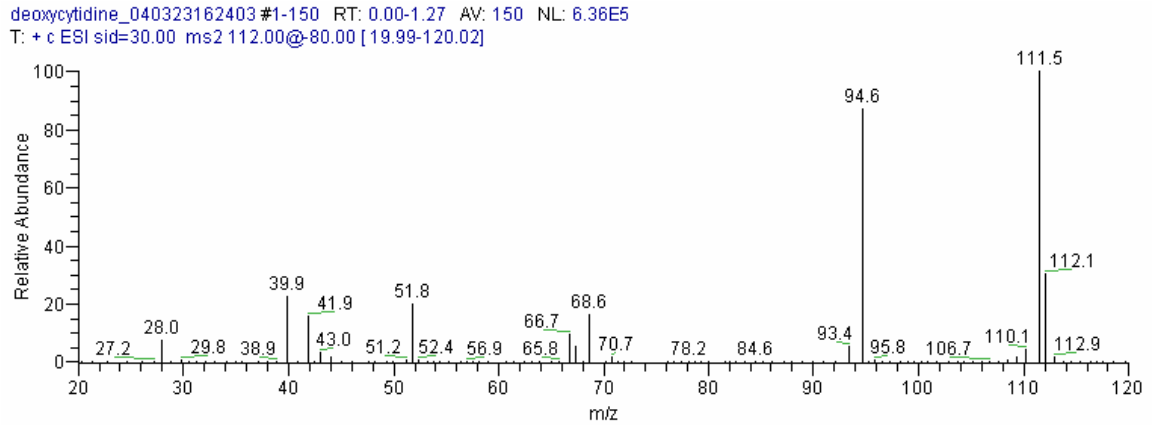

Figure 2.10. Product-ion spectrum of [**3h** + H]$^+$, *m/z* 112, produced by in-source fragmentation of protonated deoxycytidine.

The proton affinities show that amino group protonation cannot compete with protonation at the carbonyl-O or N3. With **50** present and/or accessible from **51** and **52**, ammonium ion **48** becomes available via transition state structure **138** with ΔH_{act} = 227.1 kJ/mol. We have shown elsewhere that **11h** easily ring-opens to thermodynamically more stable **12h**. We also considered whether there might be an option for ammonia elimination from a ring-opened structure. Yet, structure **137** serves as the transition state structure for the conversion of **50** and **140** and the enery requirements for this path was much too high (Table 2.3).

And this suggests the following mechanism for NH_3 elimination and formation of the large peak *m/z* 95 from [**3h** + H]$^+$. Protonation at N1 is followed by CN bond cleavage to yield **55**, protonated (*Z*)-3-isocyanatoacrylimidamide. Rotations about single bonds to rotamer **56** brings the acidic hydrogen into the vicinity of the amino group to enable the

elimination of NH_3 and the formation of **57**, cyano-N protonated (*Z*)-3-isocyanatoacrylonitrile [57].

The strong peak with *m/z* 69 shows that protonated cytosine can eliminate isocyanic acid, HNCO, and there are two paths depending on whether N1 or N3 will be part of HNCO; see resonance forms **50**-A and **50**-B, respectively. The elimination of HNCO with N3 would lead to **147** and **147** would explain the formation of protonated HCN, **56** (*m/z* 28). The elimination of HNCO with N1 would lead to **148** instead and subsequent loss of acetylene would result in protonated cyanamide (*m/z* 42). Alternatively, the HNCO elimination might be followed by a 1,2-H-shift to **148** and NH_3 elimination to protonated cyanoacetylene (*m/z* 52).

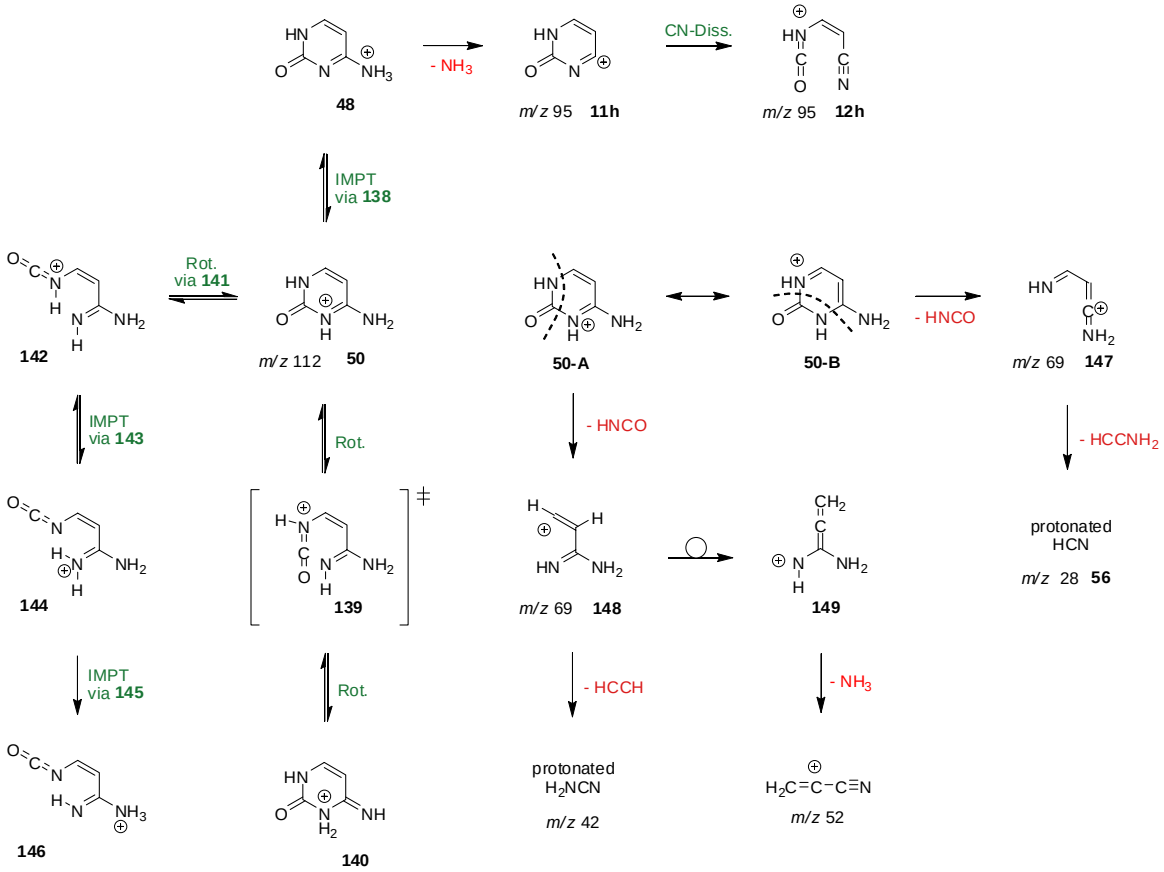

Scheme 2.8. Major fragmentation paths of protonated cytosine.

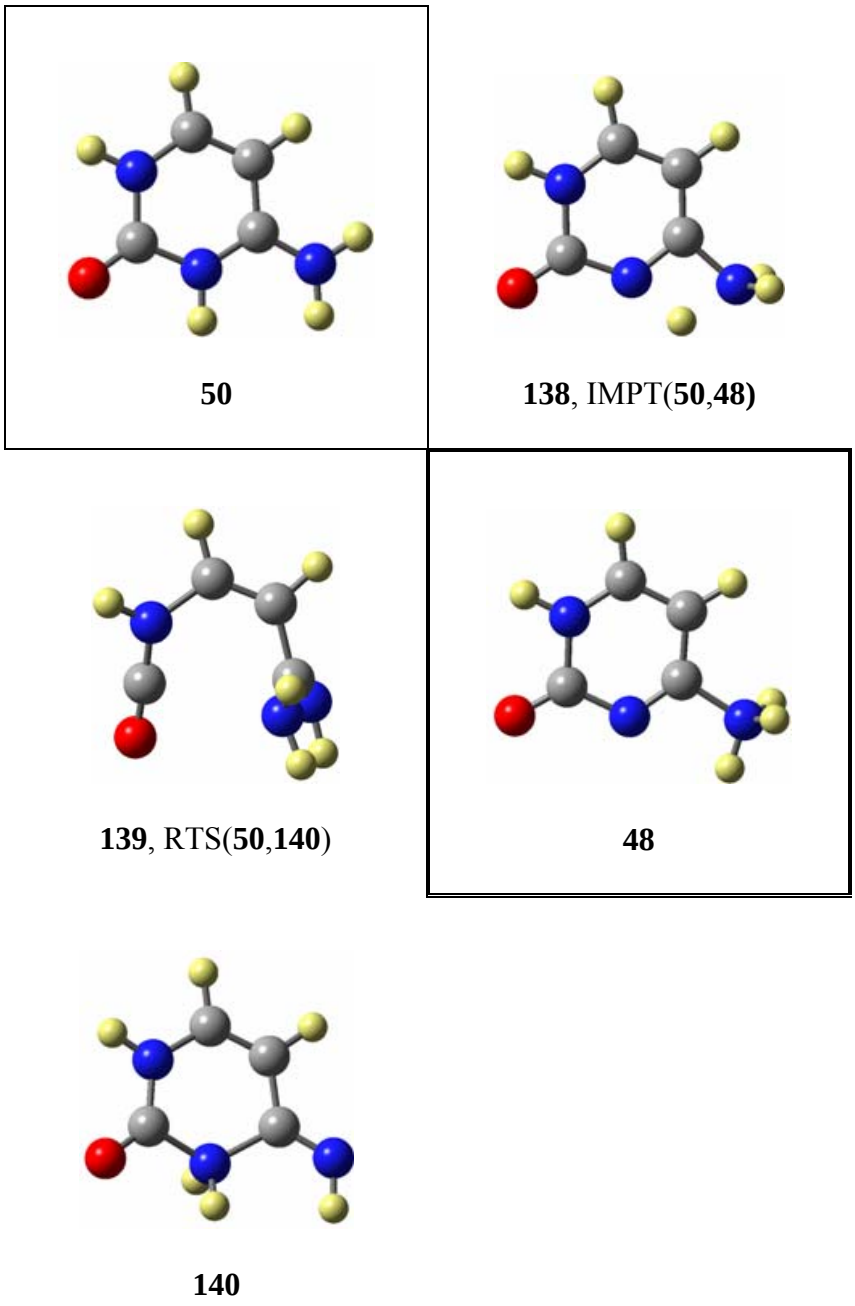

Figure 2.11. Fragmentation paths of [**3h** + H]$^+$

2.4 Conclusion

MS experiments are rather sensitive to instrument settings (Table 2.1) and there can be significant quantitative differences in fragmentation modes from one experiment to the other. Nevertheless, our study shows that the protonated nucleobases, [**1h** + H]$^+$, [**2h** + H]$^+$, and [**3h** + H]$^+$, can be observed by ESI-MS and that all observed modes of initial fragmentation can be understood mechanistically by consideration of the ion with the highest proton affinity. It is for this understanding, that we have confidence in the completeness of our study and we contend that we have observed all of the main modes of initial fragmentation.

We discussed ions **8** – **10** and **12** as possible reactive intermediates in nitrosative deamination chemistry in solution and it has been our aim to provide more direct experimental evidence for the existence of these ions. Hence, we have studied NH_3 elimination form the protonated nucleobases **1h** - **3h** and from the protonated model compounds **13h** and **14h** and Scheme 10 summarizes the key results: Every one of the postulated ions either was found to exist in the gas phase or to exist in the gas phase as a tautomer. Our results provide "semi-direct" experimental evidence for the ions because "direct" evidence would require structural characterization in the MS experiment [58] and because the new data go well beyond the "indirect evidence" stemming from inference of mechanistic studies.

The amino group hardly ever is the best protonation site of the substrate and we discussed possible mechanisms for ammonia elimination that explain how the amino group can serve as the dissociative protonation site. The acidic H and the NH_2-group can be vicinal (**24**), in a 1,3-relation (**48**), or even in a 1,4-relation (**31**, **45**, **56**). The

intramolecular proton transfer to the amino group might occur prior to elimination and an ammonium ion might exist (i.e. **46**) or IMPT and NH_3-elimination might be simultaneous events. The same kind of electrophilic catalysis applies to the elimination of H_2NCN from **30'**, of MeSH from **53**, and of MeSCN from **54**.

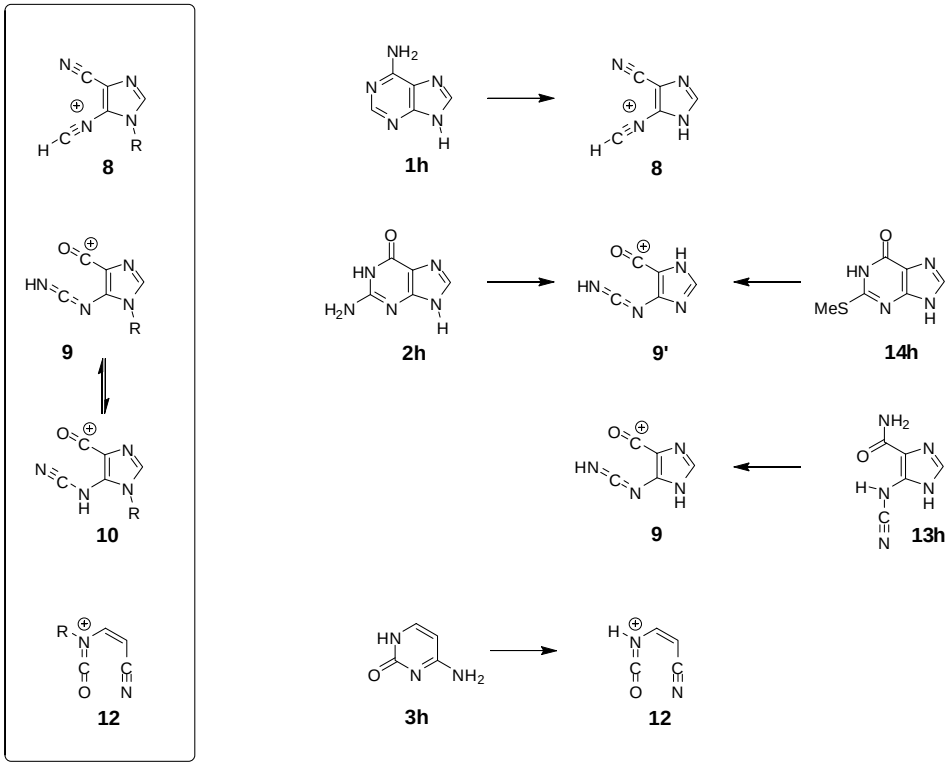

Scheme 2.9. Summary of results.

2.5 References

1. (a) Geiduschek, E. P. Reversible Denaturation of Deoxyribonucleic Acid (DNA). *Proc. Natl. Acad. Sci. USA* **1961**, *47*, 950-955. (b) Geiduschek, E. P. On the Factors Controlling the Reversibility of DNA Denaturation. *J. Mol. Biol.* **1962**, *4*, 467-487.

2. Caulfield, J. L.; Wishnok, J. S.; Tannenbaum, S. R. Nitric Oxide-Induced Interstrand Cross-Links in DNA. *Chem. Res. Tox.* **2003**, *16*, 571-574.

3. Committee on Nitrite and Alternative Curing Agents in Food. *The Health Effect of Nitrate, Nitrite, and N-Nitroso Compounds*; National Academy Press: Washington, D.C., 1981.

4. Furia, T. E. *Handbook of Food Additives*, 2nd ed.; CRC Press: Cleveland, 1972; pp 150-155.

5. Wakabayashi, K. in *Mutation and the Environment, Part E* (Albertini, R. J.; Ed.); Wiley-Liss, Inc.: New York, 1990; pp 107-116.

6. Culotta, E.; Koshland, D. E. NO News is Good News. *Science* **1992**, *258*, 1862-1865.

7. Marnett, L. J. Nitric Oxide: Chemical Events in Toxicity. *Chem. Res. Toxicol.* **1996**, *9*, 807-808.

8. Davis, K. L.; Martin, E.; Turko, I. V.; Murad, F. Novel Effects of Nitric Oxide. *Annu. Rev. Pharmacol. Toxicol.* **2001**, *41*, 203-236.

9. Jackson, A. L.; Loeb, L. A. The Contribution of Endogenous Sources of DNA Damage to the Multiple Mutations in Cancer. *Mutat. Res.* **2001**, *477*, 7-21.

10. Ohshima, H.; Bartsch, H. Chronic Infections and Inflammatory Processes as Cancer Risk Factors: Possible Role of Nitric Oxide in Carcinogenesis. *Mutat. Res.* **1994**, *305*, 253-264.

11. Tamir, S.; Tannenbaum, S. R. The Role of Nitric Oxide (NO) in the Carcinogenic Process. *Biochim. Biophys. Acta* **1996**, *1288,* F31-F36.

12. Suzuki, T.; Ide, H.; Yamada, M.; Endo, N.; Kanaori, K.; Tajima, K.; Morii, T.; Makino. K. Formation of 2'-Deoxyoxanosine from 2'-Deoxyguanosine and Nitrous Acid: Mechanism and Intermediates. *Nucleic Acids Res.* **2000**, *28*, 544-551.

13. Lucas, L. T.; Gatehouse, D.; Shuker, D. E. G. Efficient Nitroso Group Transfer from N-Nitrosoindoles to Nucleotides and 2'-Deoxyguanosine at Physiological pH. A New Pathway for N-Nitrosocompounds to Exert Genotoxicity. *J. Biol. Chem.* **1999**, *274*, 18319-18326.

14. Dong, M.; Wang, C.; Deen, W. M.; Dedon, P. C. Absence of 2'-Deoxyoxanosine and Presence of Abasic Sites in DNA Exposed to Nitric Oxide at Controlled Physiological Concentrations. *Chem. Res. Toxicol.* **2003**, *16*, 1044-1055.

15. Glaser, R.; Son, M.-S. Pyrimidine Ring Opening in the Unimolecular Dediazoniation of Guanine Diazonium Ion. An *ab Initio* Theoretical Study of the Mechanism of Nitrosative Guanosine Deamination. *J. Am. Chem. Soc.* **1996**, *118,* 10942-10943.

16. Glaser, R.; Rayat, S.; Lewis, M.; Son, M.-S.; Meyer, S. Theoretical Studies of DNA Base Deamination. 2. *Ab Initio* Study of DNA Base Diazonium Ions and of Their Linear, Unimolecular Dediazoniation Paths. *J. Am. Chem. Soc.* **1999**, *121,* 6108-6119.

17. Glaser, R.; Lewis, M. Single- and Double-Proton-Transfer in the Aggregate Between Cytosine and Guaninediazonium Ion. *Org. Lett*. **1999**, *1*, 273-276.

18. Glaser, R.; Wu, H.; Lewis, M. Cytosine Catalysis of Nitrosative Guanine Deamination and Interstrand Cross-Link Formation. *J. Am. Chem. Soc.* **2005**, *127*, 7346-7358.

19. Rayat, S.; Glaser, R. 5-Cyanoimino-4-Oxomethylene-dihydroimidazole and Nitrosative Guanine Deamination. A Theoretical Study of Geometries, Electronic Structures and *N*-Protonation. *J. Org. Chem.* **2003**, *68*, 9882-9892.

20. Rayat, S.; Majumdar, P.; Tipton, P.; Glaser, R. 5-Cyanoimino-4-oxomethylene-4,5-dihydroimidazole and 5-Cyanoamino-4-imidazolecarboxylic Acid Intermediates in Nitrosative Guanosine Deamination. Evidence from (18)O-Labeling Experiments. *J. Am. Chem. Soc.* **2004**, *126*, 9960-9969.

21. Qian, M.; Glaser, R. 5-Cyanoamino-4-imidazolecarboxamide and Nitrosative Guanine Deamination: Experimental Evidence for Pyrimidine Ring-Opening During Deamination. *J. Am. Chem. Soc.* **2004**, *126*, 2274-2275.

22. Qian, M.; Glaser, R. Demonstration of an Alternative Mechanism for G-to-G Cross-Link Formation. *J. Am. Chem. Soc.* **2005**, *127*, 880-887.

23. Hodgen, B.; Rayat, S.; Glaser, R. Nitrosative Adenine Deamination: Facile Pyrimidine Ring-Opening in the Dediazoniation of Adeninediazonium Ion. *Org. Lett.* **2003**, *5*, 4077-4080.

24. McLafferty, F. W.; Wachs, T.; Koppel, C.; Dymerski, P. P.; Bockhoff, F. M. *Advances in Mass Spectrometry*, Vol. 7b, Daly, N. R., Ed. Institute of Petroleum: London, 1978.

25. (a) Koch, W.; Holthausen, M. C. *A Chemist's Guide to Density Functional Theory*, 2nd ed. Wiley-VCH: Weinheim, 2001. (b) Parr, R. G; Weitao, Y. *Density-Functional Theory of Atoms and Molecules*, International Series of Monographs on Chemistry. Oxford University Press: Oxford, UK, 1994.

26. *Gaussian 03, Revision D.01*, Frisch, M. J.; Trucks, G. W.; Schlegel, H. B.; Scuseria, G. E.; Robb, M. A.; Cheeseman, J. R.; Montgomery, Jr., J. A.; Vreven, T.; Kudin, K. N.; Burant, J. C.; Millam, J. M.; Iyengar, S. S.; Tomasi, J.; Barone, V.; Mennucci, B.; Cossi, M.; Scalmani, G.; Rega, N.; Petersson, G. A.; Nakatsuji, H.; Hada, M.; Ehara, M.; Toyota, K.; Fukuda, R.; Hasegawa, J.; Ishida, M.; Nakajima, T.; Honda, Y.; Kitao, O.; Nakai, H.; Klene, M.; Li, X.; Knox, J. E.; Hratchian, H. P.; Cross, J. B.; Bakken, V.; Adamo, C.; Jaramillo, J.; Gomperts, R.; Stratmann, R. E.; Yazyev, O.; Austin, A. J.; Cammi, R.; Pomelli, C.; Ochterski, J. W.; Ayala, P. Y.; Morokuma, K.; Voth, G. A.; Salvador, P.; Dannenberg, J. J.; Zakrzewski, V. G.; Dapprich, S.; Daniels, A. D.; Strain, M. C.; Farkas, O.; Malick, D. K.; Rabuck, A. D.; Raghavachari, K.; Foresman, J. B.; Ortiz, J. V.; Cui, Q.; Baboul, A. G.; Clifford, S.; Cioslowski, J.; Stefanov, B. B.; Liu, G.; Liashenko, A.; Piskorz, P.; Komaromi, I.; Martin, R. L.; Fox, D. J.; Keith, T.; Al-Laham, M. A.; Peng, C. Y.; Nanayakkara, A.; Challacombe, M.; Gill, P. M. W.; Johnson, B.; Chen, W.; Wong, M. W.; Gonzalez, C.; and Pople, J. A.; Gaussian, Inc., Wallingford CT, 2004.

27. Rice, J. M.; Dudek, G. O. Mass Spectra of Nucleic Acid Derivatives. II. Guanine, Adenine, and Related Compounds. *J. Am. Chem. Soc.* **1967**, *89*, 2719-2725.

28. Barrio, M. C. G.; Scopes, D. I. C.; Holtwick, J. B.; Leonard, N. J. Syntheses of all Singly Labeled [15N]-Adenines: Mass Spectral Fragmentation of Adenine. *Proc. Natl. Acad. Sci. USA* **1981**, *78*, 3986-3988.

29. Sethi, S. K.; Gupta, S. P.; Jenkins, E. E.; Whitehead, C. W.; Townsend, L. B.; McCloskey, J. A. Mass Spectrometry of Nucleic Acid Constituents. Electron Ionization Spectra of Selectively Labeled Adenines. *J. Am. Chem. Soc.* **1982**, *104*, 3349-3353.

30. Rice, J. M.; Dudek, G. O.; Barber, M. Mass Spectra of Nucleic Acid Derivatives. Pyrimidines. *J. Am. Chem. Soc*. **1965**, *87*, 4569-4576.

31. Fryčák, P.; HušKová, R.; Tomáš, A.; Lemr, K. Atmospheric Pressure Ionization Mass Spectrometry of Purine and Pyrimidine Markers of Inherited Metabolic Disorders. *J. Mass. Spectrom*. **2002**, *37*, 1242-1248.

32. Wilson, M. S.; McCloskey, J. A.. Chemical ionization mass spectrometry of nucleosides. Mechanisms of ion formation and estimations of proton affinity. *J. Am. Chem. Soc.* **1975**, *97*, 3436-3444.

33. Nelson, C. C.; McCloskey, J. A.. Collision-Induced Dissociation of Adenine. *J. Am. Chem. Soc.* **1992**, *114*, 3661-3668.

34. Gregson, J. M.; McCloskey, J. A.. Collision-Induced Dissociation of Protonated Guanine. *Int. J. Mass Spectro. Ion Proc.* **1997**, *165/166*, 475-485.

35. Tureček, F.; Chen, X. Protonated Adenine: Tautomers, Solvated Clusters, and Dissociation Mechanisms. *J. Am. Soc. Mass Spectro.* **2005**, *16*, 1713-1726.

36. Curtiss, L. A.; Redfern, P. C.; Frurip, D. J. Theoretical methods for computing enthalpies of formation of gaseous compounds. *Rev. Comput. Chem.* **2000**, *15*, 147-211.

37. Giese, B.; McNaughton, D. Density Functional Theoretical (DFT) and Surface-Enhanced Raman Spectroscopic Study of Guanine and Its Alkylated Derivatives. Part 1. DFT Calculations on Neutral, Protonated and Deprotonated Guanine. *Phys. Chem. Chem. Phys*. **2002**, *4*, 5161-5170.

38. Jang, Y. H.; Goddard III, W. A.; Noyes, K. T.; Sowers, L. C.; Hwang, S.; Chung, D. S. pK_a Values of Guanine in Water: Density Functional Theory Calculations Combined with Poisson-Boltzmann Continuum-Solvation Model. *J. Phys. Chem. B.* **2003**, *107*, 344-357.

39. Greco, F.; Liguori, A.; Sindona, G.; Uccella, N. Gas-Phase Proton Affinity of Deoxyribonucleosides and Related Nucleobases by Fast Atom Bombardment Tandem Mass Spectrometry. *J. Am. Chem. Soc.* **1990**, *112*, 9092-9096.

40. Chandra, A. K.; Nguyen, M. T.; Uchimaru, T.; Zeegers-Huyskens, T. Protonation and Deprotonation Enthalpies of Guanine and Adenine and Implications for the Structure and Energy of Their Complexes with Water: Comparison with Uracil, Thymine, and Cytosine. *J. Phys. Chem. A* **1999**, *103*, 8853-8860.

41. Taft, R. W. *Proton Transfer Reaction*; Caldin, E. F., Gold, V., Eds.; Wiley-Halstead: New York, 1975; Chapter 2.

42. Lias, S. G.; Bartmess, J. E.; Liebman, J. F.; Holmes, J. L.; Levin, R. D.; Mallard, W. G. Gas-Phase Ion and Neutral Thermochemistry. *J. Phys. Chem. Ref. Data, Suppl. 1* **1988**, 17.

43. Karpas, Z.; Berant, Z.; Stimac, R. M. An Ion Mobility Spectrometry / Mass Spectro-metry (IMS/MS) Study of the Site of Protonation in Anilines. *Struct. Chem.* **1990**, *1*, 201-204.

44. Flammang, R.; Dechamps, N.; Pascal, L.; Van Haverbeke, Y.; Gerbaux, P.; Nam, P.-C.; Nguyen, M. T. Ring versus Nitrogen Protonation of Anilines. *Lett. Org. Chem.* **2004**, *1*, 23-30.

45. Tu, Y.-P. Dissociative Protonation Sites: Reactive Centers in Protonated Molecules Leading to Fragmentation in Mass Spectrometry. *J. Org. Chem.* **2006**, *71*, 5482-5488.

46. Paizs, B.; Suhai, S. Fragmentation pathways of protonated peptides. *Mass Spectrom. Rev.* **2005**, *24*, 508-548.

47. Mouls, L.; Subra, G.; Aubagnac, J.-L.; Martinez, J.; Enjalbal, C. Tandem mass spectrometry of amidated peptides. *J. Mass Spectrom.* **2006**, *41*, 1470–1483.

48. Csonka, I. P.; Paizs, B.; Suhai, S. Modeling of the gas-phase ion chemistry of protonated arginine. *J. Mass Spectrom.* **2004**, *39*, 1025-1035.

49. Cooper, T.; Talaty, E.; Grove, J.; Van Stipdonk, M.; Suhai, S.; Paizs, B. Isotope Labeling and Theoretical Study of the Formation of a3* Ions from Protonated Tetraglycine. *J. Am. Soc. Mass Spectrom.* **2006**, *17*, 1654–1664.

50 Morgan, K. M. Reaction mechanisms. Part (iii) Pericyclic reactions. *Annu. Rep. Prog. Chem. B* **2005**, *101*, 284-304.

51. Tordini, F.; Bencini, A.; Bruschi, M.; Gioai, L. D.; Zampella, G.; Fantucci, P. Theoretical Study of Hydration of Cyanamide and Carbodiimide. *J. Phys. Chem. A* **2003**, *107*, 1188-1196.

52. Lin, H. Y.; Ridge, D. P.; Uggerud, E.; Vulpius, T. Unimolecular Chemistry of Protonated Formamide. Mass Spectrometry and ab Initio Quantum Chemical Calculations**.** *J. Am. Chem. Soc*. **1994**, *116*, 2996-3004.

53. Yang, S.; Glaser, R., to be published.

54. Marynick, D. S.; Scanion, K.; Eades, R. A.; Dixon, D. A. Absolute Proton Affinities of PH_3 and H_2S. *J. Phys. Chem.* **1981**, *85*, 3364-3366.

55. Haney, M. A.; Franklin, J. L. Mass Spectrometric Determination of the Proton Affinities of Various Molecules. *J. Phys. Chem.* **1969**, *73*, 4328-4331.

56. Polce, M. J.; Kim, Y.; Wesdemiotis, C. First experimental characterization of aminocarbene. *Int. J. Mass Spectrom. Ion Proc.* **1997**, *167/168*, 309-315.

57. Glaser, R.; Wu, H.; Saint Paul, F. v. Chemical Carcinogens in Non-Enzymatic Cytosine Deamination: 3-Isocyanatoacrylonitrile. *J. Mol. Model.* **2006**, *12*, 731-737.

58. Cooper, H. J.; Hakansson, K.; Marshall, A. G. The role of electron capture dissociation in biomolecular analysis. *Mass Spectrometry Reviews* **2005**, *24*, 201-222.

CHAPTER 3: Computational Study of Protonated 5-(Iminomethylenamino)-1*H*-Imidazole-4-Carboxamide

3.1 Introduction

Nitrosative guanine deamination[1,2,3] and interstrand cross-link formation[4,5,6] result from endogenous DNA damage and causes various diseases via mutagenesis and cytotoxicity. It has been studied since the very discovery of guanine. The major product of guanine deamination is xanthosine that is formed by direct nucleophilic substitution in homogeneous solution.[7,8,9] The second major product of guanine deamination is oxanosine.[10,11,12] We suggested one reaction mechanism that involves the unimolecular dediazoniation of guaninediazonium ion with pyrimidine ring-opening and results in the formation of 5-cyanoimino-4-oxomethylene-4,5-dihydroimidazole after deprotonation.[13,14] It is a highly reactive intermediate and can react with water via two protonated isomers [**1** + H]$^+$ and [**2** + H]$^+$ by two different pathways to form oxanosine(Scheme 3.1).[15]

Our particular interest here is molecule **1** because of its relevance to the guanine deamination. The synthesis of cyanoamine **1e** (**1**, ether R = $CH_2OCH_2CH_2OH$) and study of its cyclization reaction and cross-link formation chemistry were reported.[16,17] The cycliztion of **1** was under the condition of room temperature in 0.2M K_2HPO_4/KH_2PO_4 buffer solution (pH = 6.0, 7.0, 8.0, 9.0). Guanine and the isoguanine were the two products of this cycliztion reaction. The formation of guanine from **1** is a nucleophilic addition of the weakly nucleophilic amide-amino group to the cyanoamine, and this reaction most likely was acid catalyzed. One reaction mechanism was proposed to

explain the formation of isoguanine. The first step of this mechanism was **1** cyclized to oxanine-1-imine. The second step was the ring-opening of oxanine-1-imine to form keteninine. The final step was the ring-closing of keteninine to form isoguanine.(Scheme 3.1).

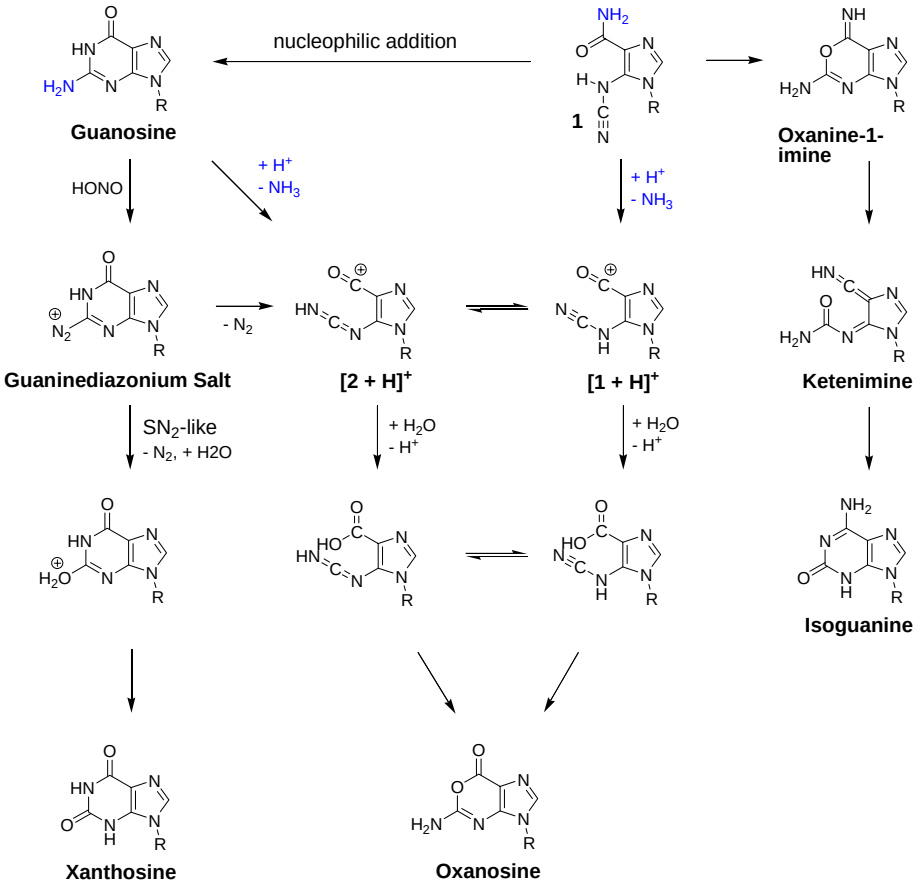

Scheme 3.1. Involvement of the conjugate acids of cyanoamine **1** and carbodiimide **2** in deamination of guanine derivatives. Deamination can be effected either via nitrosation or by proton-catalyzed ammonia elimination.

We reported the NH_3 elimination of the replacement of the R-group by an H-atom to form protonated cyanoamine **1** and nucleobases based on the theoretical and mass

spectrometric study that provided compelling evidence for pyrimidine ring-opened species.[18] The computed proton affinities of nucleobases were within five percent of the experimental values of them. The protonated cyanoamine **1** eliminates the ammonia and then loses the CN group. A likely mechanism for fragmentations was given. The potential energy surfaces of **1** and protonated **1** are somewhat complex because the molecule **1** exists in equilibrium between cyanoamine **1** and carbodiimide **2**. The two exocyclic bonds of **1** also make it more complex by giving different conformations. The conformational and isomer preferences of cyanoamine 1 and carbodiimide 2 and on their conjugate acids is studied (Scheme 3.2). The proton affinities of N- and O-sites were computed for of all rotamers and tautomers of cyanoamine **1** and carbodiimide **2** (Scheme 3.2) to begin the discussion of the gas-phase ion chemistry. Several reaction paths for isoguanosine formation and ammonia elimination from cyanoamine 1 and carbodiimide 2 also have been computed.

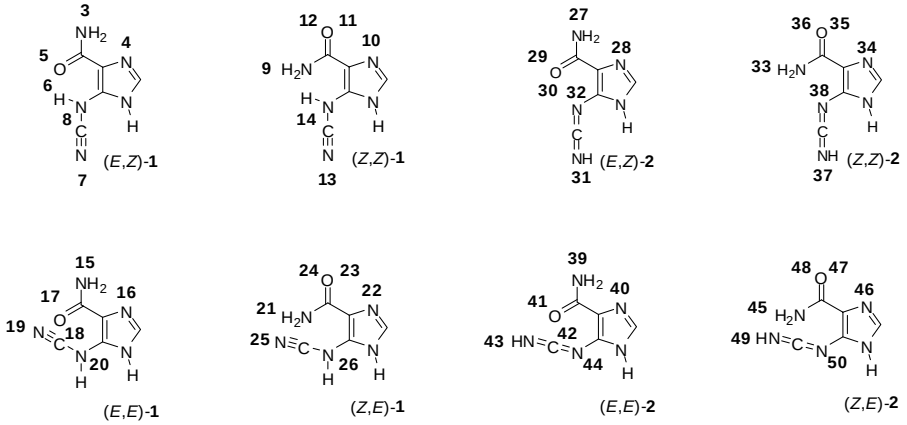

Scheme 3.2. Numbering of conjugate acids considered for the four potential conformers of cyanoamine **1** and carbodiimide **2**.

3.2 Computational Methods

All structures various intermediates and transition states along relevant reaction paths were determined with density functional theory (DFT).[19] The hybrid method B3LYP was employed in conjunction with the 6-31++G** basis set, B3LYP/6-31++G**, and the calculations were performed with *Gaussian03*[20] on a 64-processer SGI Altix system. Structures were optimized and vibrational analysis was performed for each structure to confirm that the structure was in fact stationary, to confirm the character of the stationary structure, and to determine thermochemical data. Total energies *E*, vibrational zero-point energies *VZPE*, thermal energies *TE*, and entropies *S* are given in Table 3.1 and Cartesian coordinates of all optimized structures are provided as supporting information.

Table 3.1. Total energies and thermodynamical data[a-c]

Parameter	*E*	*VZPE*	*TE*	*S*	*N*
(*E*,*Z*)-**1**	-542.559084	71.26	77.41	97.79	0
(*Z*,*Z*)-**1**	-542.536039	71.23	77.38	98.07	0
RTS(**1**, (*E*,*Z*) → (*Z*,*Z*))	-542.530486	70.53	76.63	100.38	1
(*E*,*Z*)-**2**	-542.547380	70.35	76.70	100.05	0
(*Z*,*Z*) -**2**	-542.541026	70.26	76.58	99.61	0
(*E*,*E*) -**2**	-542.557703	70.64	76.83	97.25	0
(*Z*,*E*) -**2**	-542.539767	70.42	76.67	98.90	0
RTS(**2**, (*E*,*Z*) → (*Z*,*Z*))	-542.534246	70.06	75.97	96.09	1
RTS(**2**, (*E*,*Z*) →(*E*,*E*))	-542.546765	70.24	76.10	95.38	1
RTS(**2**, (*Z*,*E*) → (*Z*,*Z*))	-542.536099	70.23	75.99	94.50	1
RTS(**2**, (*Z*,*E*) → (*E*,*E*))	-542.536904	70.31	76.10	95.18	1
3	-542.888433	78.59	85.07	100.41	0
4	-542.903909	78.60	85.02	100.71	0
5	-542.900724	79.31	85.61	98.17	0
6	-542.894173	79.90	85.95	97.94	0
7	turns into **30**				
8	turns into **6**				
9	turns into **21**				

10	-542.899510	79.62	85.91	99.21	0
11	-542.895675	79.56	85.78	99.44	0
12	-542.879170	79.26	85.52	100.85	0
13	turns into **33**				
14	turns into **21**				
15	-542.878008	79.40	85.85	99.75	0
16	turns into **4**				
17	-542.893502	79.24	85.54	98.11	0
18	-542.899153	79.41	85.47	96.05	0
19a	-542.921794	80.57	85.99	91.07	0
19b	-542.914560	80.47	85.94	91.53	0
20	turns to **6**				
21	-542.862140	79.11	85.47	98.94	0
22	-542.898911	79.66	85.82	97.35	0
23	-542.901767	79.68	85.74	96.21	0
24	-542.883712	79.15	85.36	97.31	0
25	turns to **19a**				
26	turns to **21**				
27	-542.896519	78.59	85.07	100.41	0
28	-542.904857	78.60	85.02	100.71	0
29	-542.911201	78.51	84.85	98.96	0
30	-542.921524	79.05	85.15	96.88	0
31	turns to **43**				
32	turns to **30**				
33	-542.885169	78.61	84.97	99.38	0
34	-542.921173	78.92	85.18	98.48	0
35	-542.921173	79.03	85.16	97.35	0
36	-542.905899	78.53	84.78	97.92	0
37	turns to **43**				
38	turns to **33**				
39	-542.900961	78.76	85.17	99.26	0
40	-542.915859	78.77	85.08	98.22	0
41	-542.912686	78.48	84.83	98.74	0
42	-542.912396	78.93	85.03	96.74	0
43	-542.950270	80.86	86.30	90.25	0
44	turns to **19**				

45	-542.875448	78.68	85.04	99.08	0
46	-542.918888	78.85	85.14	98.66	0
47	-542.916659	79.15	85.20	96.37	0
48	-542.897356	78.43	84.77	99.27	0
49	turns to **43**				
50	turns to **44**				

[a] All calculations are determined at B3LYP/6-31++G**.
[b] Total energies (E_{tot}) in hartrees, vibrational zero-point energies (*VZPE*) and thermal energies (*TE*) in kcal/mol, and entropies (*S*) in cal/mol K.
[c] Number of imaginary frequencies (NIF).

These data allow for the determination of relative and reaction energies ΔE, enthalpies $\Delta H_0 = \Delta(E+VZPE)$ and $\Delta H_{298} = \Delta(E+TE)$, and free energies $\Delta G = \Delta(E+TE-298.15 \cdot S)$. The affinities for protonation at the various sites are the negative reaction enthalpies $\Delta\Delta H_{298}$ of the formations of the respective protonated system X; (*E*,*Z*)-**1** + H^+ → X (Table 3.3).

3.3 Results and Discussion

Conformational and Isomer Preferences

The molecule **1** should have four different cyanoamine forms and four carbodiimide forms in theory. However, there are only six of them existing. The neutral (*E*,*E*) and (*Z*,*E*) of cyanoamine **1** don't exist and they directly turn into (*E*,*Z*) and (*Z*,*Z*) of cyanoamine **1**. The neutral (*E*,*Z*)-rotamer of cyanoamine **1** is preferred over any of the carbodiimides **2** and the (*Z*,*Z*)-rotamer of cyanoamine **1**, that the (*E*,*Z*)-rotamer of cyanoamine **1** is preferred by only ΔH = 1.2 kJ/mol over the (*E*,*E*)- tautomer of carbodiimide **2** that is secondly preferred. Interestingly, all the carbodiimides are preferred over (*Z*,*Z*)-rotamer of cyanoamine **1**. (Table 3.2) Computed structures of

conformers of cyanoamine **1** and carbodiimide **2** and their rotational transition state structures for their interconversion are shown in Figure 3.1 and Figure 3.2.

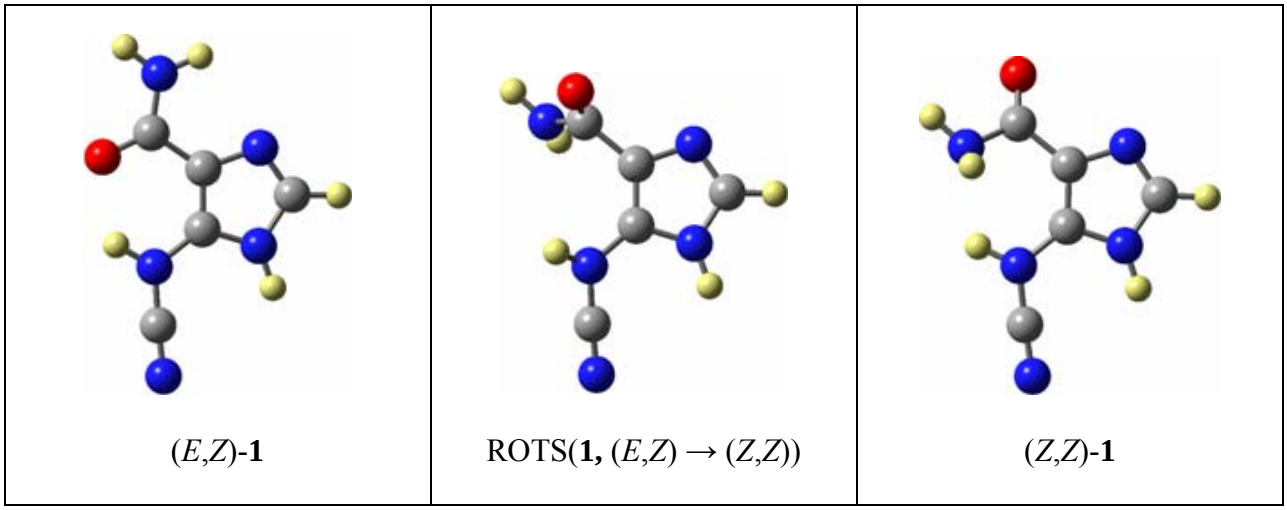

Figure 3.1. Computed structures of conformers of cyanoamine **1** and of the rotational transition state structure (ROTS) for their interconversion.

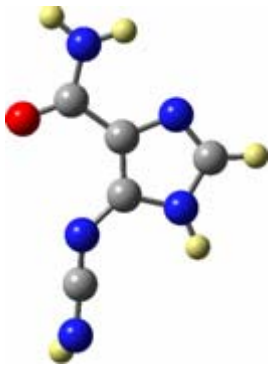	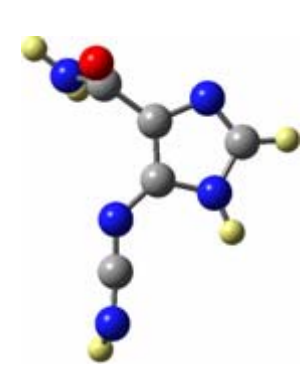	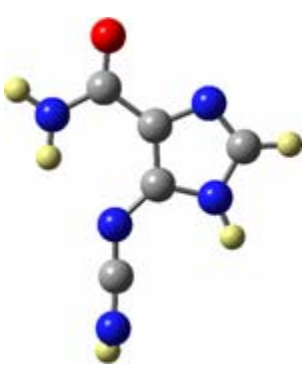
(*E*,*Z*)-**2**	ROTS(**2**, (*E*,*Z*) → (*Z*,*Z*))	(*Z*,*Z*)-**2**
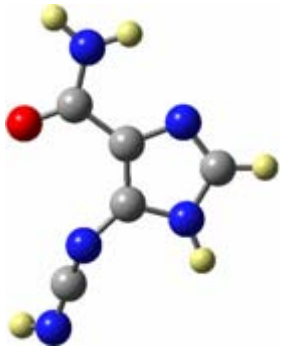		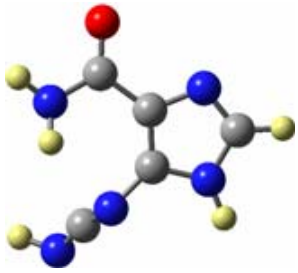
ROTS(**2**, (*E*,*Z*) → (*E*,*E*))		ROTS(**2**, (*Z*,*Z*) → (*Z*,*E*))
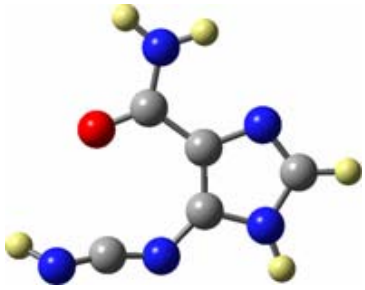	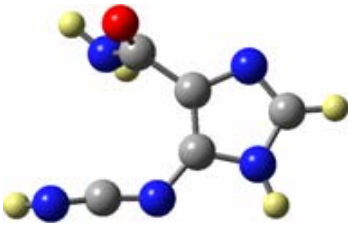	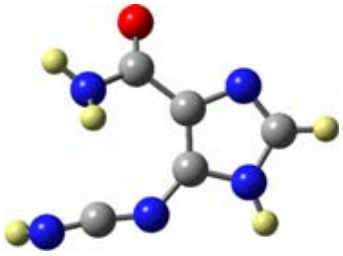
(*E*,*E*)-**2**	ROTS(**2**, (*E*,*E*) → (*Z*,*E*))	(*Z*,*E*)-**2**

Figure 3.2. Computed structures of conformers of carbodiimide **2** and of the rotational transition state structure (ROTS) for their interconversion.

Table 3.2. Relative energies and activation barriers for rotational isomerizations of conformers of cyanoamines **1** and carbodiimides **2**[a]

Parameter	ΔE_0	ΔE_{298}	ΔH_{298}	ΔG_{298}
E_{rel}(**1**, (*Z*,*Z*) *vs.* (*E*,*Z*))	15.15	15.12	15.12	15.04
E_{act}(**1**, (*E*,*Z*) → (*Z*,*Z*))	18.80	18.07	18.02	17.25
E_{act}(**1**, (*Z*,*Z*) → (*E*,*Z*))	3.65	2.95	2.90	2.21
E_{rel}(**2**, (*Z*,*Z*) *vs.* (*E*,*Z*))	4.18	4.09	4.06	4.19
E_{act}(**2**, (*Z*,*Z*) → (*E*,*Z*))	4.46	4.26	3.85	4.90
E_{act}(**2**, (*E*,*Z*) → (*Z*,*Z*))	8.64	8.35	7.91	9.09
E_{rel}(**2**, (*E*,*Z*) *vs.* (*E*,*E*))	6.79	6.50	6.66	5.82
E_{act}(**2**, (*E*,*Z*) → (*E*,*E*))	0.40	0.29	-0.20	1.20
E_{act}(**2**, (*E*,*E*) → (*E*,*Z*))	7.19	6.79	6.46	7.02
E_{rel}(**2**, (Z,*E*) *vs.* (*Z*,*Z*))	0.83	0.99	0.92	1.13
E_{act}(**2**, (Z,*E*) → (*Z*,*Z*))	2.41	2.22	1.73	3.04
E_{act}(**2**, (*Z*,*Z*) → (*Z*,*E*))	3.24	3.21	2.65	4.17
E_{rel}(**2**, (Z,*E*) *vs.* (*E*,*E*))	11.79	11.57	11.63	11.14
E_{act}(**2**, (Z,*E*) → (*E*,*E*))	1.88	1.77	1.31	2.42
E_{act}(**2**, (*E*,*E*)→ (*Z*,*E*))	13.68	13.35	12.95	13.56
E_{rel}(**2**, (*E*,*Z*) *vs.***1**, (*E*,*Z*))	7.70	6.79	6.99	6.31
E_{rel}(**2**, (*Z*,*Z*) *vs.* **1,** (*E*,*Z*))	11.87	10.87	11.04	10.50
E_{rel}(**2**, (*E*,*E*) *vs.***1,** (*E*,*Z*))	0.91	0.29	0.33	0.49
E_{rel}(**2**, (*Z*,*E*) *vs.***1,** (*E*,*Z*))	12.70	11.86	11.96	11.63

[a] All data are in kcal/mol. and determined at B3LYP/6-31++G**.

Conjugate Acids

All Computed structures of conjugate acids of cyanoamine **1** are shown in Figure 3.3 and Figure 3.4, and the structures of conjugate acids of carbodiimide **2** are shown in Figure 3.5 and Figure 3.6. We computed the proton affinities for every possible site of rotamers and tautomers of cyanoamine **1** and carbodiimide **2**. The proton affinities and related data are listed in Table 3.3 and Table 3.4.

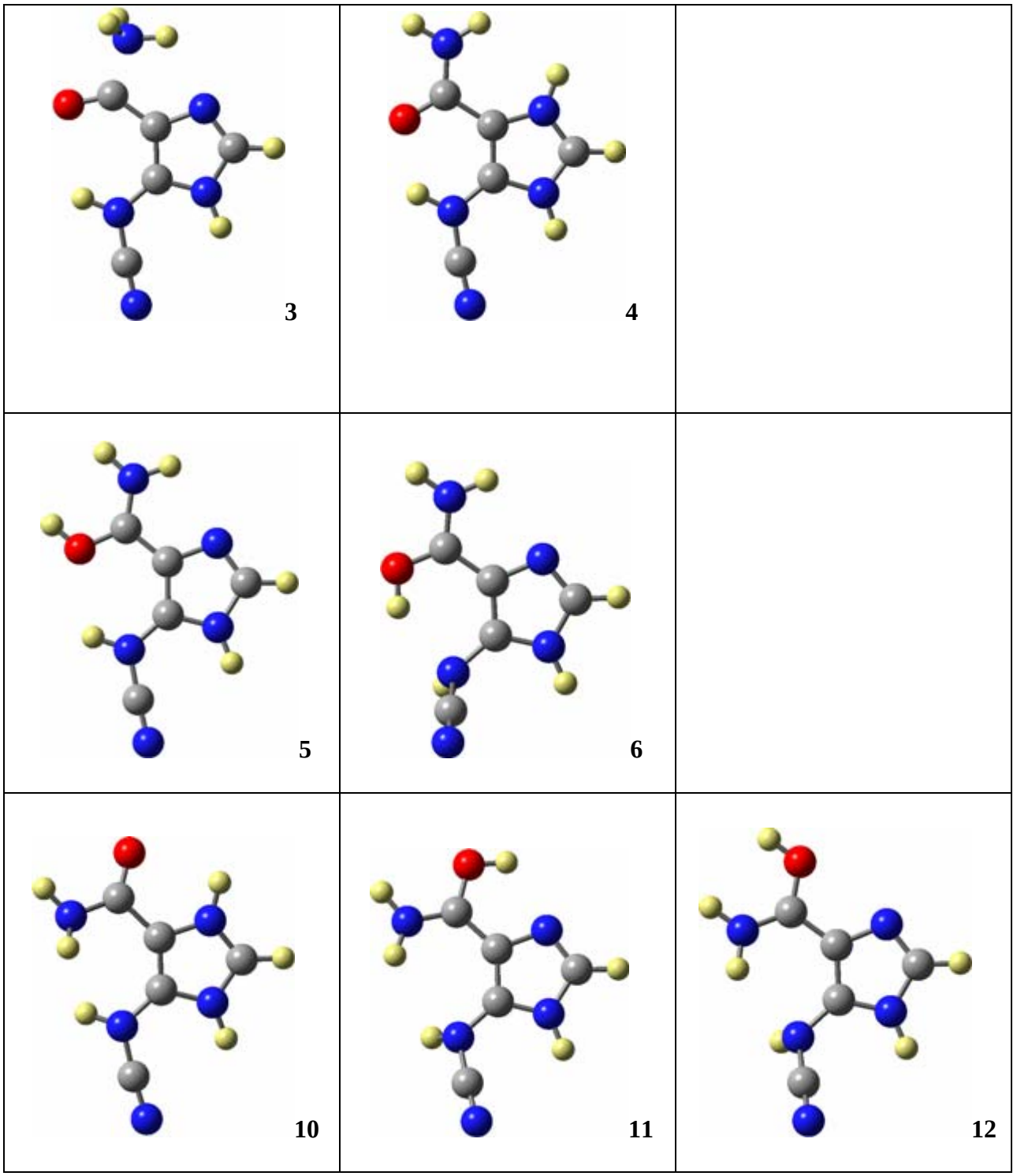

Figure 3.3. Computed structures of protonated **1** with *Z*-arm of the NCN moiety.

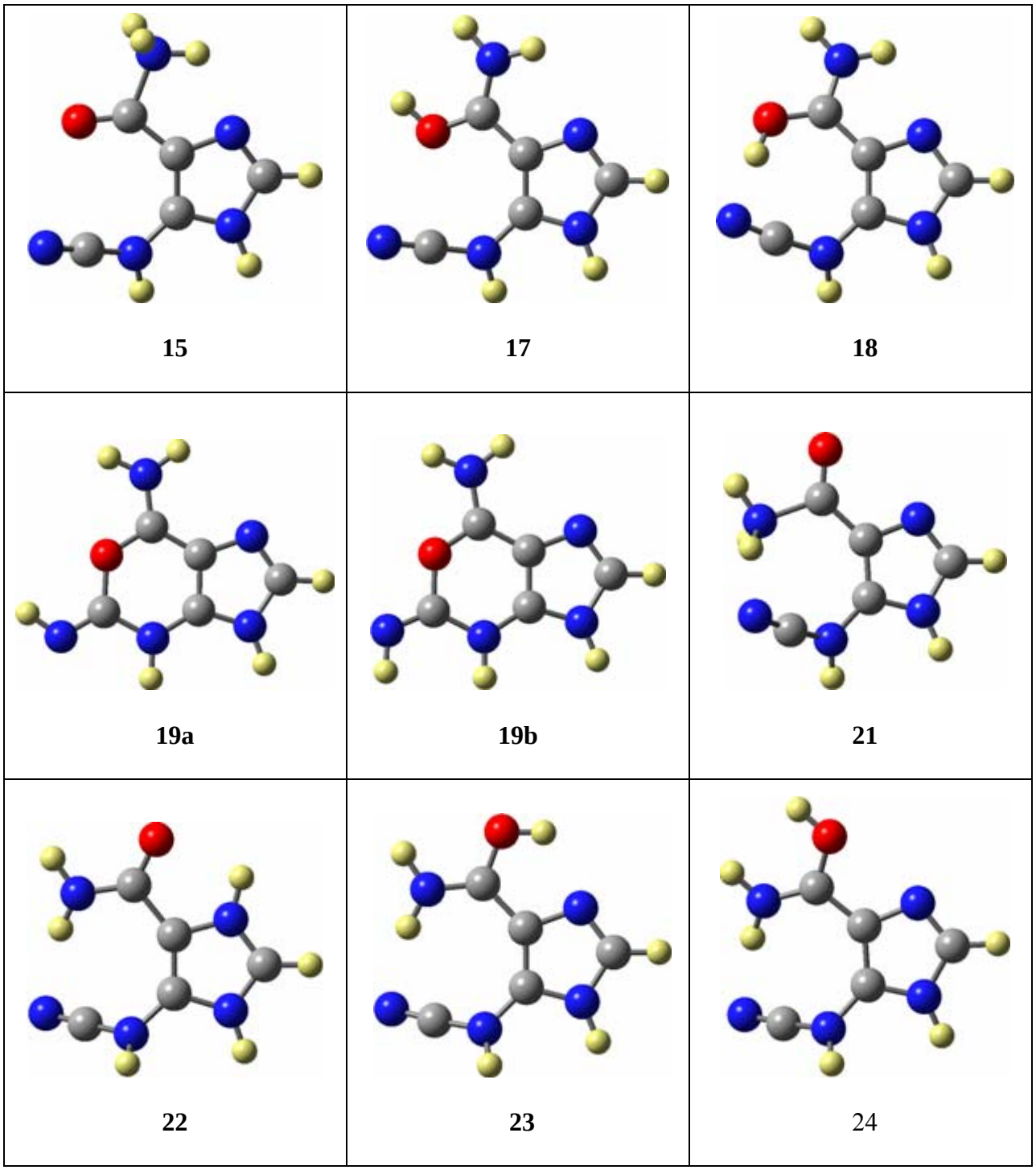

Figure 3.4. Computed structures of protonated **1** with *E*-arm of the NCN moiety.

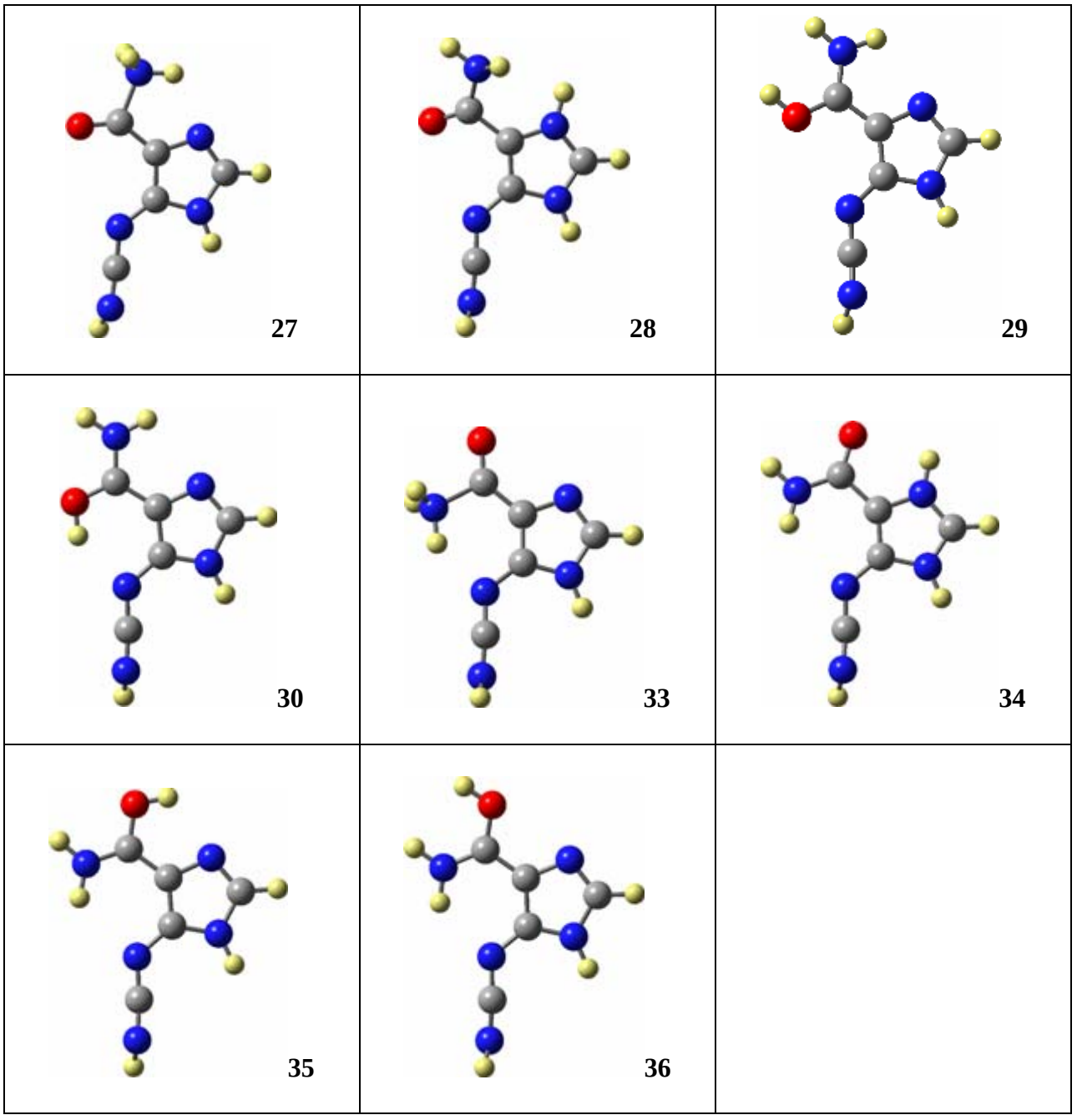

Figure 3.5. Computed structures of protonated **2** with *Z*-arm of the NCN moiety.

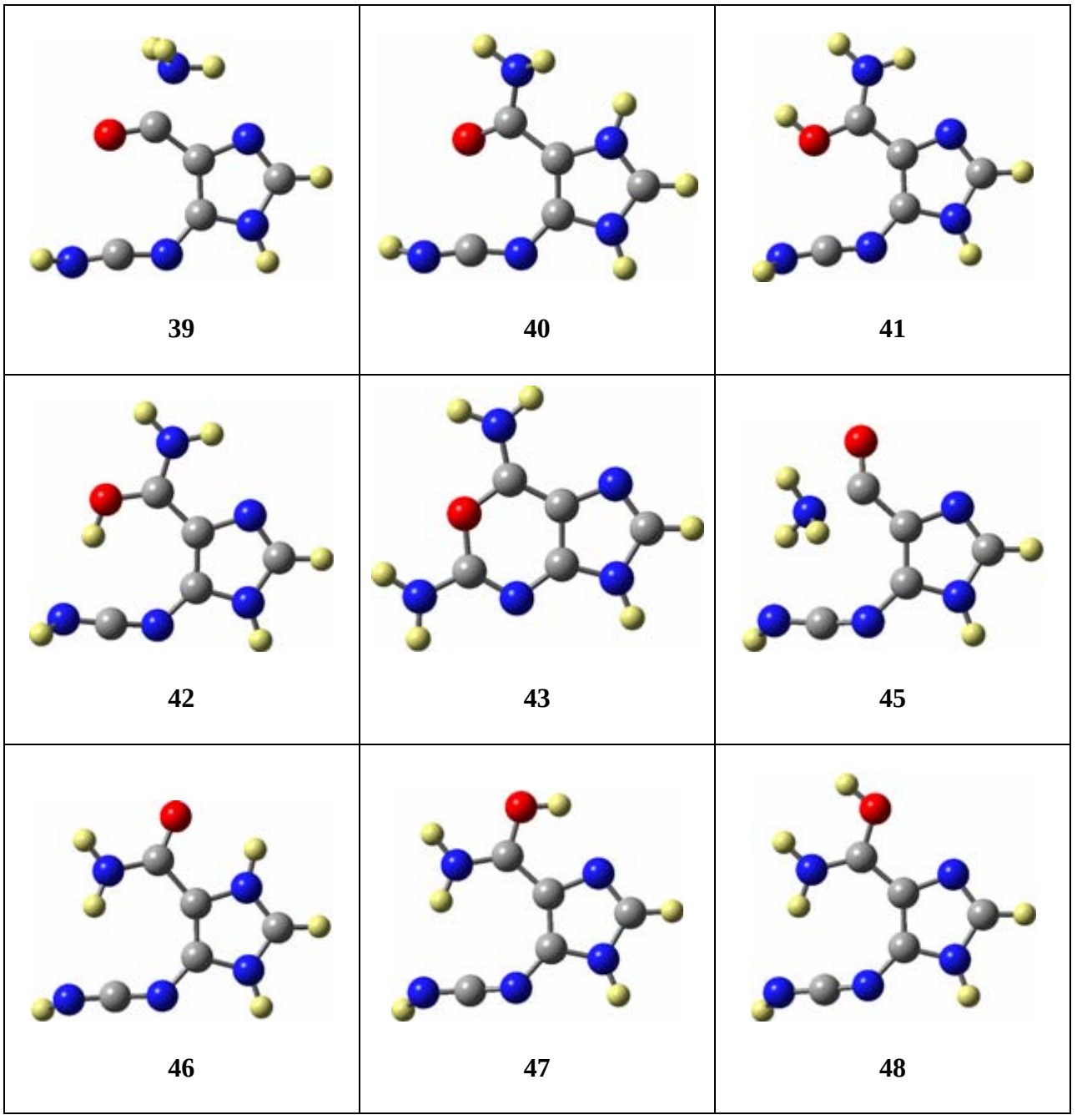

Figure 3.6. Computed structures of protonated **2** with *E*-arm of the NCN moiety.

Table 3.3. All data of proton affinities in kJ/mol computed at B3LYP/6-31++G**.

Parameter	ΔE_0	ΔE_{298}	ΔH_{298}	ΔG_{298}
PA(**3**)	828.39	831.33	833.82	803.13
PA(**4**)	871.03	873.72	876.20	848.03
PA(**5**)	862.48	865.55	868.03	836.28
PA(**6**)	842.80	846.95	849.43	817.39
PA(**10**)	857.99	857.41	857.41	859.19
PA(**11**)	848.16	847.90	847.90	849.96
PA(**12**)	806.15	805.68	805.69	809.50
PA(**15**)	802.51	801.25	801.25	803.69
PA(**17**)	843.82	843.18	843.18	843.59
PA(**18**)	857.92	858.31	858.31	856.14
PA(**19a**)	912.47	915.54	915.54	907.17
PA(**19b**)	893.89	896.76	896.77	888.97
PA(**21**)	762.08	761.22	761.22	762.66
PA(**22**)	856.24	856.20	856.20	855.66
PA(**23**)	863.63	864.03	864.04	862.07
PA(**24**)	818.52	818.27	818.27	817.68
PA(**27**)	854.45	853.05	853.05	856.33
PA(**28**)	876.26	875.15	875.16	878.79
PA(**29**)	893.30	892.50	892.50	893.96
PA(**30**)	918.09	918.34	918.34	917.21
PA(**33**)	824.57	823.71	823.71	825.70
PA(**34**)	917.74	917.29	917.30	918.16
PA(**35**)	919.12	919.18	919.18	918.64
PA(**36**)	879.31	878.90	878.90	879.06
PA(**39**)	865.39	864.29	864.30	866.13
PA(**40**)	904.41	903.77	903.77	904.31
PA(**41**)	897.28	896.48	896.48	897.67
PA(**42**)	894.65	894.89	894.89	893.58
PA(**43**)	985.92	988.91	991.39	869.52
PA(**45**)	798.80	797.93	797.94	799.55
PA(**46**)	912.02	911.46	911.46	912.55
PA(**47**)	904.91	905.36	905.36	903.59
PA(**48**)	857.29	856.53	856.53	858.39

Table 3.4. Proton affinities (ΔH) in kJ/mol computed at B3LYP/6-31++G**.

Mol.	Protonation Site	(*E*,*Z*)	(*Z*,*Z*)	(*E*,*E*)	(*Z*,*E*)
1	NH_2	833.82		801.25	761.22
	N7	876.20	857.41		856.20
	C6–O, N7	868.03	847.90	858.31	864.04
	C6–O, NH_2	849.43	805.69	843.18	818.27
	NCN, cyano			**915.54**	
	NCN, amino				
2	NH_2	853.05	823.71	864.30	797.94
	N7	875.16	917.30	903.77	911.46
	C6–O, N7	**918.34**	919.18	894.89	905.36
	C6–O, NH_2	892.50	878.90	896.48	856.53
	NCN, cyano			**991.39**	
	NCN, amino				

Isoguanosine Formation

The highest proton affinity, by far, is associated with cyano-N protonation of (*E*,*E*)-**2** leading to the formation of the **43**, ΔH (PA) = 991.4 kJ/mol. The formation of (*E*,*E*)-**2** can be obtained from (*E*,*Z*)-**1** via (*E*,*Z*)-**2** by internal proton transfer. It is easy to get (*E*,*E*)-**2** in solution but is hard in gas phase because of high activation barrier. The formation of ion **43** must start form the protonated (*E*,*Z*)-**1** (Scheme 3.3) because neutral (*E*,*E*)-**2** is not available. Cyano-*N* protonation of (*E*,*Z*)-**1** does not form a stable nitrilium ion **7** but the O-protonated carbodiimide species **30** is formed instead. Ion **43** is easily accessible by internal proton transfer by **41** or **42**, which are obtained by simple rotation of **29** and **30** respectively.

Interestingly, all other the cyano-N protonated carbodiimides **31**, **37**, and **49** directly form **43** (Scheme 3.3). Ions **19a** and **19b** are conformational isomers and **19a** is preferred by ΔH = 18.8 kJ/mol over **19b**. The formation of **43** also can be accomplished by

intramolecular proton transfer from **19a**, which is another path that starts form either **44** or **50**. Ion **50** is obtained from the amide group rotation of **44**. Ion **19a** is then accessible by intramolecular cyclization of **44**. Oxanosine may be formed by hydrolysis of **43.** However, the deprotonation of **43** is much faster than hydrolysis of **43**. Oxanine-1-imine is formed instead of Oxanosine. According to our previous study, the formation of isoguanosine is obtained if the oxanine-1-imine is formed.

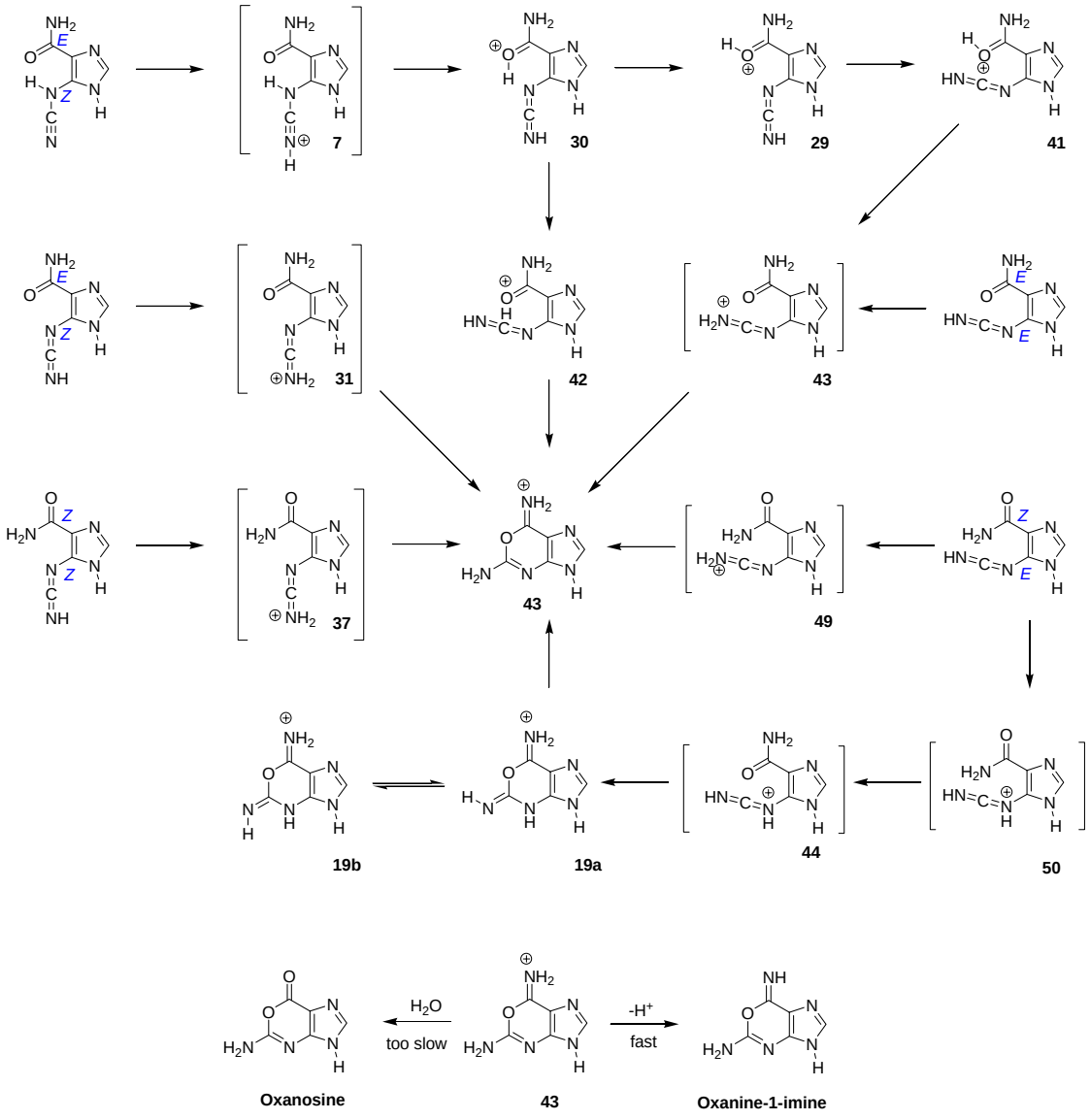

Scheme 3.3. Cyclizations initiated by protonation of tautomers of carbodiimide **2**.

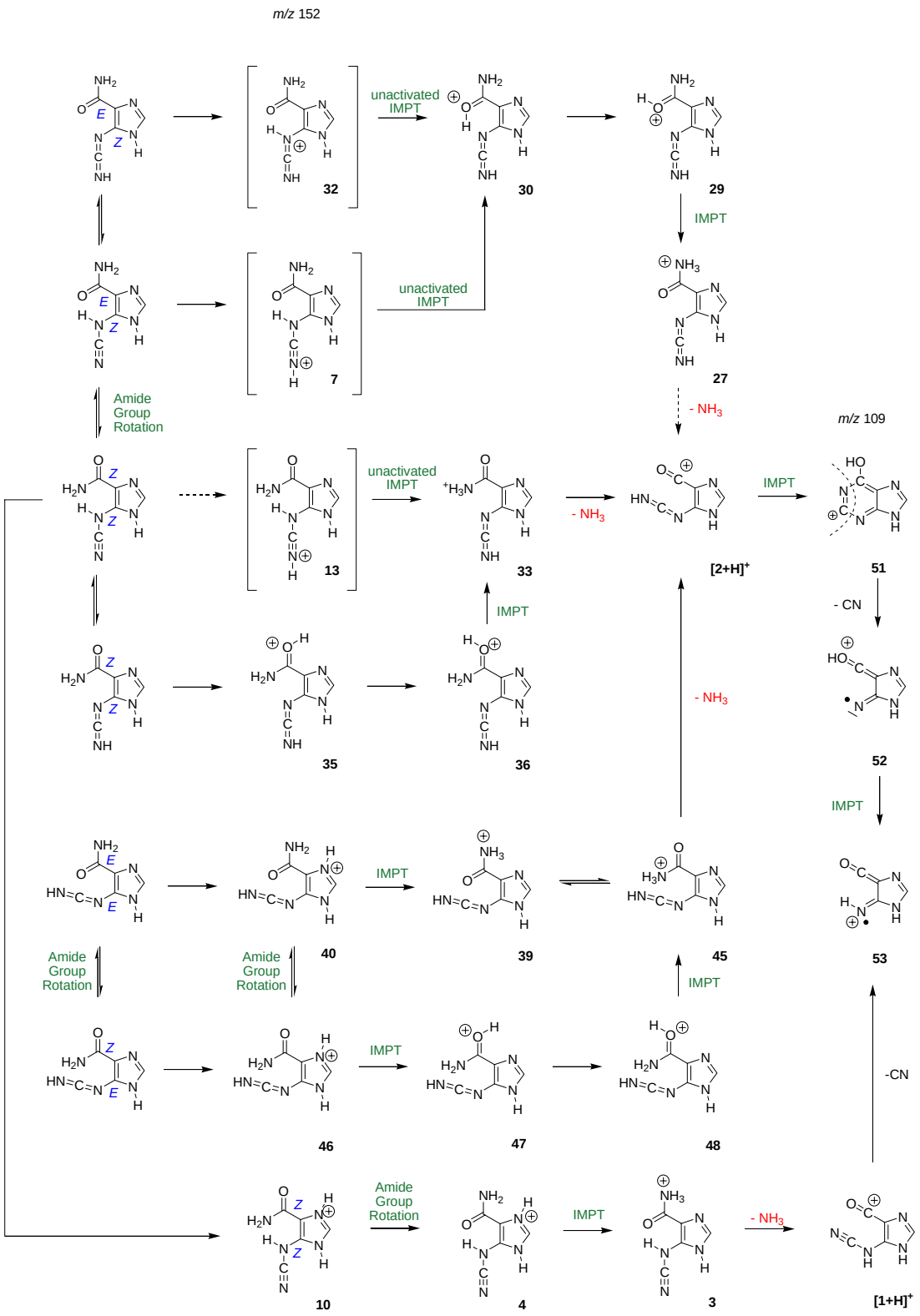

Scheme 3.4. Possible paths of protonated **5** beginning with NH_3 elimination.

Implications for Mechanisms of Ammonia Elimination

The amino group is *not* the best protonation site for the molecule **1**, and we have to discuss how the amino group can serve as the dissociative protonation site[21] or consider possible mechanisms for ammonia elimination. Some guidance is provided by the emerging understanding of NH_3 elimination from peptides.[22] The "mobile proton model" holds that intramolecular proton migration to various protonation sites can occur before fragmentation. The presence of basic amino acids impedes the proton mobility,[23] and the actual mechanisms of ammonia elimination can be more complex.[24,25]

Studies of NH_3 elimination from amides strongly suggest that ammonia elimination occurs only from the ammonium ion[26] does *not decarbonylate* and the ion loses CN instead to form *m/z* 109 based on the previous study. A most likely mechanism for ammonia elimination of protonated **1** and **2** is outlined in Scheme 3.4. We computed the proton affinities for every possible site of the two rotamers and four tautomers of **1**. Cyano-*N* protonation is the best option for cyanoamine (*E*,*Z*)-**1** and ion $[\mathbf{2} + H]^+$ becomes accessible via ammonia elimination via one path that start from cyanoamine (*E*,*Z*)-**1**. The first step of the path is the formation of **30** that is the product of the unactivated intramolecular proton transfer from **7**. O-inversion from **30** to **29** is endothermic by 25.8 kJ/mol. The formation of $[\mathbf{2} + H]^+$ is possible after the process of intramolecular proton transfer from **29** to **27** that is endothermic by 39.4 kJ/mol. This path also can start from **32** and **30** that has the highest proton affinities among protonated ions of carbodiimide (*E*,*Z*)-**2.** Ion **30** is formed by the unactivated intramolecular proton transfer from **32**.

Cyanoamine (*Z*,*Z*)-**1** could form the ion $[\mathbf{1} + H]^+$ and $[\mathbf{2} + H]^+$ via different paths. The path to the ion $[\mathbf{1} + H]^+$ is via the imidazolium ion **10** that is best protonated ion for

cyanoamine (*Z*,*Z*)-**1**. Formation of $[\mathbf{1} + H]^+$ involves initial amide rotation from **10** to **4** which is then followed by proton transfer to the amide-NH_2 protonated carbodiimide species **3**; this sequence is endothermic by 29.8 kJ/mol. The path to the Ion $[\mathbf{2} + H]^+$ is achieved by ammonia elimination from **33** that is formed unactivated intramolecular proton transfer from **13**. The ion **35,** the best option for carbodiimide (*Z*,*Z*)-**2,** could also form the ion $[\mathbf{2} + H]^+$ via ammonia elimination of **33**. The first step of this path is the O-inversion that is exothermic by 40.3 kJ/mol and then is followed by the proton transfer from **36** to **33**.

For carbodiimide (*Z*,*E*)-**2** the formation of the ion **46** is preferred. The ion $[\mathbf{2} + H]^+$ is formed via ammonia elimination via two paths that start from **46,** one with amide rotation via **40** and **39** another one without amide rotation via **47** and **48**. The ion **39** that is also the best option for carbodiimide (*E*,*E*)-**2**, after amide rotation to **40** and intramolecular proton transfer from **40** to **39**, could lead to NH3 elimination and the formation of $[\mathbf{2} + H]^+$; this sequence is endothermic by 47.2 kJ/mol. The alternative path to $[\mathbf{2} + H]^+$ involves initial proton transfer from **46** to **47** and subsequent O-inversion is endothermic by 48.8 kJ/mol.

The *E*-conformation about the C-(N_2CH) bond is preferred in the ions $[\mathbf{2} + H]^+$ and $[\mathbf{1} + H]^+$, and the intramolecular proton transfer equilibrium between the N in $[\mathbf{2} + H]^+$ and the O in **51** should be fast. The accessibility of **51** provides a rational for CN elimination to form radical cation **52** or **53**.

.

3.4 Conclusion

We discussed the conformational and isomer preferences of cyanoamine 1 and carbodiimide 2 and on their conjugate acids. The (*E*,*Z*)-**1** is the most stable and (*Z*,*Z*)-**1** is the least stable. The discussion of isoguanosine formation suggests that there are several possible paths to complete this cycliztion reaction that can start from ions **19a**, **31**, **37**, and **43**. It helps us to understand the cycliztion reaction mechanisms of cyanoamine **1** and carbodiimide **2**.

We have studied NH_3 elimination from the protonated cyanoamine **1** and carbodiimide **2** and computed the proton affinities for all possible structures**.** Every one of the postulated ions either was found to exist in the gas phase or to exist in the gas phase as a tautomer. The formation of reactive intermediates $[\mathbf{1} + H]^+$ and $[\mathbf{2} + H]^+$ via different paths that start form the protonated cyanoamine **1** and carbodiimide **2**. The amino group hardly ever is the best protonation site of the substrate and we discussed possible mechanisms for ammonia elimination that explain how the amino group can serve as the dissociative protonation site. The NH_3 elimination was always obtained from the intramolecular proton transfer to the amino group.

3.5 Reference

1. Strecker, A. *Annals* **1861**, *118*, 151-177.
2. Kossel, A. *Berichte* **1985**, *18*, 1929-1930.
3. Kossel, A., and Neumann, A. *Z. Physiol. Chem.* **1894**, *27*, 2215-2222.
4. Geiduschek, E. P. *Proc. Natl. Acad. Sci. U.S.A.* **1961**, *47*, 950-955.
5. Geiduschek, E. P. *J. Mol. Biol.* **1962**, *4*, 467-487.
6. Caulfield, J. L., Wishnok, J. S., and Tannenbaum, S. R. *Chem. Res.Toxicol.* **2003**, *16*, 571-574.
7. Rayat, S. Ph.D. Dissertation, University of Missouri-Columbia, 2003.
8. Qian, M., and Glaser, R. *J. Am.Chem.Soc.* **2004**, *126*, 2274-2275.
9. Rayat, S., Majumdar, P., Tipton, P., and Glaser, R. *J. Am. Chem.Soc.* **2004**, *126*, 9960-9969.
10. Suzuki, T.; Yamaoka, R.; Nishi, M.; Ide, H.; Makino, K. *J. Am. Chem.Soc.* **1996**, *118*, 2515-2516.
11. Lucas, L. T.; Gatehouse, D.; Shuker, E. G. *J. Biol. Chem.* **1999**, *274*, 18319-18326.
12. Dong, M.; Wang, C.; Deen, W. M.; Dedon, P. C. *Chem. Res. Toxicol.* **2003**, *16*, 1044-1055.
13. Glaser, R.; Son, M.-S. *J. Am. Chem. Soc.* **1996**, *118*, 10942-10943.
14. Glaser, R.; Rayat, S.; Lewis, M.; Son, M.-S.; Meyer, S. *J. Am. Chem. Soc.* **1999**, *121*, 6108-6119.
15. Rayat, S.; Wu, Z.; Glaser, R. *Chem. Res. Tox.* **2004**, *17*, 1157-1169.
16. Qian, M.; Glaser, R. *J. Am. Chem. Soc.* **2004**, *126*, 2274-2275.

17. Qian, M.; Glaser, R. *J. Am. Chem. Soc.* **2005**, *127*, 880-887.

18. Qian, M.; Yang, S.; Wu, H.; Majumdar, P.; Leigh, N.; Glaser, R. *J. Am. Soc. Mass Spectrometry (JAMAS)* **2007**, *18*, Accepted.

19. (a) Koch, W.; Holthausen, M. C. *A Chemist's Guide to Density Functional Theory*, 2nd ed. Wiley-VCH: Weinheim, 2001. (b) Parr, R. G; Weitao, Y. *Density-Functional Theory of Atoms and Molecules,* International Series of Monographs on Chemistry. Oxford University Press: Oxford, UK, 1994.

20. *Gaussian 03, Revision D.01*, Frisch, M. J.; Trucks, G. W.; Schlegel, H. B.; Scuseria, G. E.; Robb, M. A.; Cheeseman, J. R.; Montgomery, Jr., J. A.; Vreven, T.; Kudin, K. N.; Burant, J. C.; Millam, J. M.; Iyengar, S. S.; Tomasi, J.; Barone, V.; Mennucci, B.; Cossi, M.; Scalmani, G.; Rega, N.; Petersson, G. A.; Nakatsuji, H.; Hada, M.; Ehara, M.; Toyota, K.; Fukuda, R.; Hasegawa, J.; Ishida, M.; Nakajima, T.; Honda, Y.; Kitao, O.; Nakai, H.; Klene, M.; Li, X.; Knox, J. E.; Hratchian, H. P.; Cross, J. B.; Bakken, V.; Adamo, C.; Jaramillo, J.; Gomperts, R.; Stratmann, R. E.; Yazyev, O.; Austin, A. J.; Cammi, R.; Pomelli, C.; Ochterski, J. W.; Ayala, P. Y.; Morokuma, K.; Voth, G. A.; Salvador, P.; Dannenberg, J. J.; Zakrzewski, V. G.; Dapprich, S.; Daniels, A. D.; Strain, M. C.; Farkas, O.; Malick, D. K.; Rabuck, A. D.; Raghavachari, K.; Foresman, J. B.; Ortiz, J. V.; Cui, Q.; Baboul, A. G.; Clifford, S.; Cioslowski, J.; Stefanov, B. B.; Liu, G.; Liashenko, A.; Piskorz, P.; Komaromi, I.; Martin, R. L.; Fox, D. J.; Keith, T.; Al-Laham, M. A.; Peng, C. Y.; Nanayakkara, A.; Challacombe, M.; Gill, P. M. W.; Johnson, B.; Chen, W.; Wong, M. W.; Gonzalez, C.; and Pople, J. A.; Gaussian, Inc., Wallingford CT, 2004.

21. Tu, Y.-P. *J. Org. Chem.* **2006**, *71*, 5482-5488.

22. Paizs, B.; Suhai, S. *Mass Spectrom. Rev.* **2005**, *24*, 508-548.

23. Mouls, L.; Subra, G.; Aubagnac, J.-L.; Martinez, J.; Enjalbal, C. *J. Mass Spectrom.* **2006**, *41*, 1470-1483.

24. Csonka, I. P.; Paizs, B.; Suhai, S. *J. Mass Spectrom.* **2004**, *39*, 1025-1035.

25. Cooper, T.; Talaty, E.; Grove, J.; Van Stipdonk, M.; Suhai, S.; Paizs, B. *J. Am. Soc. Mass Spectrom.* **2006**, *17*, 1654–1664.

26. Lin, H. Y.; Ridge, D. P.; Uggerud, E.; Vulpius, T. *J. Am. Chem. Soc.* **1994**, *116*, 2996-3004.